

BESS実験

—測定器と反陽子流束測定—

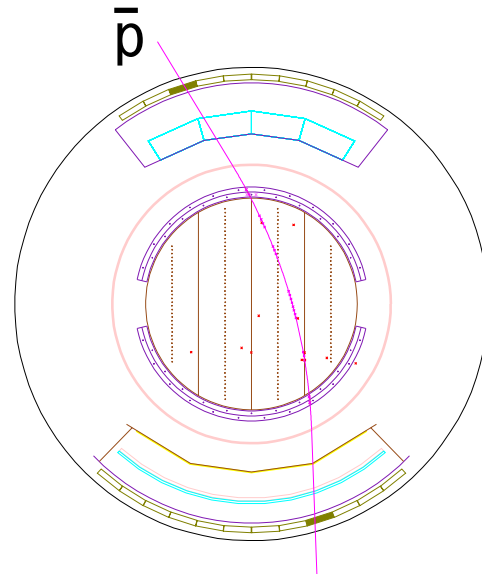
BESS Collaboration
Balloon-borne Experiment
with a **Superconducting Spectrometer**

宇宙線研究所セミナー

東大・理 浅岡陽一

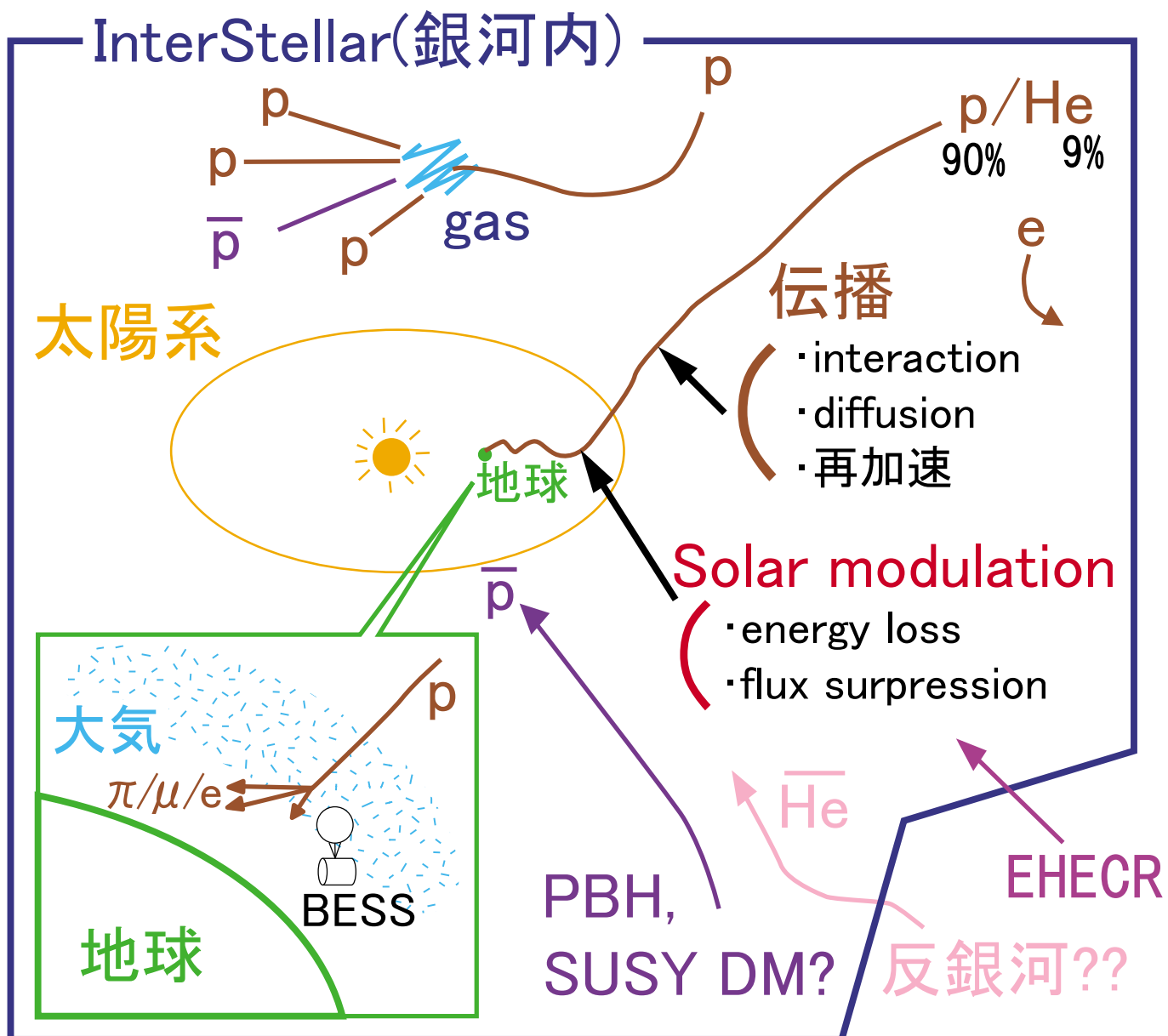
Contents

1. Introduction
2. Detectors
3. \bar{P} Flux Measurements
4. Efficiency Calibration
5. Solar Modulation
6. Summary



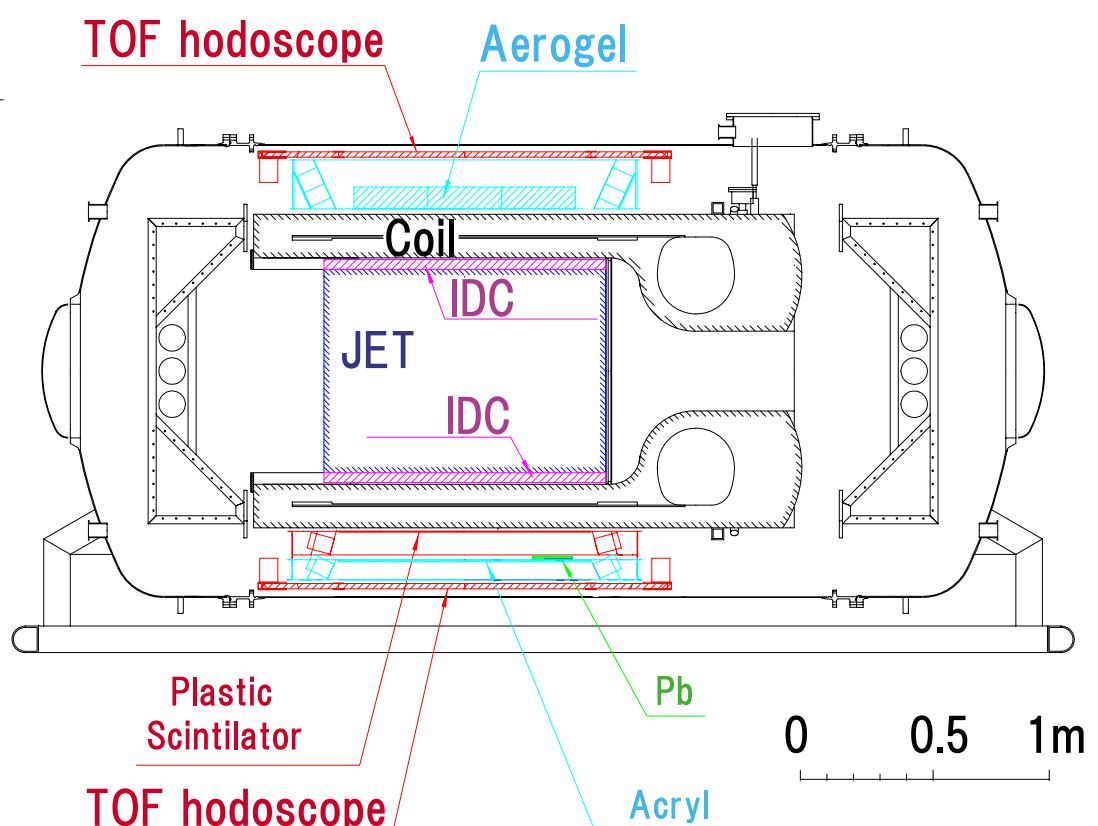
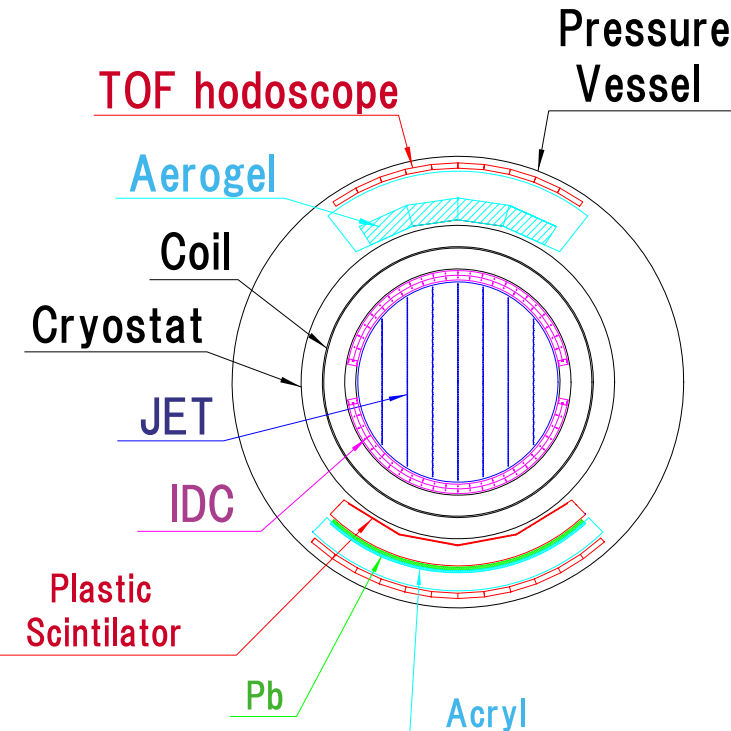
BESS実験: 宇宙における素粒子現象の探求を目的とする気球実験

- ・原始ブラックホール (PBH) の Hawking radiation による蒸発
- ・SUSY Dark Matter (neutralino) の対消滅
⇒ 低エネルギー反陽子 (一次起源)



BESS 測定器

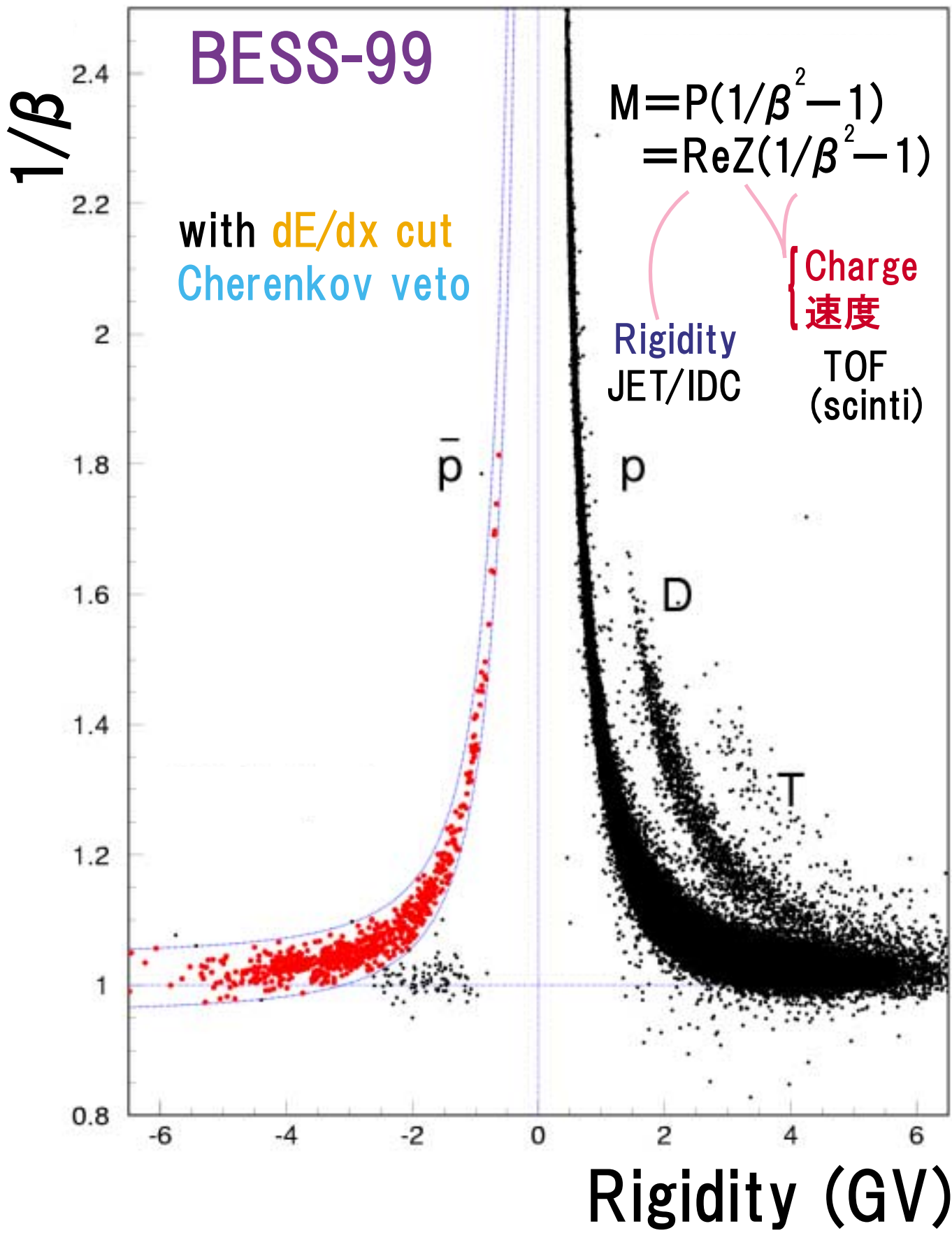
TOF $\Rightarrow \beta$
 Tracking \Rightarrow Rigidity = 運動量/電荷



特徴

- ・薄肉超伝導ソレノイド \Rightarrow 大面積・大立体角 \Leftrightarrow high statistics
- ・強力な粒子識別能力 \Rightarrow 質量の同定(β -Rigidity)
 dE/dx , Aerogel Cherenkov
- ・simple な構造 \Rightarrow 一様な性能 \Leftrightarrow low systematics

Particle ID (質量の同定)



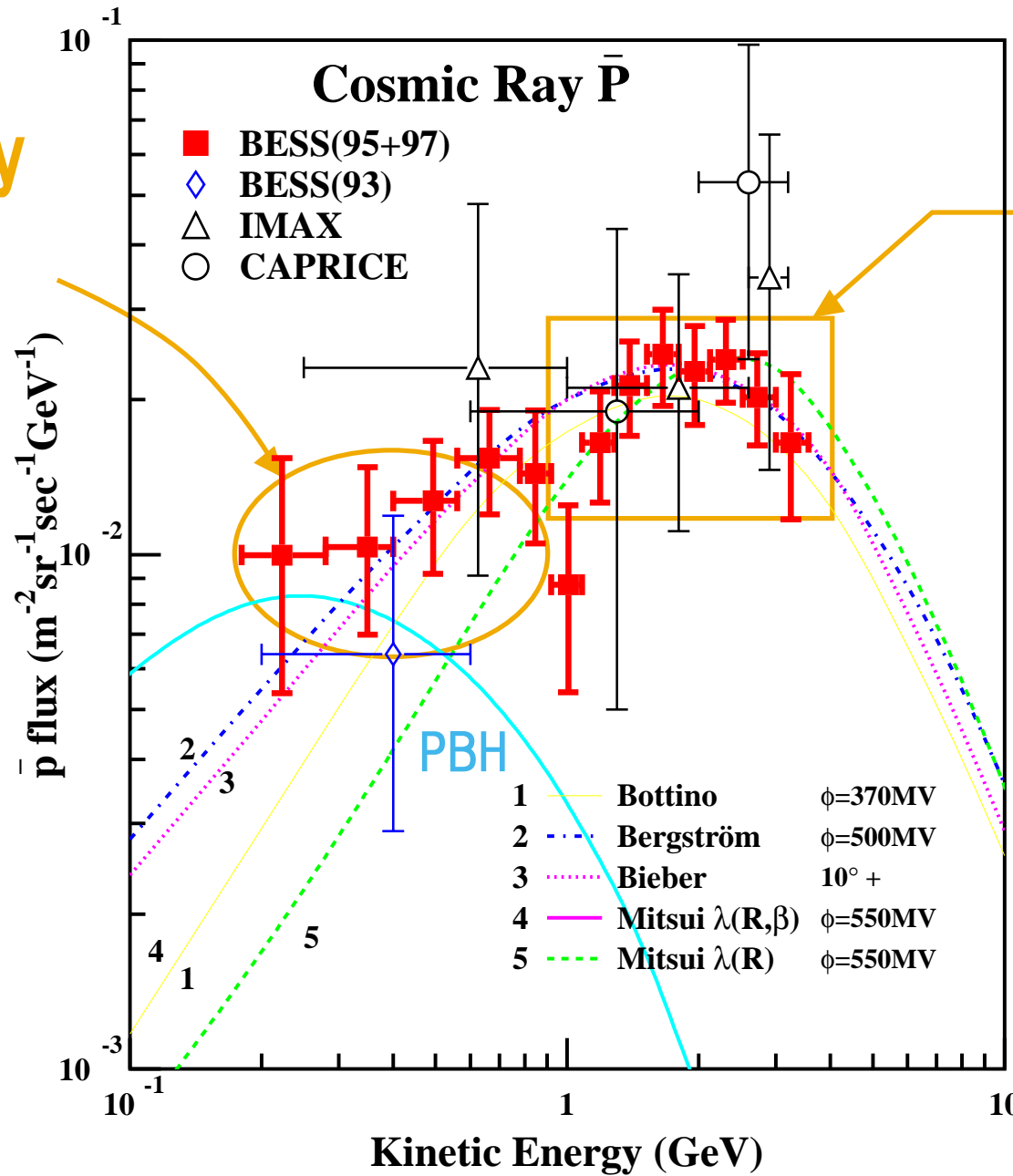
\bar{P} spectrum の測定 @ solar minimum

low energy region

2次起源流束
⇒ 減少
(kinematics)

primary sources
の探索が可能

- PBH蒸発
- SUSY DM の annihilation



peak region

2次起源 dominant



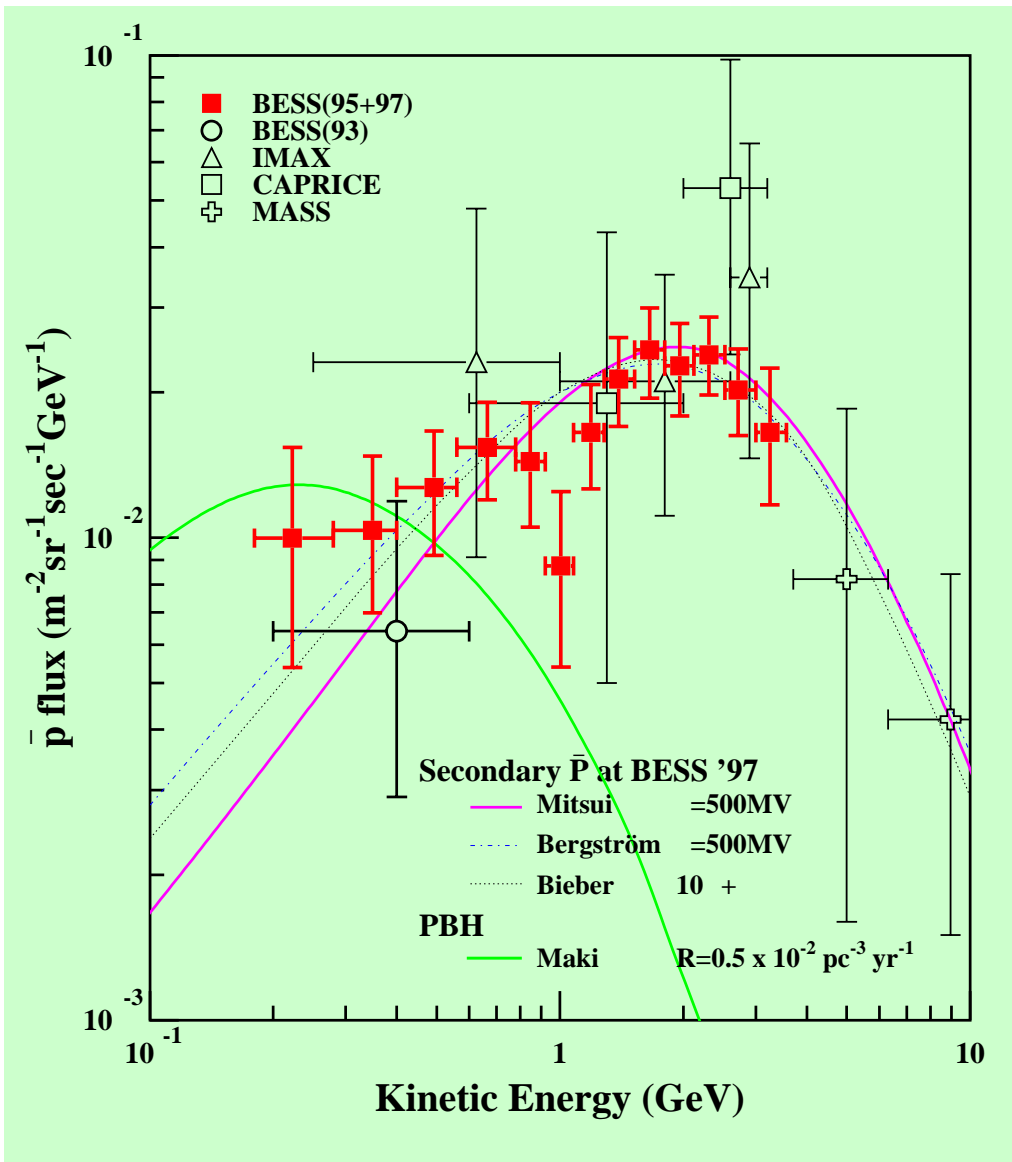
[IS proton flux
 \bar{p} flux @ peak
⇒ 伝播 model
の検証

Input, Output
共に BESS で
測定可能

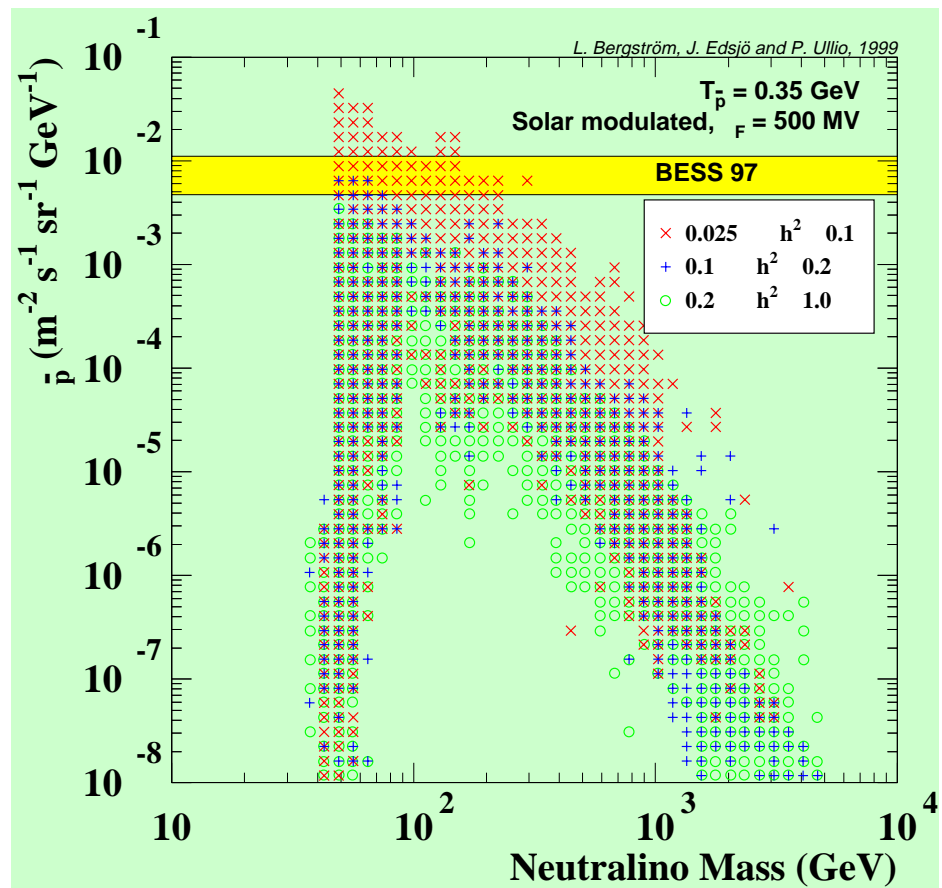
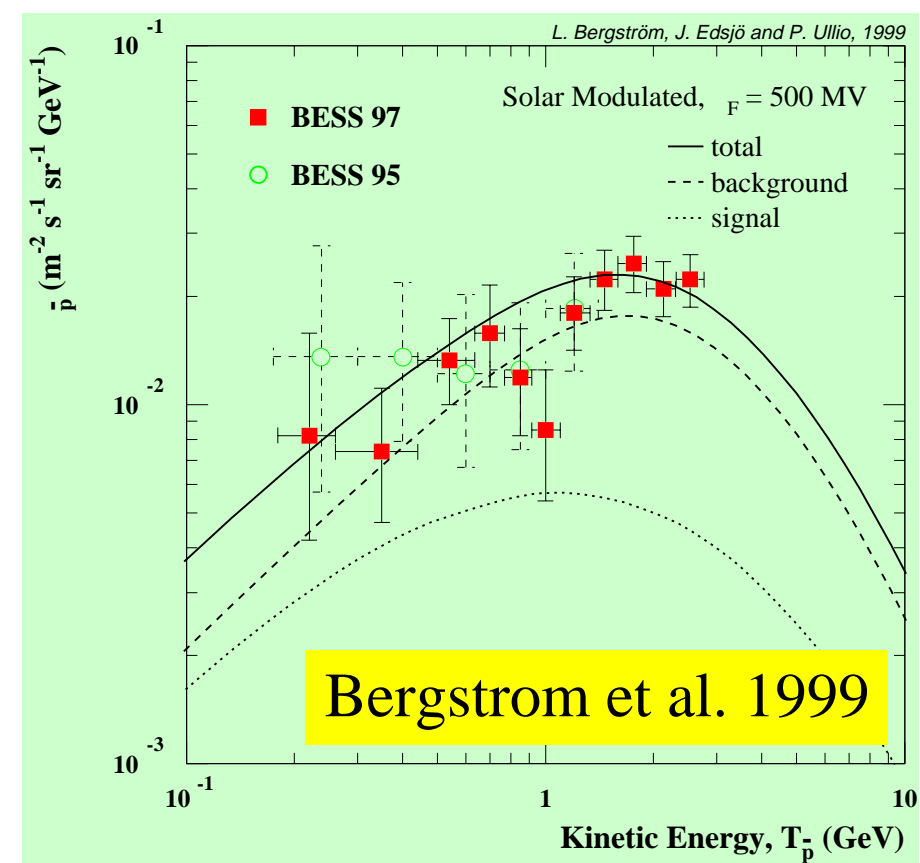
Evaporation of Primordial Black holes

“Black hole explosion ?”
S. W. Hawking, Nature, 1974

- PBHs might be formed by fluctuations in the early Universe.
- $M \sim 5 \times 10^{14} g$ now evaporating.
- Distinct spectrum compared to secondary background.
- BESS data limit the evaporation rate
 - Maki et al, 1996.
 - $R < 10^{-2} \text{ pc}^{-3} \text{ yr}^{-1}$
 - More stringent than gamma-ray limits.



Indirect search for SUSY Dark matter



- Background is larger at low energies than we expected.
- Difficult to distinguish signal from background by means of spectral shape.

BESS data has limited parameter space for SUSY.

- Bergstrom et al, 1999.
- Bottino et al, 1998.

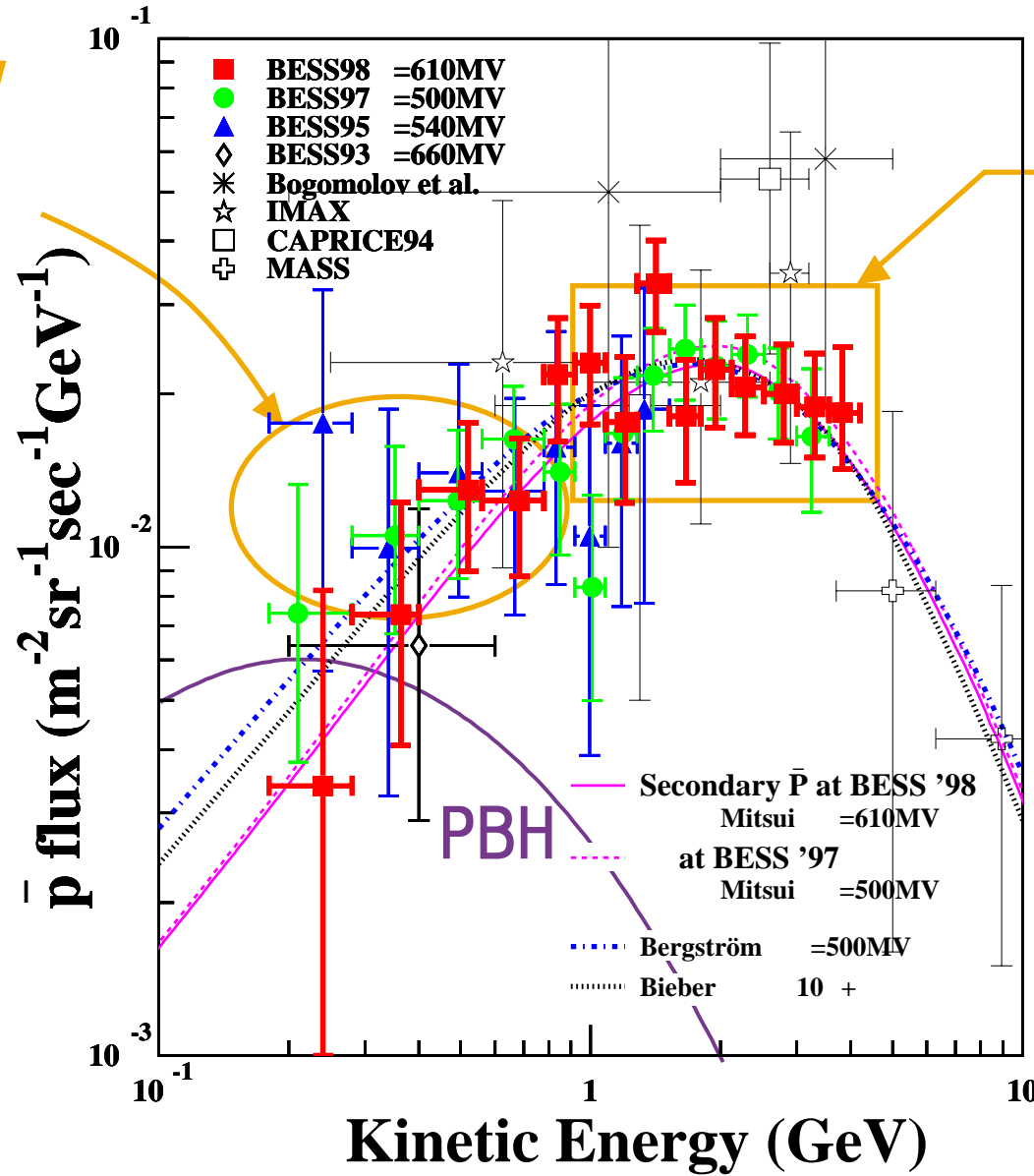
\bar{p} spectrum の測定(93-98)

low energy region

2次起源流束
⇒ 減少
(kinematics)

primary sources
の探索が可能

- PBH蒸発
- SUSY DM の annihilation



peak region

2次起源 dominant



[IS proton flux
-p flux @ peak
⇒ 伝播 model
の検証

流束の経年変化
⇒ solar modulation
の理解

History

87 Proposals S. Orito et al.

⋮	⋮
92	Ready 後帰国(MOU)
93	初 Flight 6 p
94	2nd Flight 2 p
95	3rd Flight 43 p
96	気球に穴があいており、となり町との間に落下。 大変な回収の後、2回目のチャンスを待つが時間切れ。
97	4th Flight 415 p
98	5th Flight 1 season 2回のflightを狙うも、 398 p 山火事の影響で時間切れ。
99	気球破裂し、湖に落ちる。1週間でリカバーし、 6th Flight 668 p 2回目のチャンスを捉える。
00	7th Flight 2週間以上の天気待ち。打ち上げ時 558 p 気球に穴が発見されるがテープで塞ぐ。

折戸研入り

キャンペーン参加

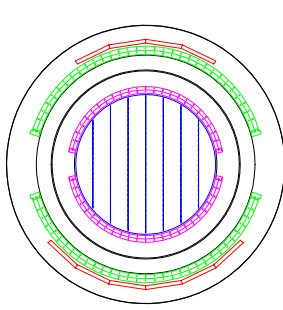
- ・過去7回地磁気緯度の低いCanada, Lynnlake でのFlightに成功した。
- ・Detectorが原因で予定を遅らせたことはない。 Balloonの事故にはけっこう遭っている。

Year by Year Improvement of the Detector

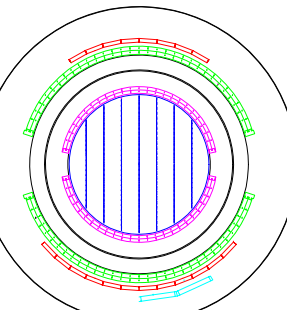
気球実験だからこそ可能！

TOF, JET, Solenoid
のConceptは維持

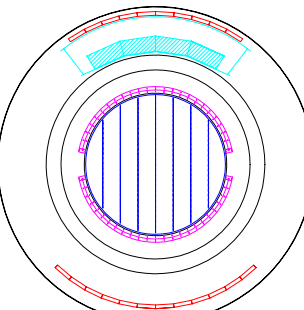
BESS-93,94



BESS-95

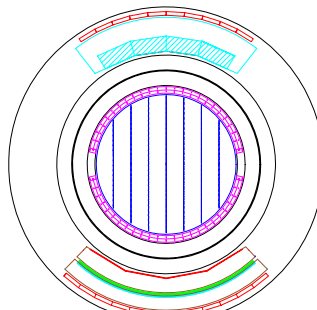


BESS-97,98



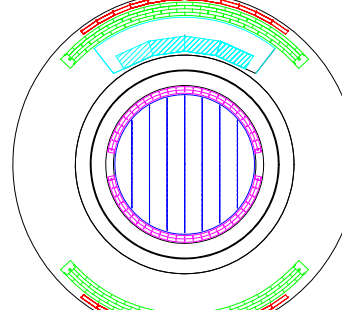
AMS Technical Flight

BESS-99,00

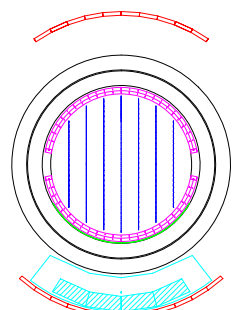


⇒ Future

BESS-TeV



BESS-Polar



Larger Vessel

$$\sigma_{\text{TOF}} = 300 \text{ ps}$$

$$\sigma_{\text{TOF}} = 110 \text{ ps}$$

$$\sigma_{\text{TOF}} = 70 \text{ ps}$$

Aerogel C

97 $n=1.03$
 $\bar{p} 0.2-3.5 \text{ GeV}$
98 $n=1.02$

$$\bar{p} 0.2-0.6 \text{ GeV}$$

$$\bar{p} 0.2-1.4 \text{ GeV}$$

$$\bar{p} 0.2-4.2 \text{ GeV}$$

$$6, 2$$

$$43$$

$$415, 398$$

Shower Counter

2X₀ Lead
 e/μ sep.

$$\bar{p} 0.2-4.2 \text{ GeV}$$

$$668, 558$$

Larger Vessel

New ODC's
New JET/IDC's

No Vessel

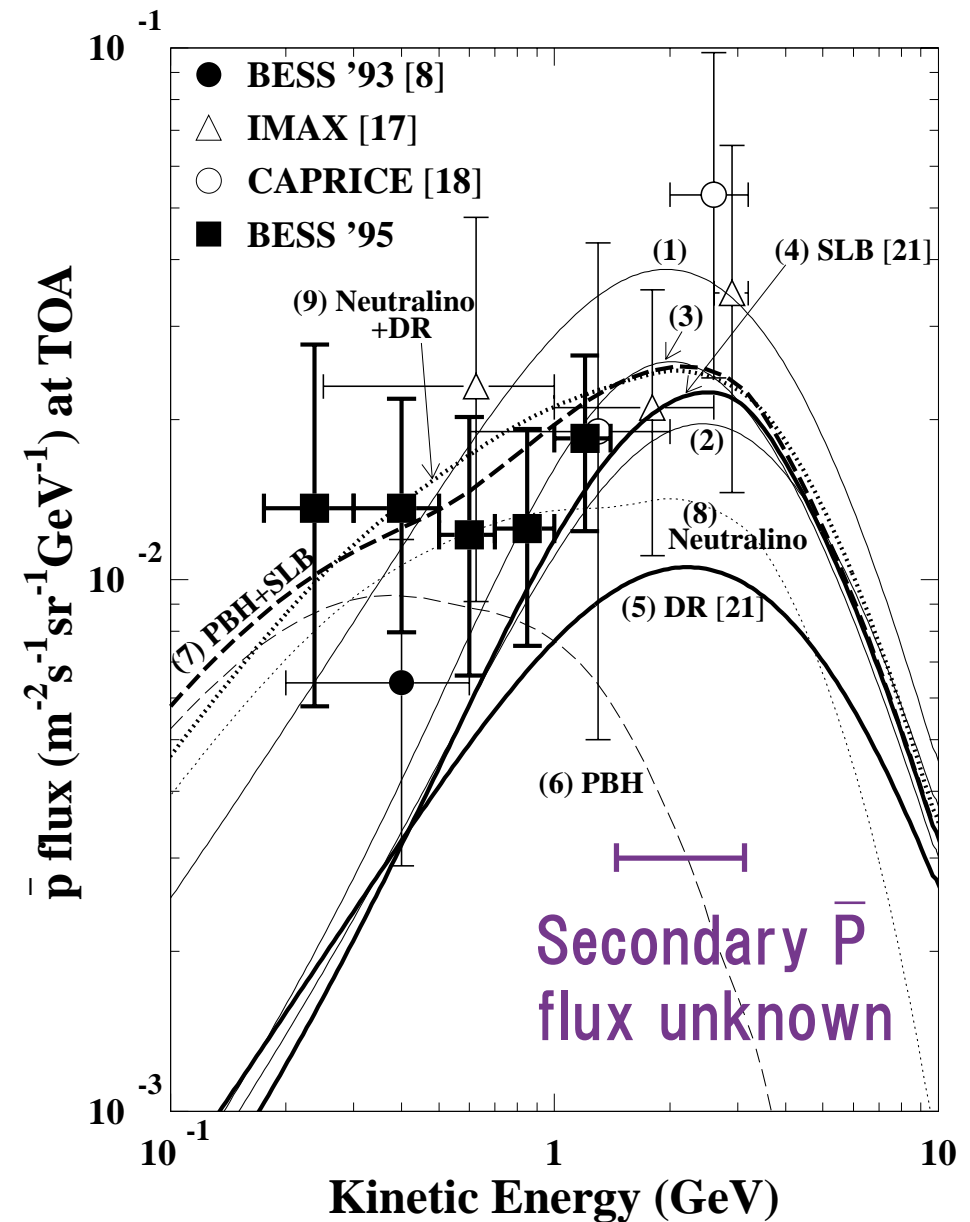
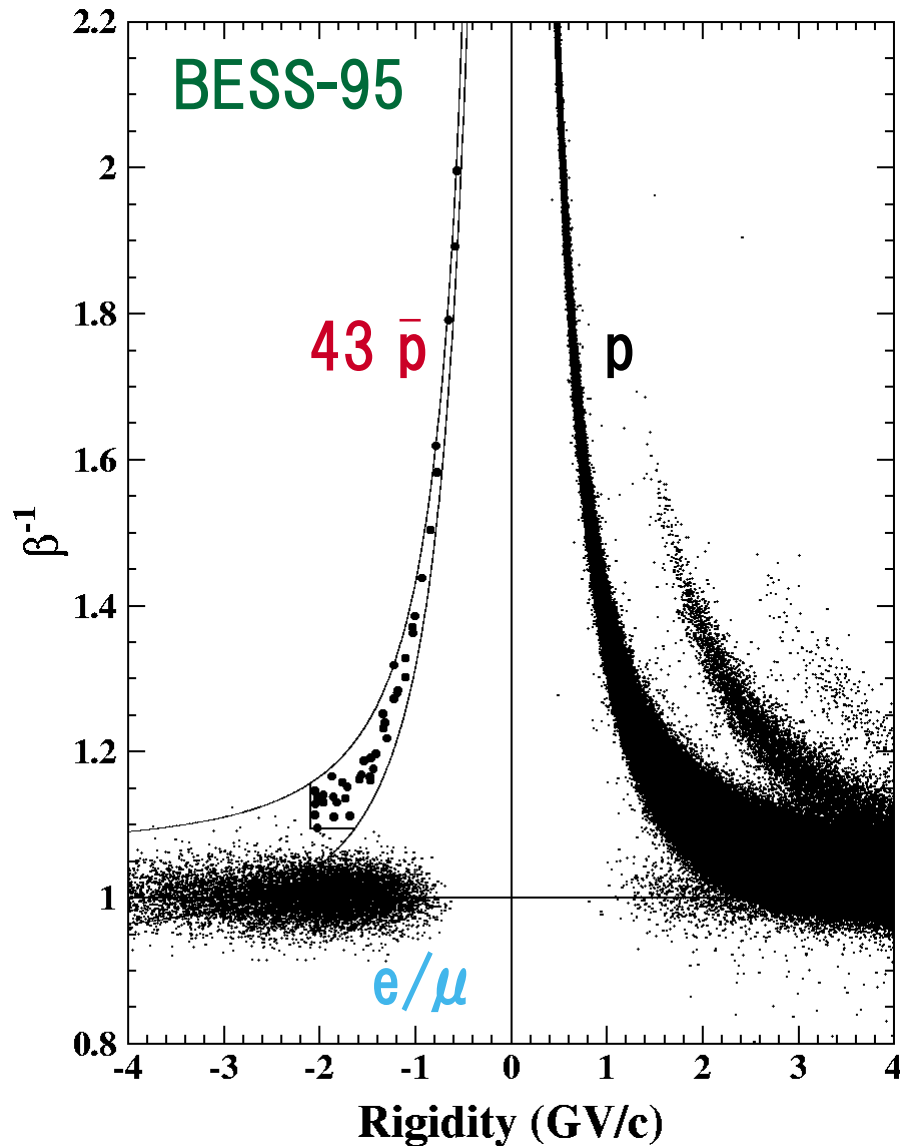
New Mag
(ultra thin)

p/He up to 1 TeV

$$\bar{p} 0.2-4.2 \text{ GeV} \quad \bar{p} 0.1-4.2 \text{ GeV}$$

↔ No. of \bar{p} 's

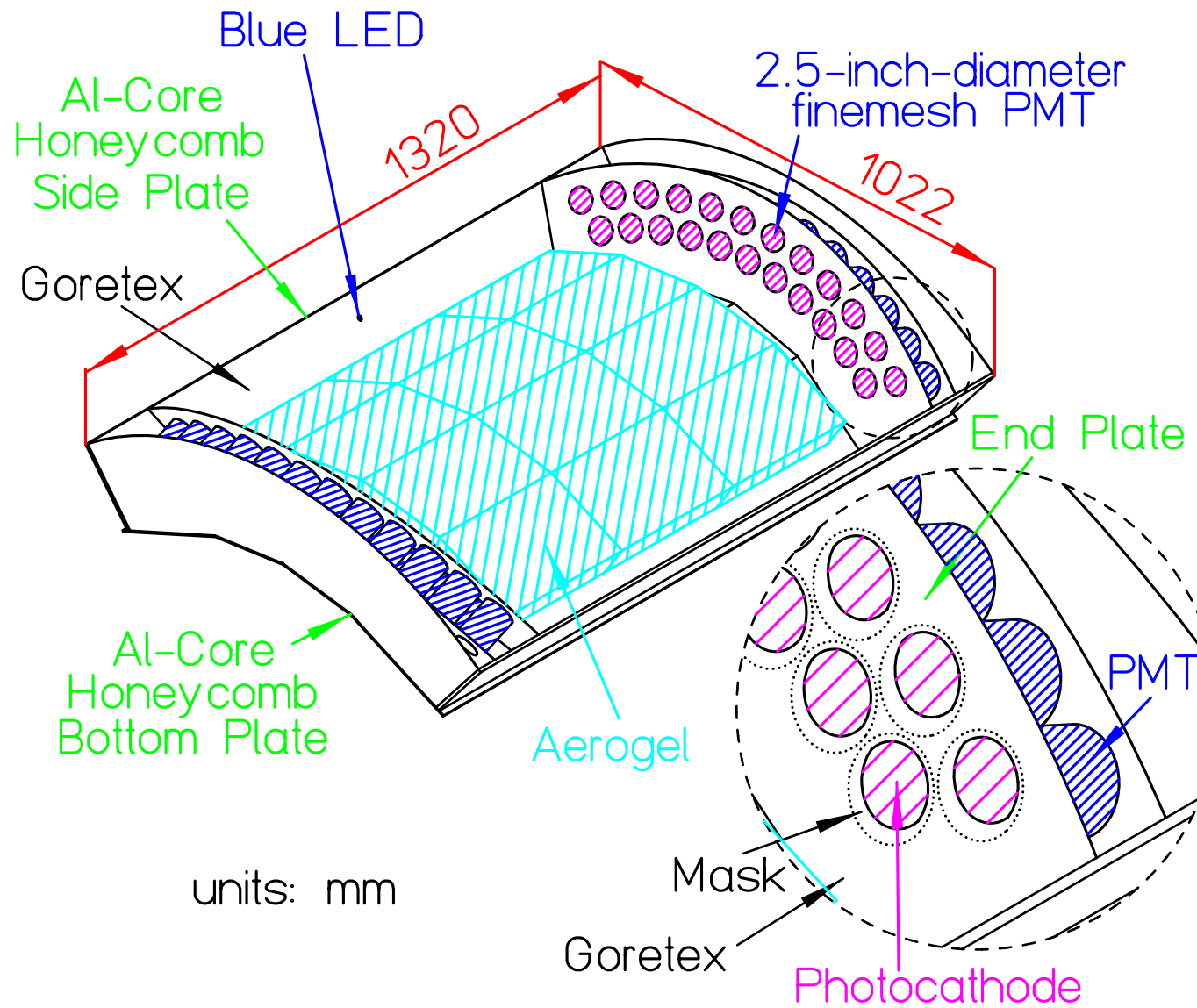
Antiproton Measurement (Before Aerogel)



H. Matsunaga et al, PRL, 1998.

Aerogel Cherenkov Counter

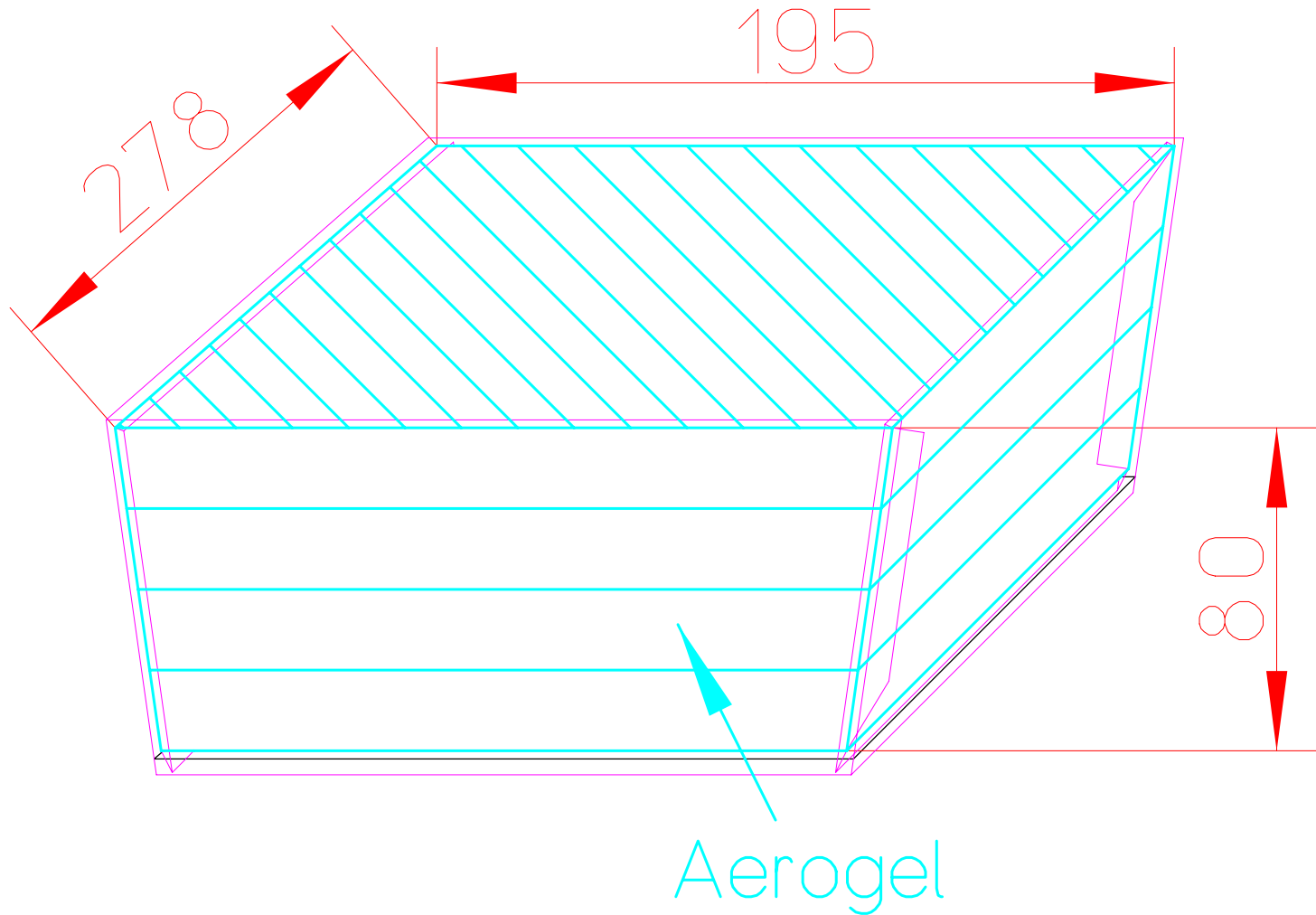
Y.Asaoka et al, NIMA 416 (1998) 236-242



- ・大面積大立体角
- ・PMT 稠密配置
- ・反射材 Goretex
- ・LEDによるPMT gain calibration

Aerogel

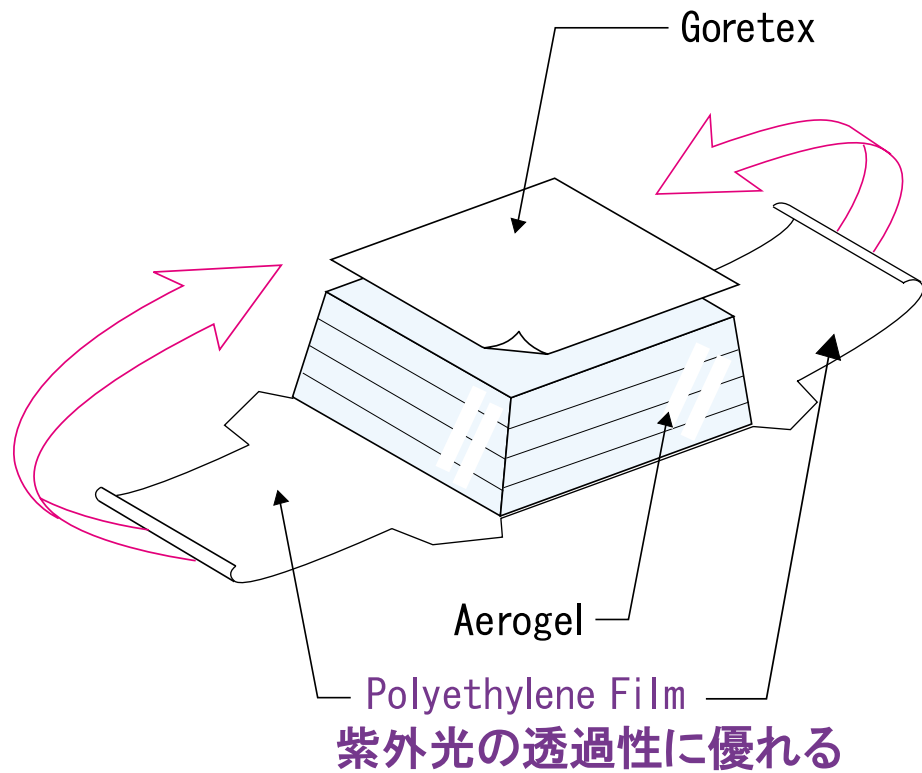
疎水性・透明度に優れる R&D by KEK(住吉さん他)
非常にfragile ⇔ 振動の多い気球実験でのfeasibility



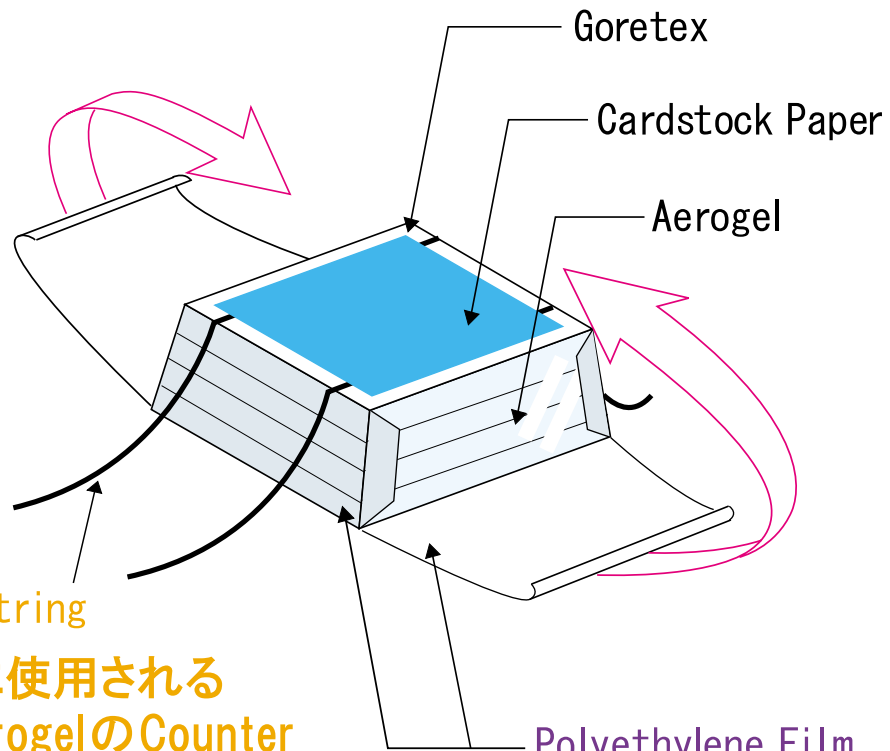
- 97 n=1.03 茂利製油
waterjetでcut
- 98~ n=1.02 KEK(BELLEの協力)
テーパーのついた型
…忘れられないシラザンのにおい

Wrapping of Aerogels

Step1:

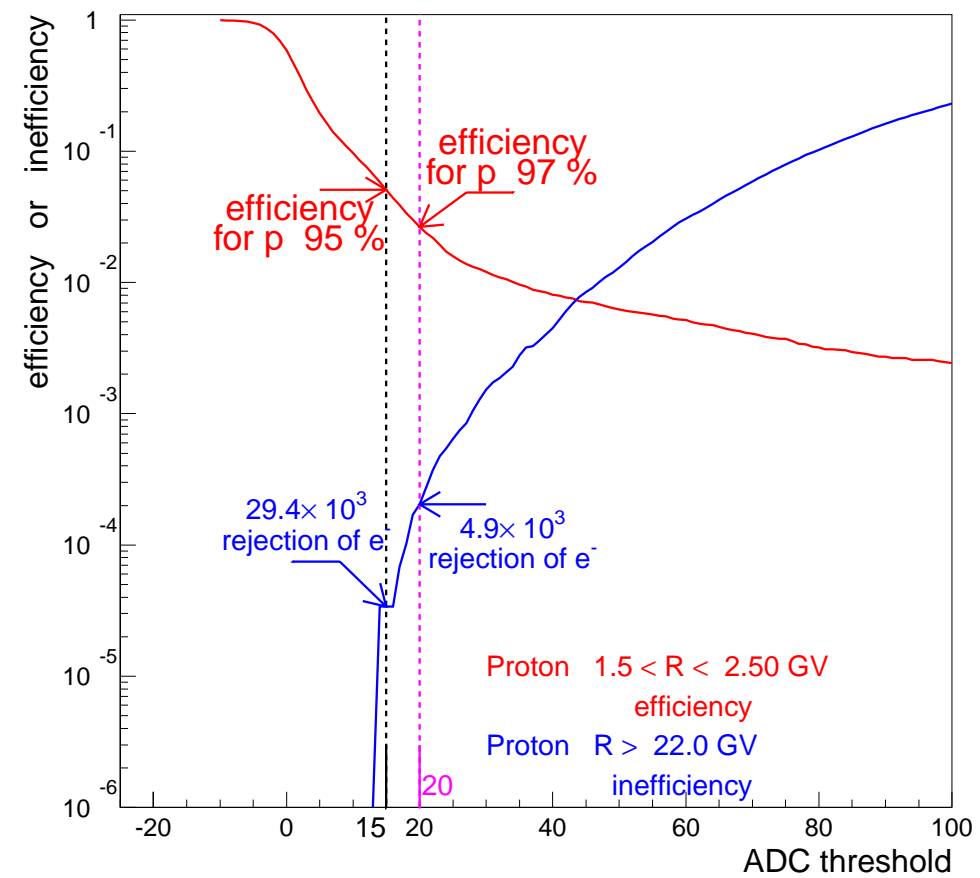
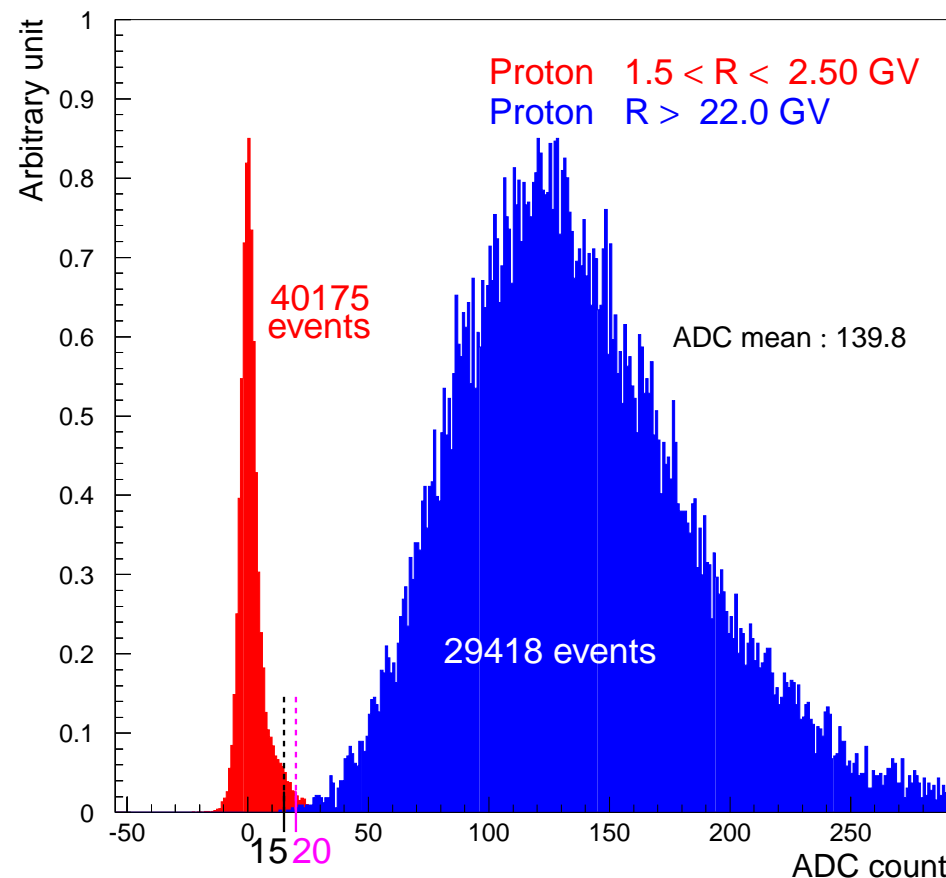


Step2:



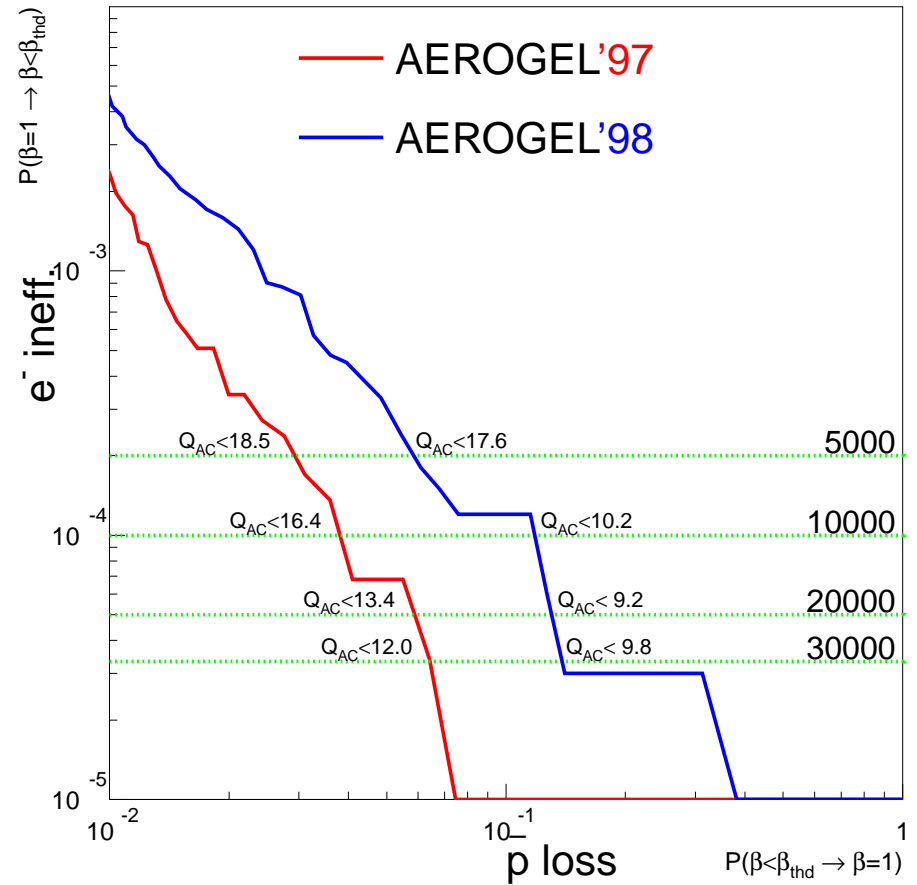
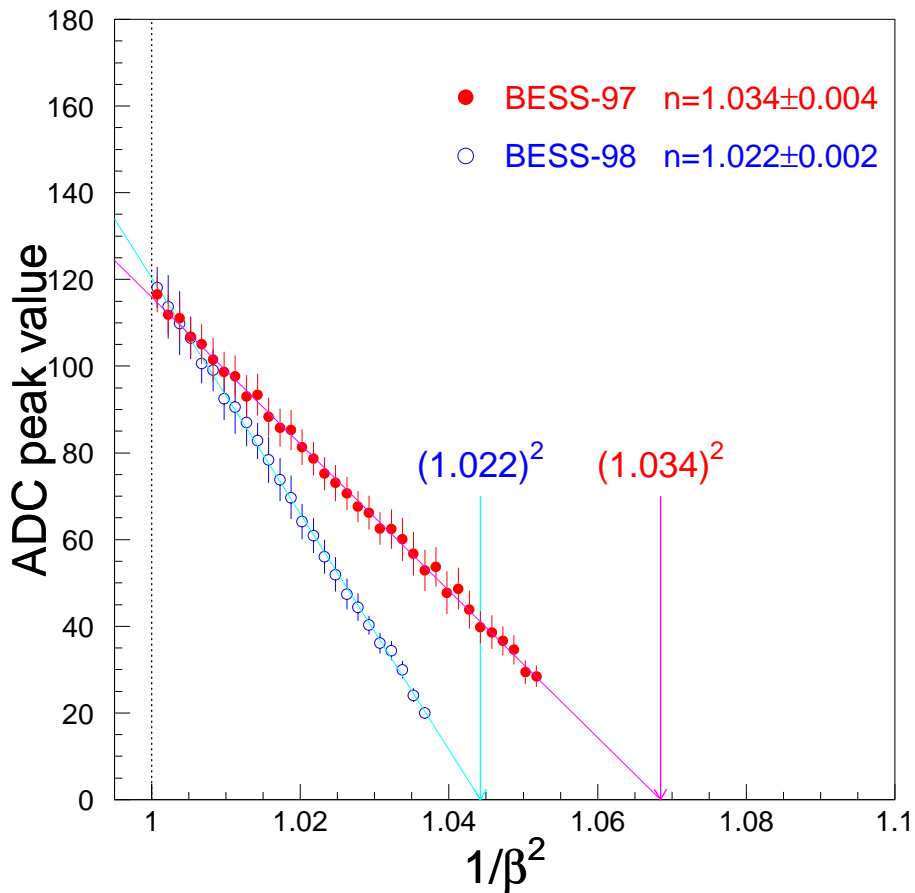
Aerogel-97 e/μ Rejection Power

$n=1.03$



Rejection power was estimated as a function of ADC threshold using high energy proton samples.

Aerogel-97, 98 Comparison

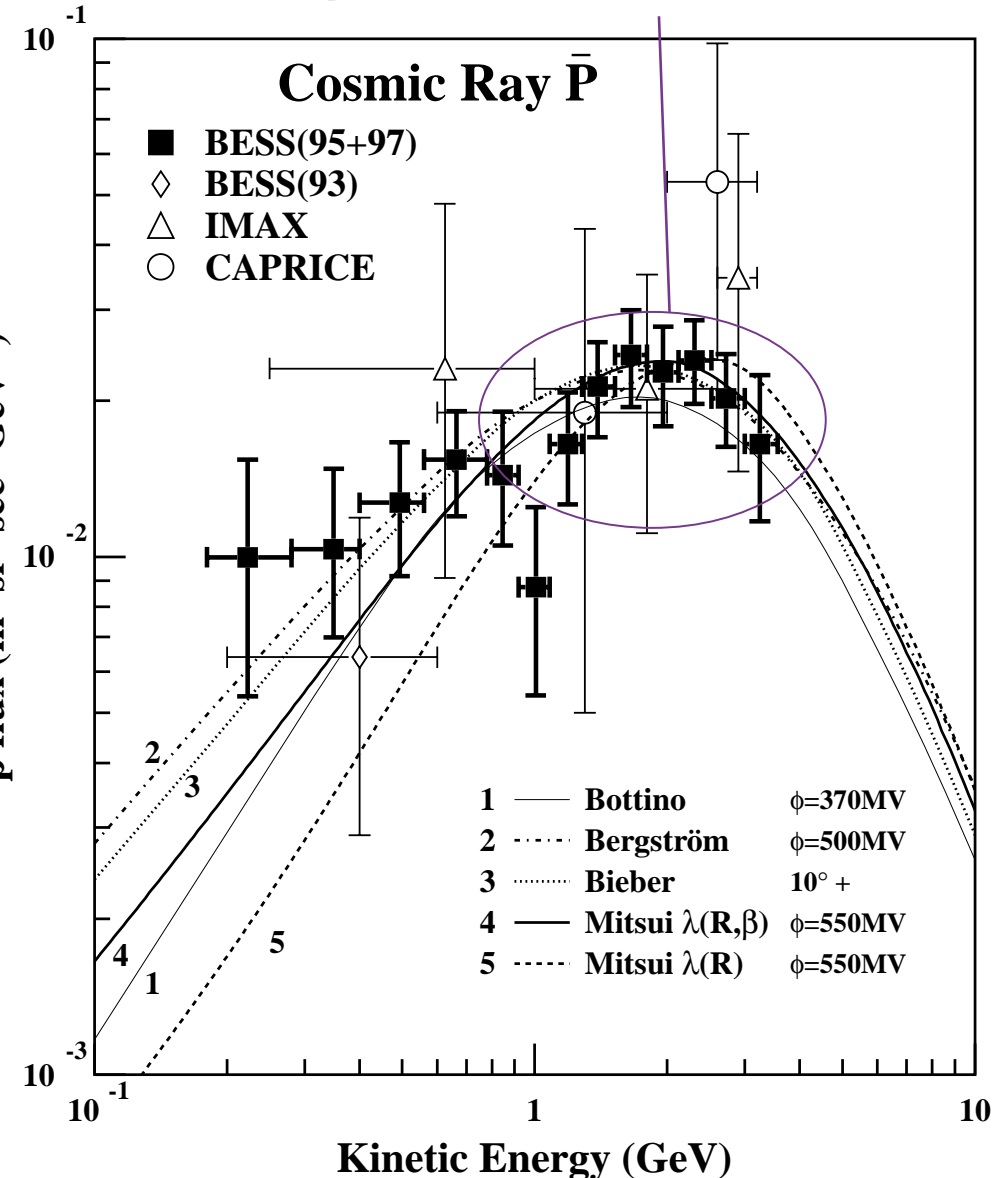
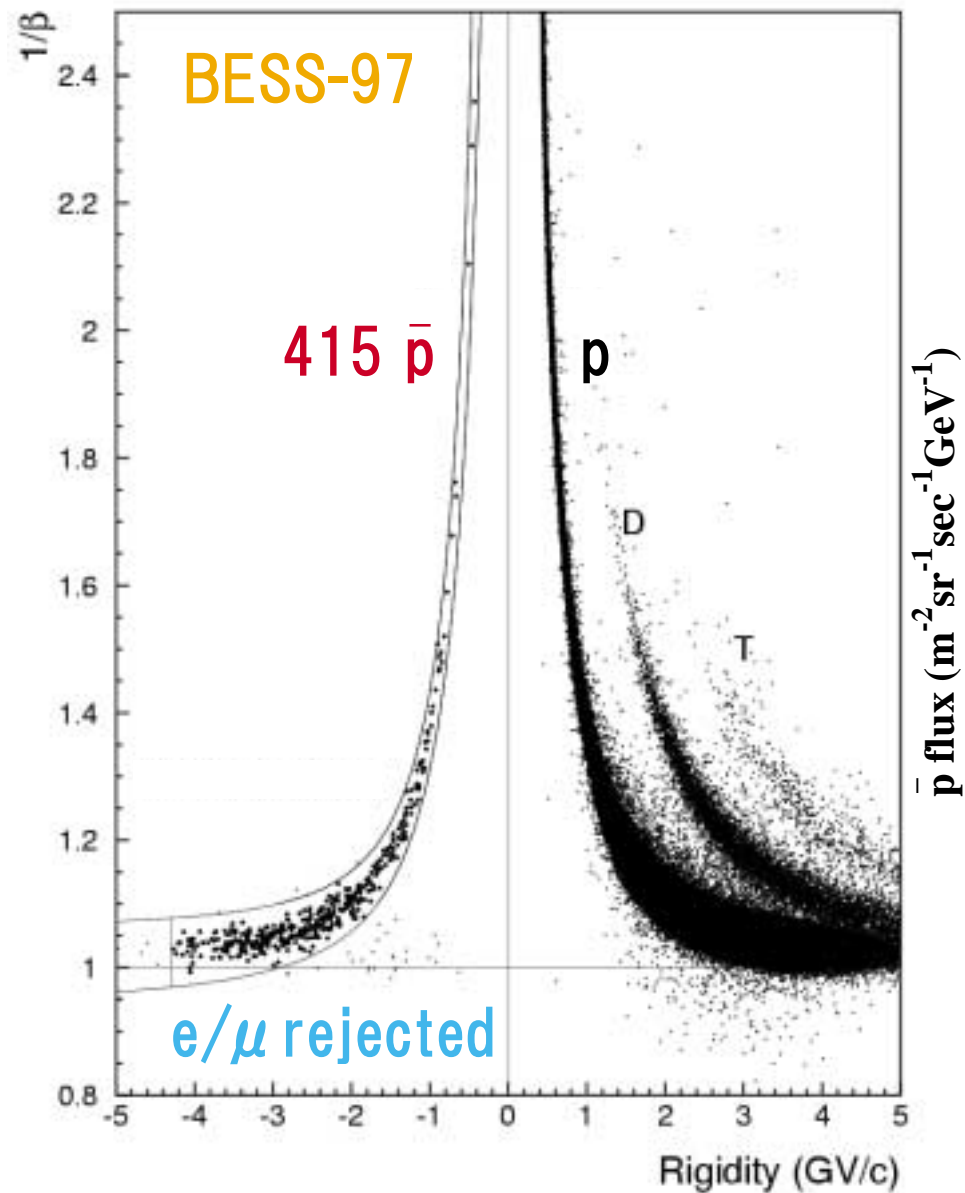


$$n=1.03 \Rightarrow n=1.02$$

- produced photon: $\sim 66\%$
- collected photo electron: $\sim 90\% \Rightarrow \text{Excellent Transparency}$

Antiproton Measurement (After Aerogel)

Secondary \bar{p} flux determined ($\pm 15\%$)



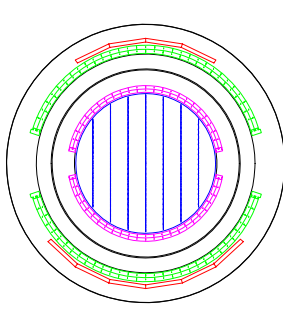
S. Orito et al, PRL, 2000.

Year by Year Improvement of the Detector

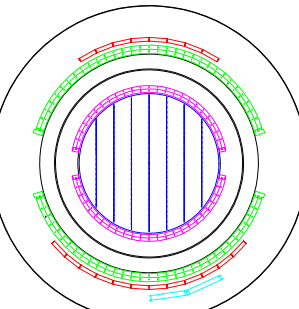
気球実験だからこそ可能！

TOF, JET, Solenoid
のConceptは維持

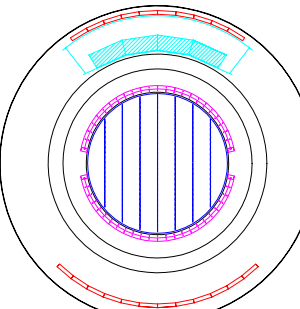
BESS-93,94



BESS-95

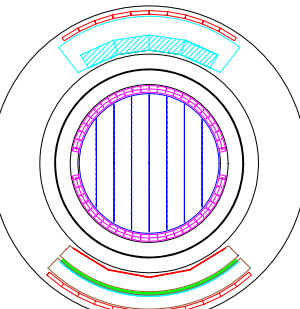


BESS-97,98



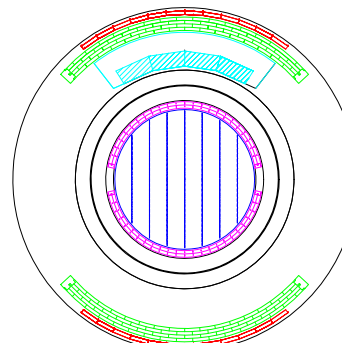
AMS Technical Flight

BESS-99,00

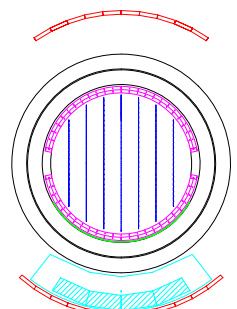


⇒ Future

BESS-TeV



BESS-Polar



Larger Vessel

$$\sigma_{\text{TOF}} = 300 \text{ ps}$$

$$\sigma_{\text{TOF}} = 110 \text{ ps}$$

$$\sigma_{\text{TOF}} = 70 \text{ ps}$$

Aerogel C

97 $n=1.03$
 $\bar{p} 0.2-3.5 \text{ GeV}$
98 $n=1.02$

$$\bar{p} 0.2-0.6 \text{ GeV}$$

$$\bar{p} 0.2-1.4 \text{ GeV}$$

$$\bar{p} 0.2-4.2 \text{ GeV}$$

Shower Counter

2X₀ Lead
 e/μ sep.

$$\bar{p} 0.2-4.2 \text{ GeV}$$

6, 2

43

415, 398

668, 558

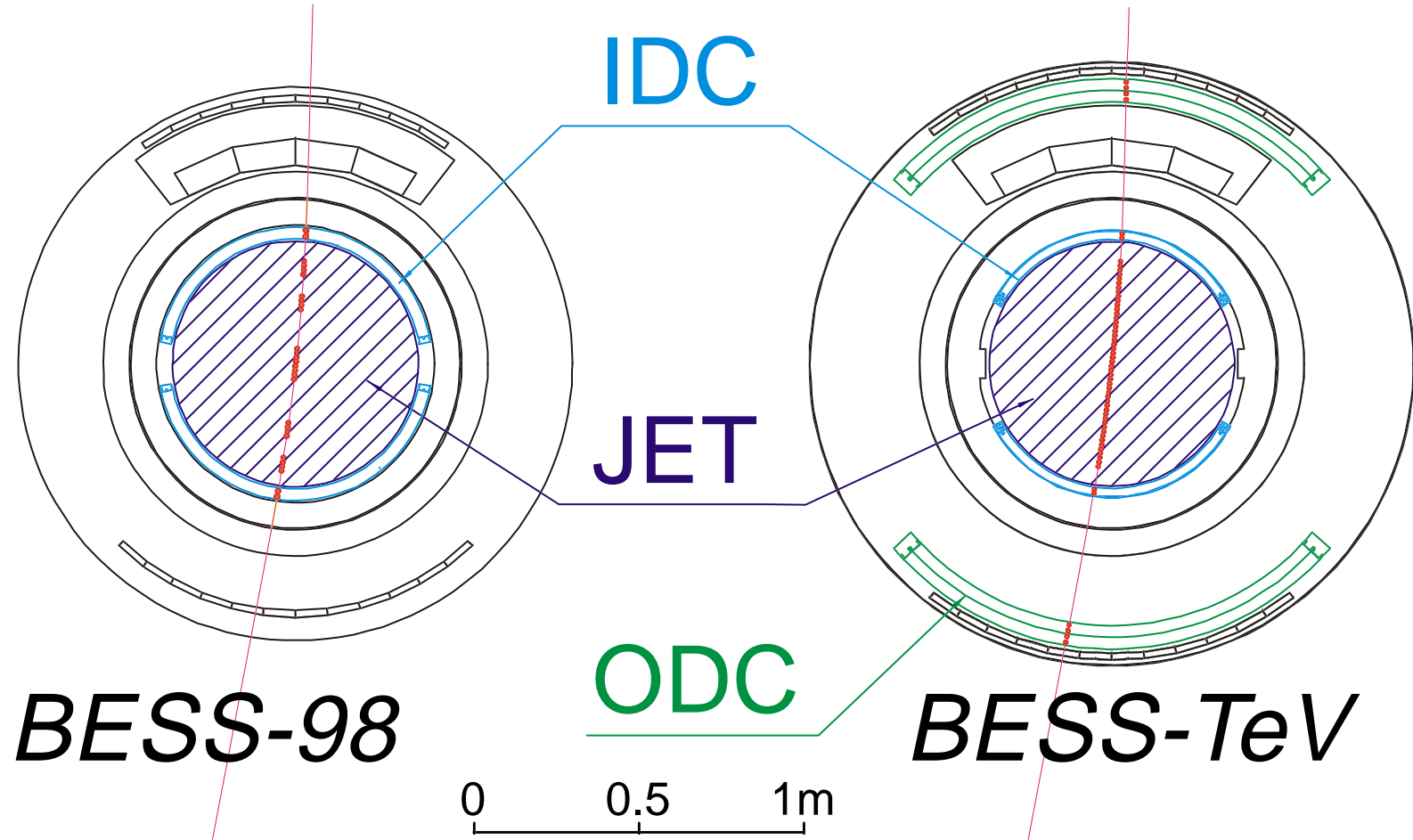
p/He up to 1 TeV

$$\bar{p} 0.2-4.2 \text{ GeV}$$

$$\bar{p} 0.1-4.2 \text{ GeV}$$

↔ No. of \bar{p} 's

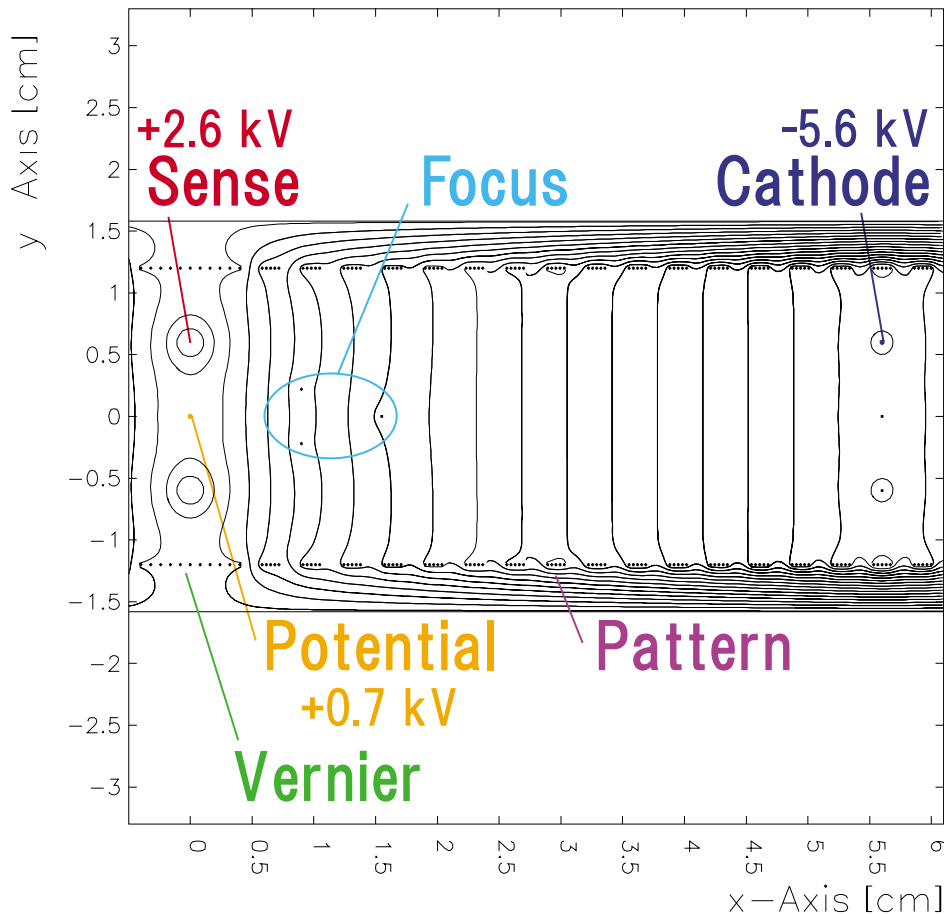
BESS TeV Project



- ODC \Rightarrow track length X 2
- 位置resolution 向上 (New Chambers) \Rightarrow MDR > 1 TeV (現 200 GeV)
P/He up to 500 GeV
+ lead μ^- up to 500 GeV
- 測定点增加 (28 \rightarrow 60)

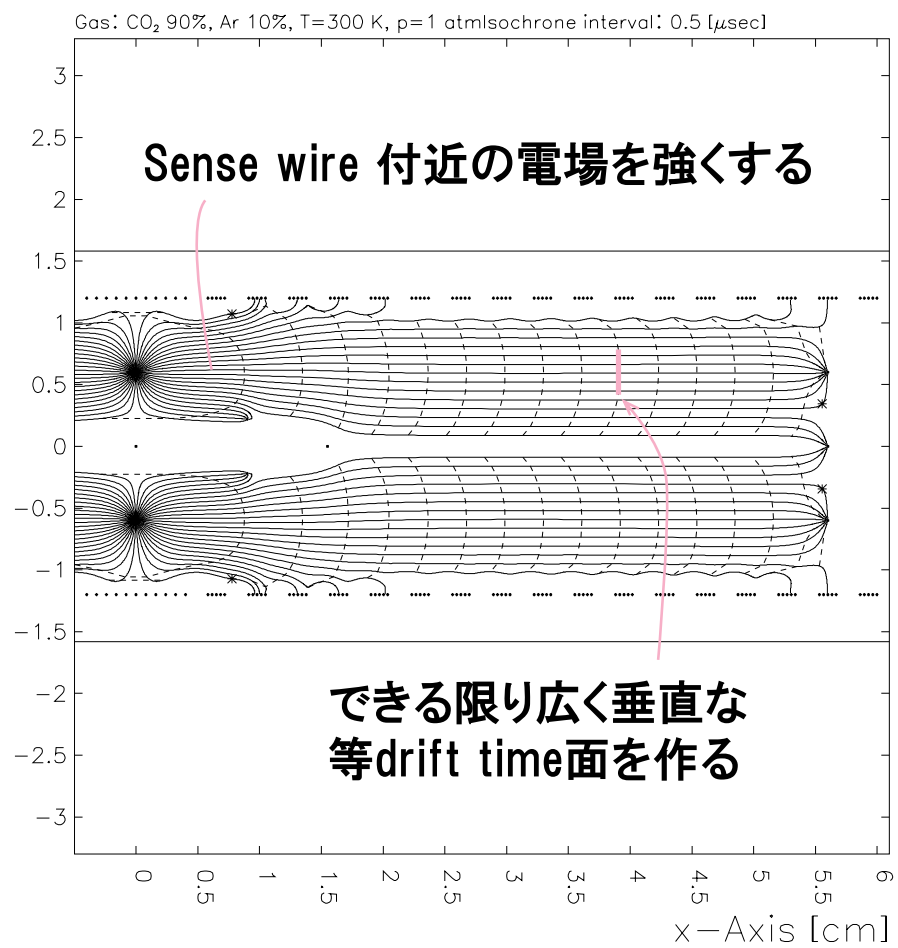
Cell Design using garfield

Contours of V



Plotted at 22.32.59 on 07/04/00 with Garfield version 6.33.

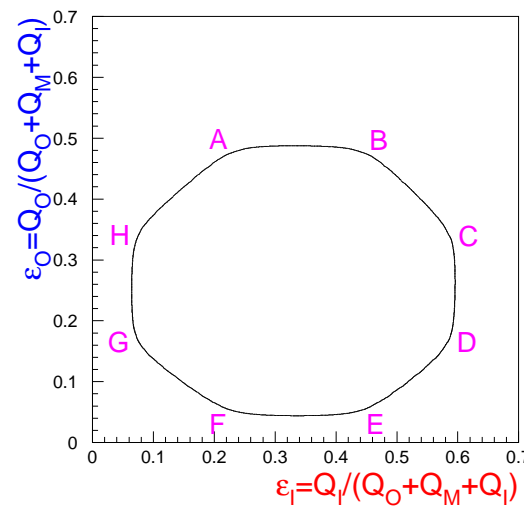
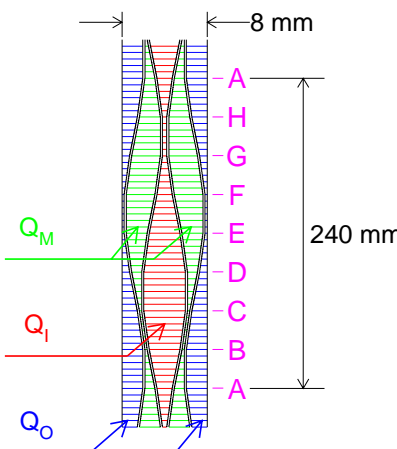
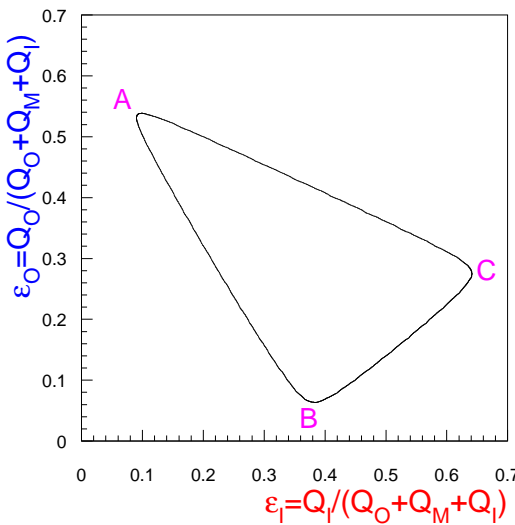
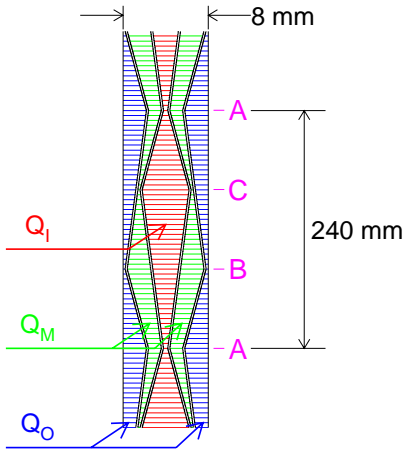
Electron drift lines



Plotted at 22.55.37 on 07/04/00 with Garfield version 6.33.

- Garfield による signal simulation を用いた optimization
- 現 IDC による simulation の妥当性の評価

Vernier strips



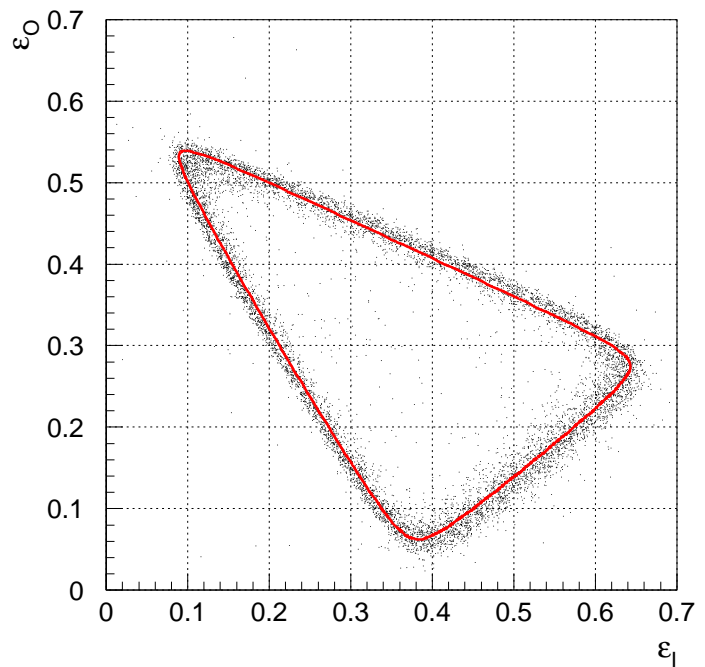
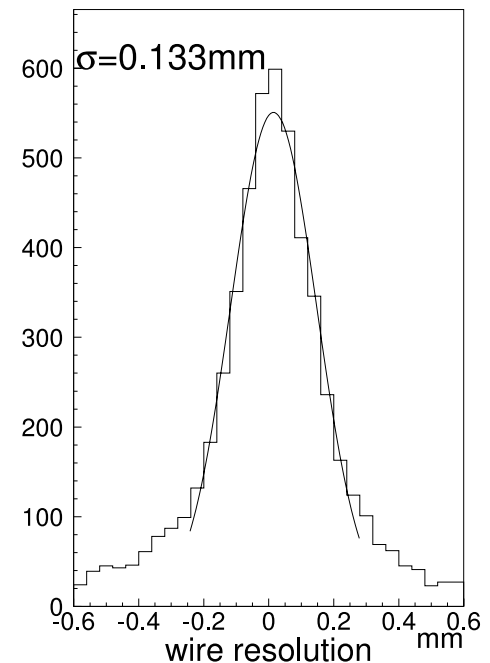
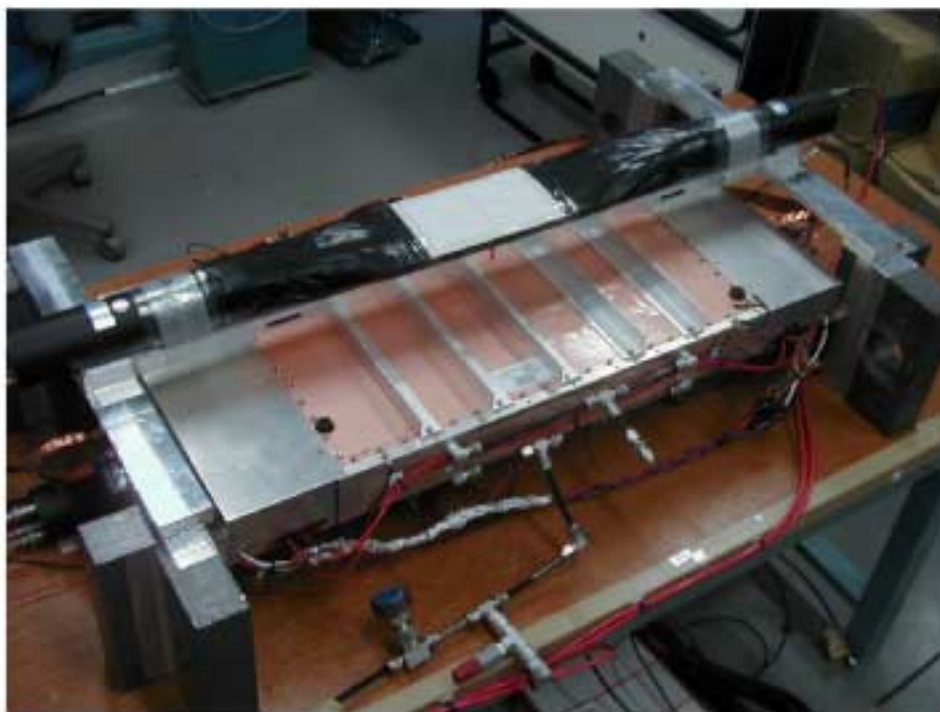
- 各パターンの charge の比
⇒ 周期的な z 座標の測定

- 3 vernier
↔ 現 IDC: 2 vernier

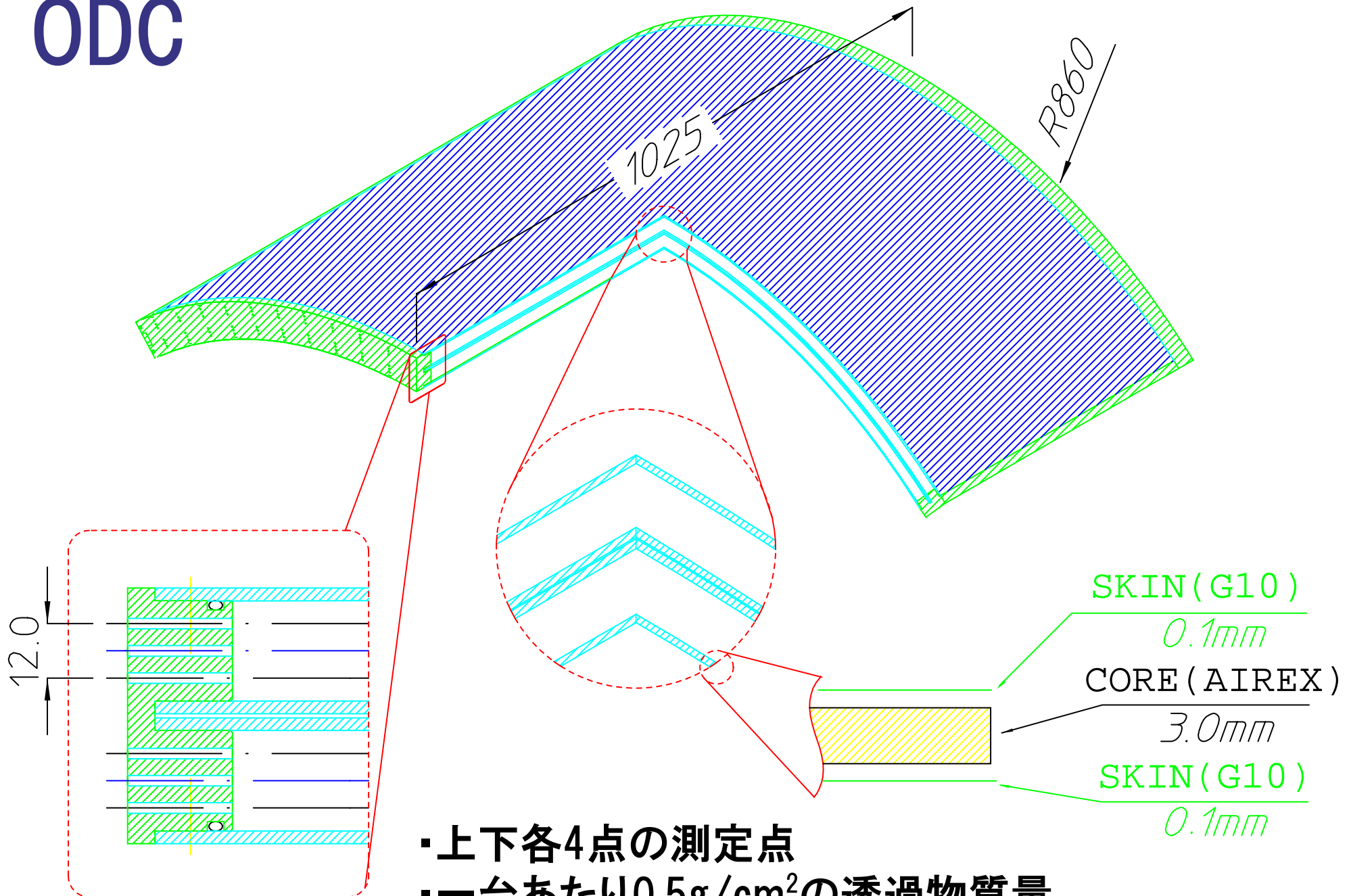
- 周期/位相を変えて z 座標
を解く

Prototype (R&D)

- Performance (cosmi)
 - r- ϕ : <150 μm
 - z : $\sim 1 \text{ mm}$ の resolution
- Feasibility
 - gas seal/ HV まわり/
 - 組み立て/ Elec mount/ etc.



ODC



- ・上下各4点の測定点
- ・一台あたり $0.5\text{g}/\text{cm}^2$ の透過物質量
- ・ $\text{CO}_2(90\%), \text{Ar}(10\%)$ の混合ガス

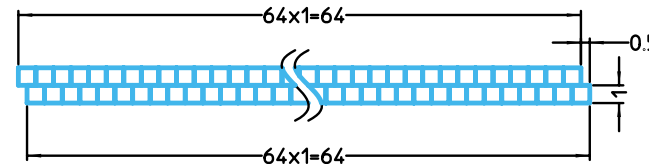
Scintillation Fiber

目的:

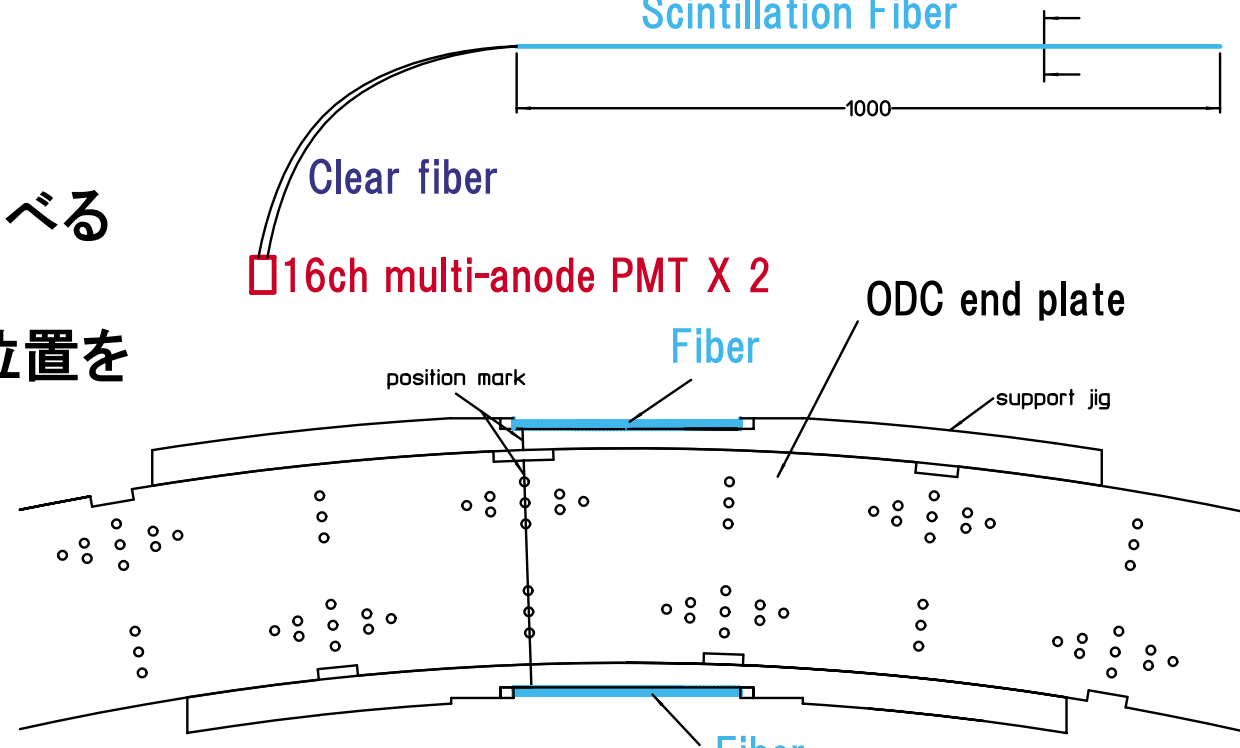
ODC x-t relation の
absolute calibration
を正確に行なう
⇒ TeV へのカギ

- 64本のfiberを2層並べる
- それぞれのfiberの位置を
顕微鏡で測定
- ODC 1 cell の
上下に配置
- Trigger に組み込む

Cross Sectional View

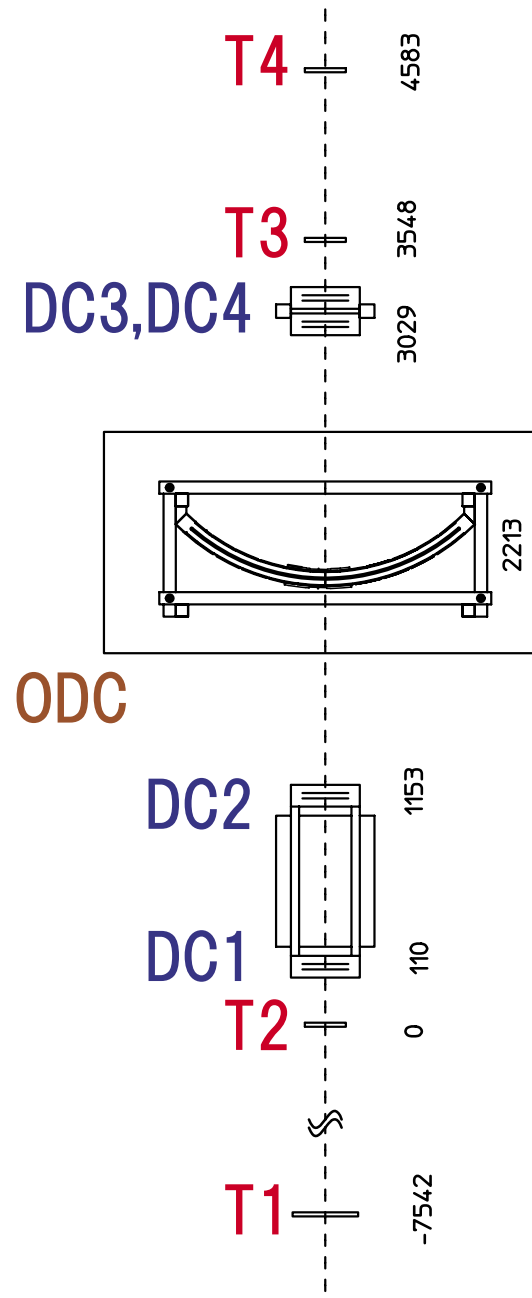


Scintillation Fiber



ODC Beamtest

@ π 2 KEK-PS 2000年12月

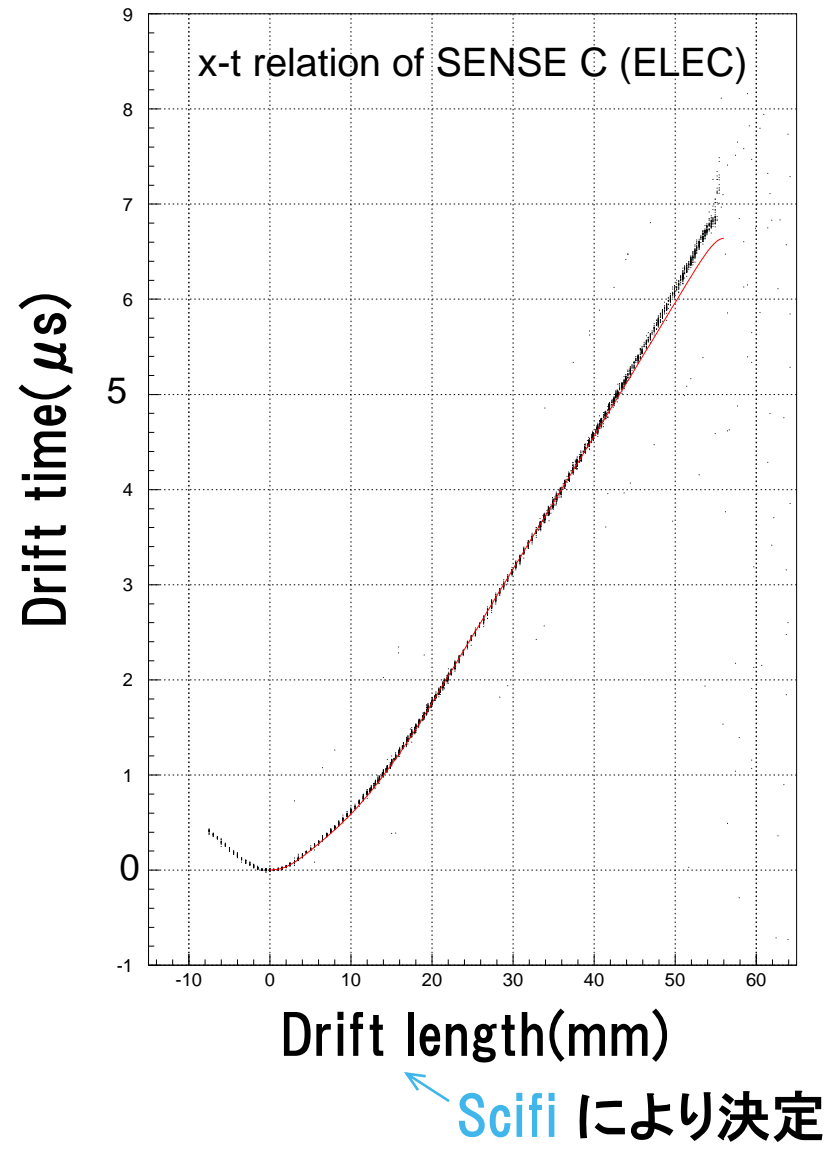
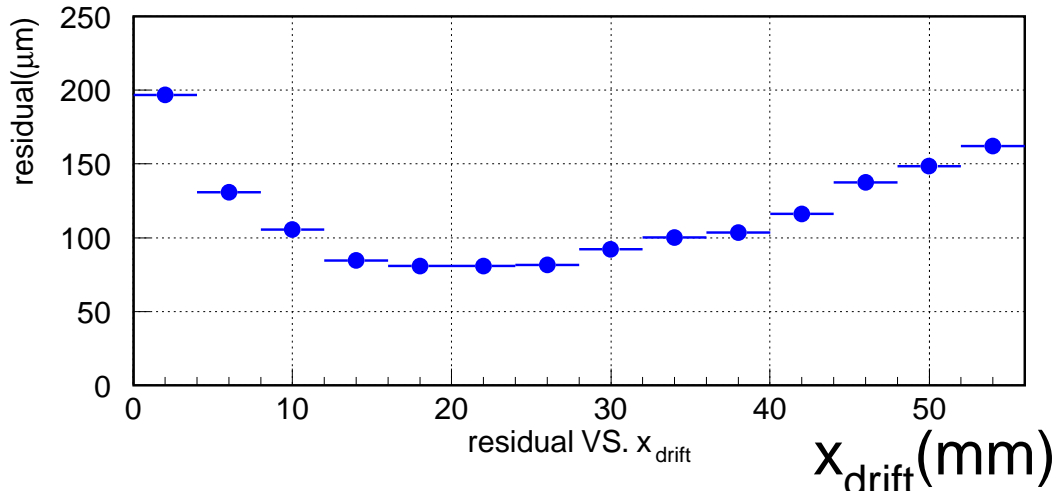
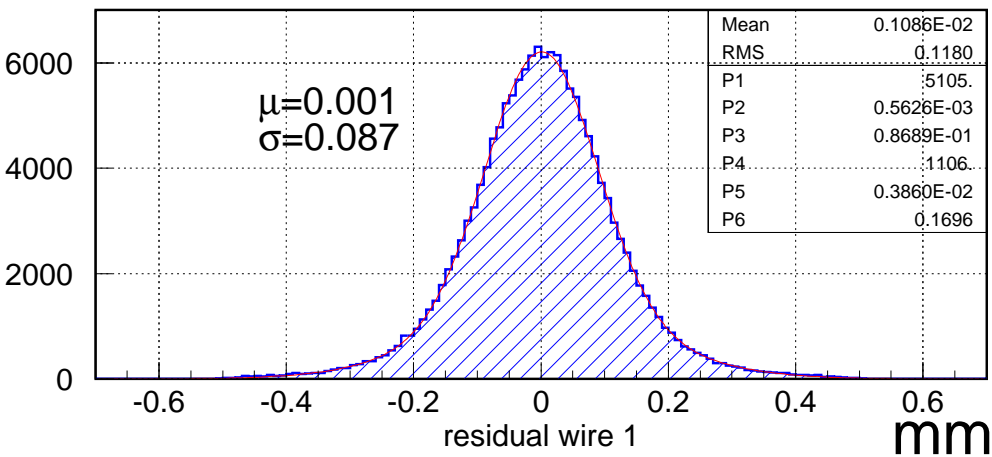


- ・完成直後
- ・串刺し実験
- ・少人数

- 性能評価
- ・resolution
 - ・X-t relation

ODC Beamtest Results

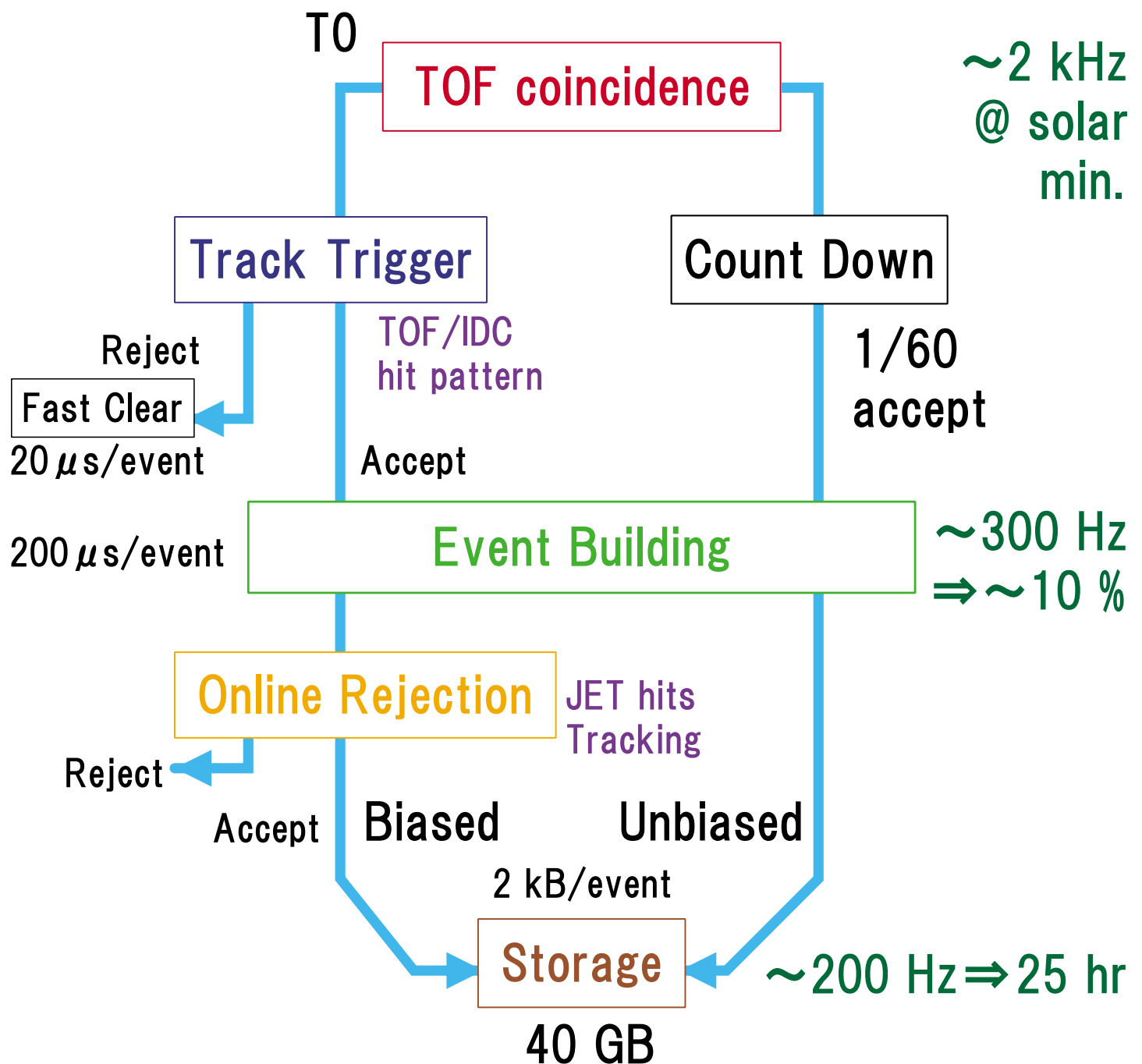
- X-t relation を **Scifi** により決定
- near sense $\sim 200 \mu\text{m}$
- central region $< 100 \mu\text{m}$ を達成



Trigger System

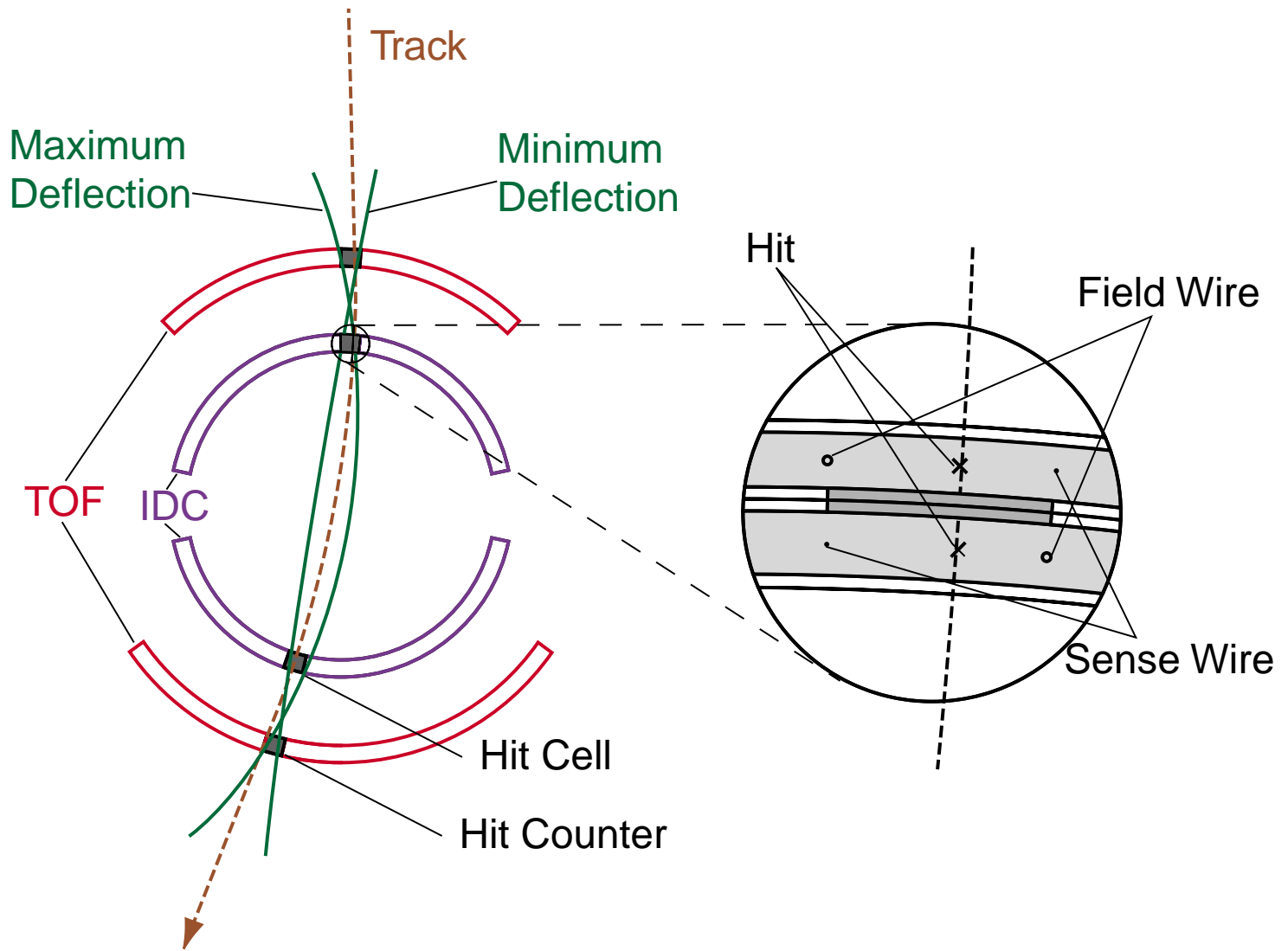
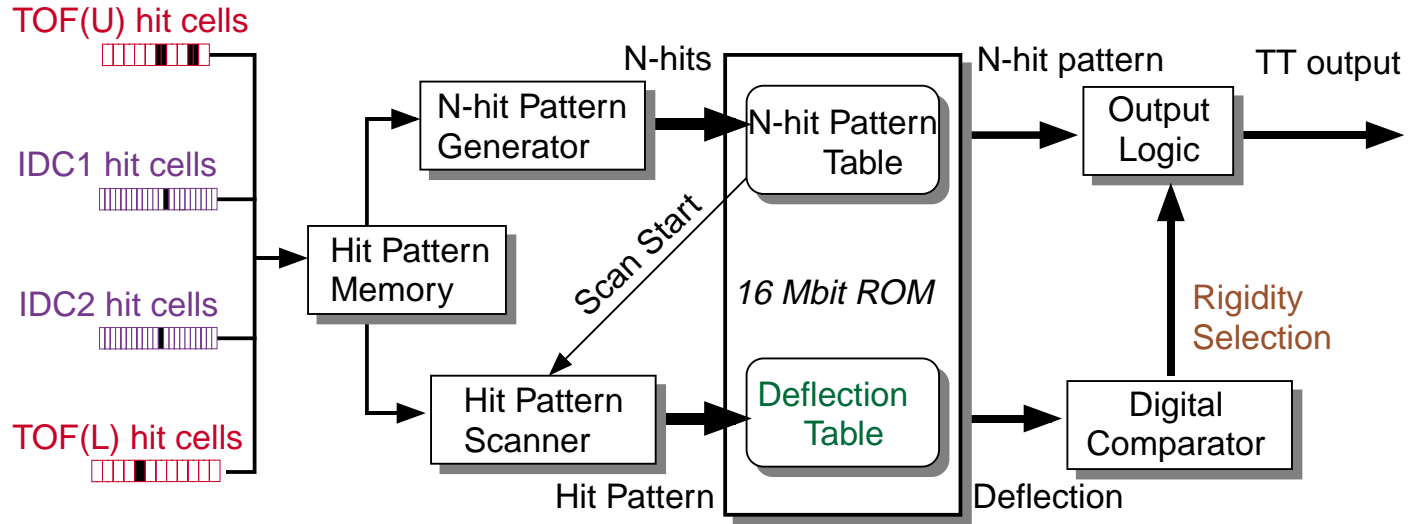
Flight Time, Data Capacity を有効に利用するために、2つの mode がある。

Unbiased ... Proton/Junk
Biased ... negative charge



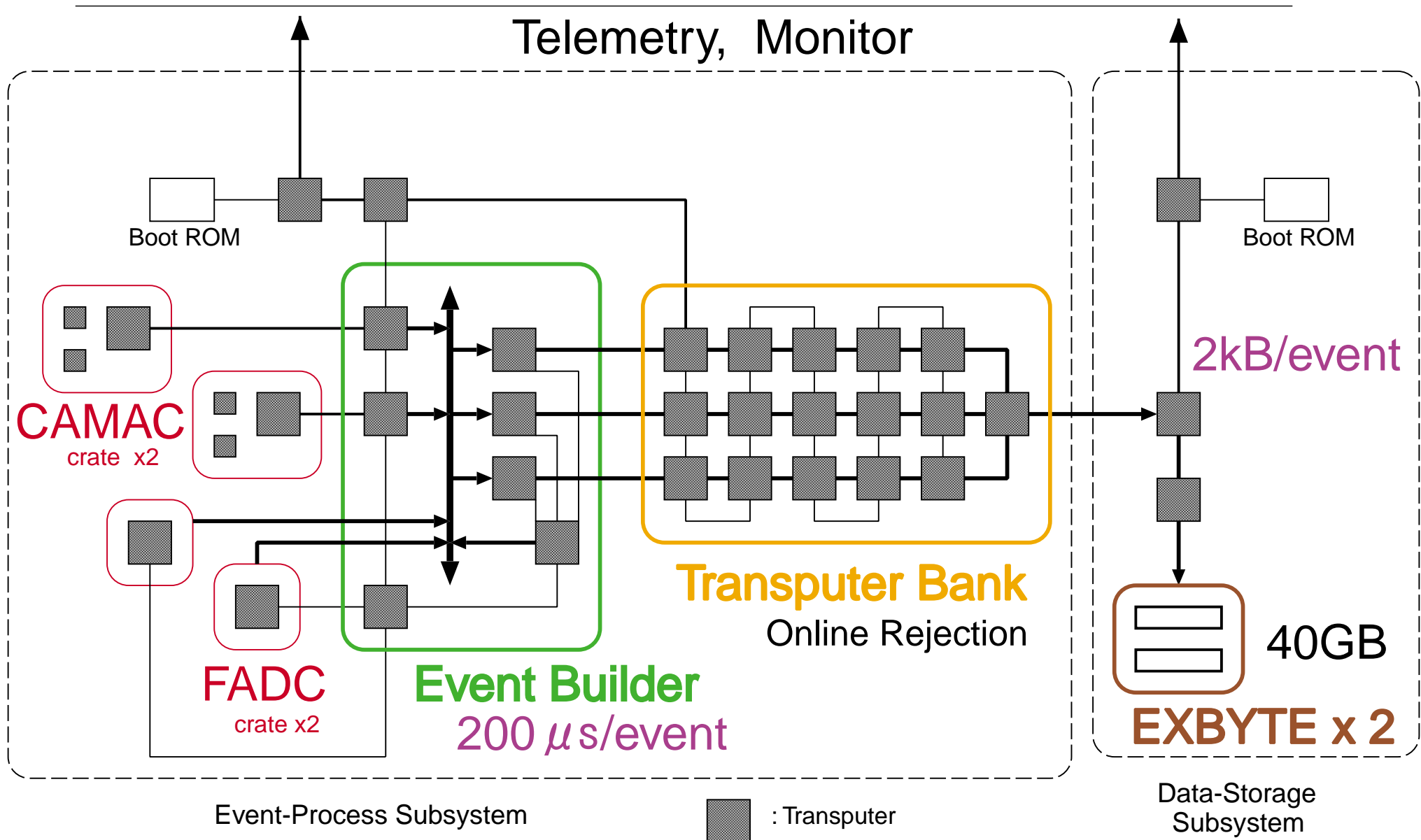
Track Trigger

Hit pattern selection / Rough rigidity selection



Data Acquisition

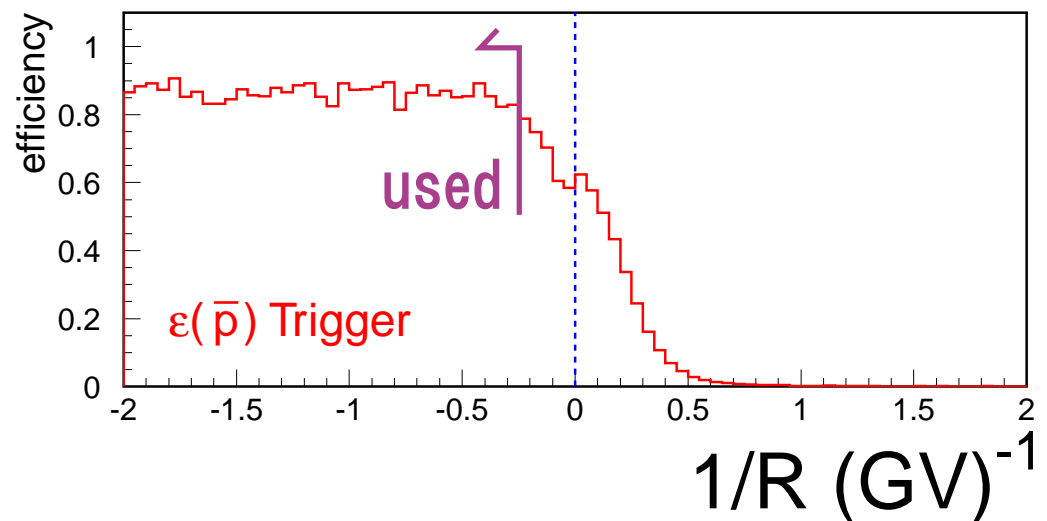
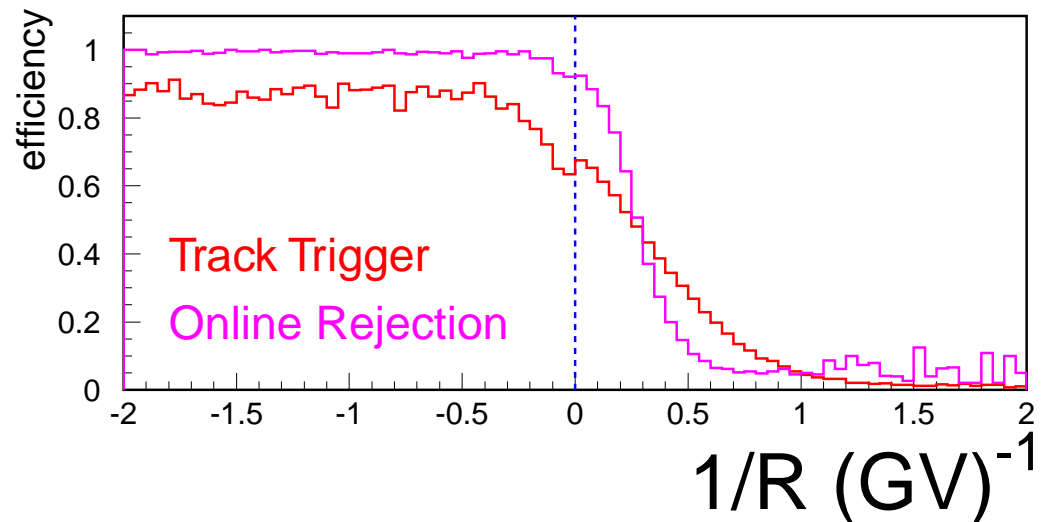
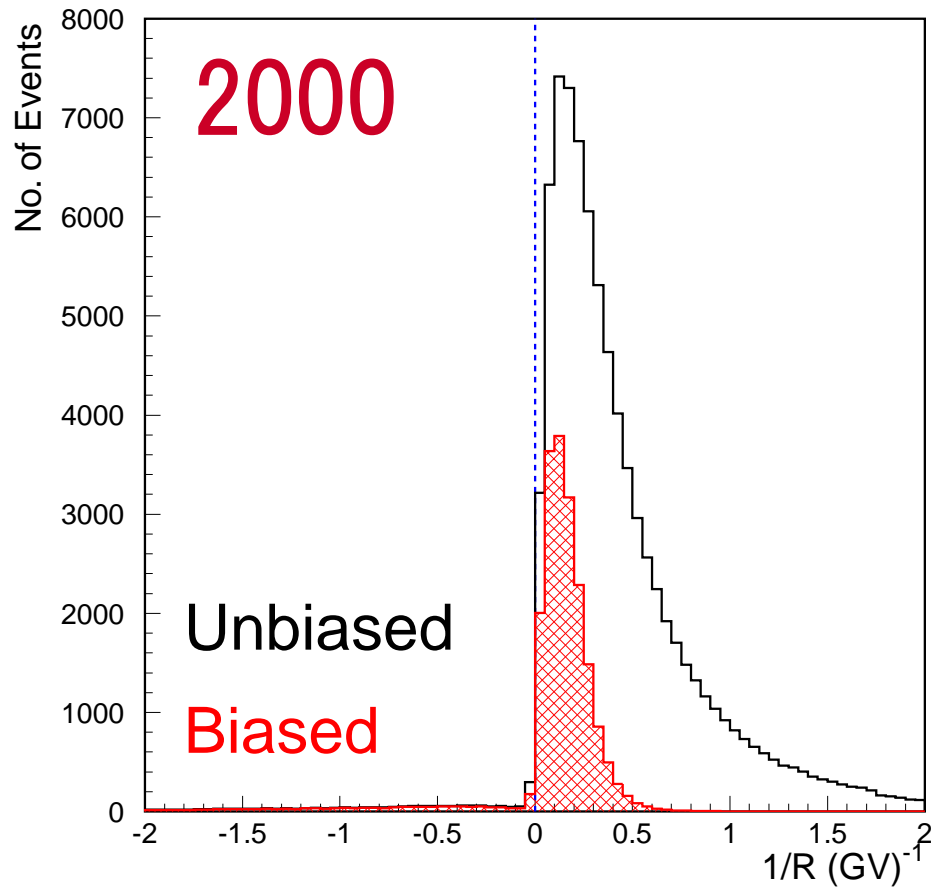
Dead Time Fraction, Data Capacity



Trigger Mode for Antiproton

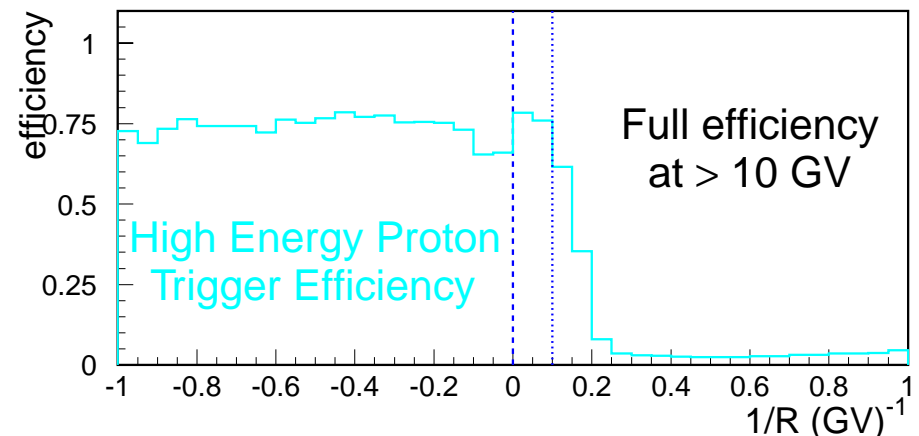
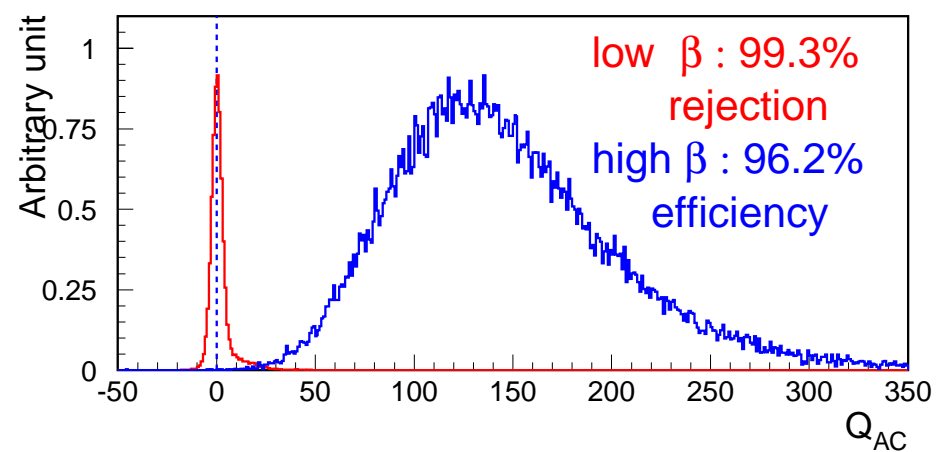
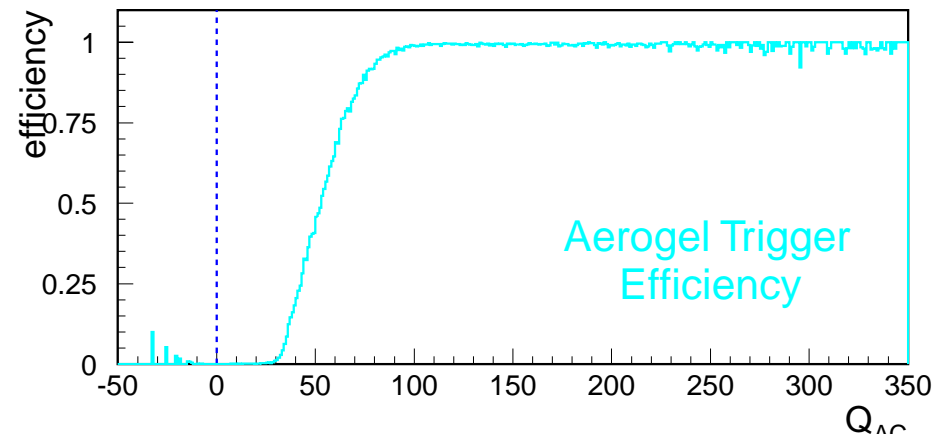
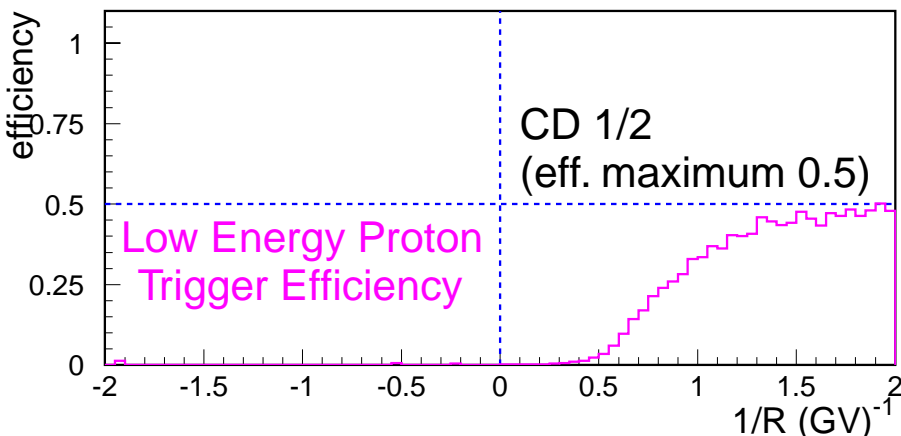
- eff. for high energy \bar{p}
- rej. of high energy p

⇒ Optimization

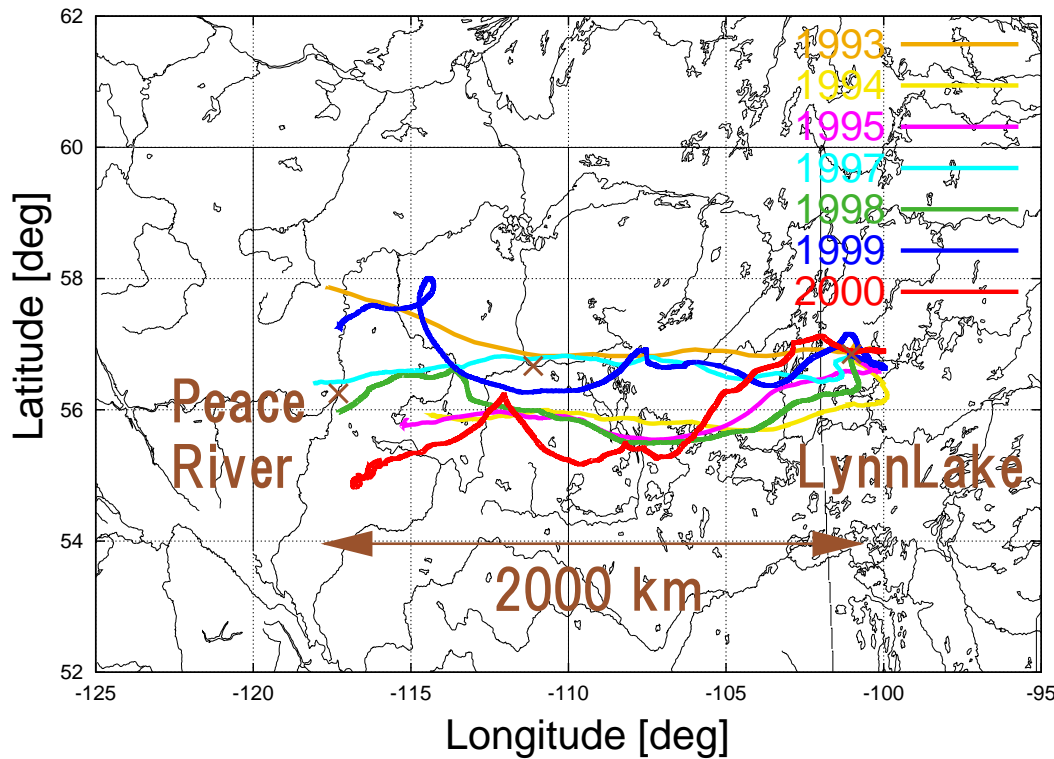


Other Trigger Modes

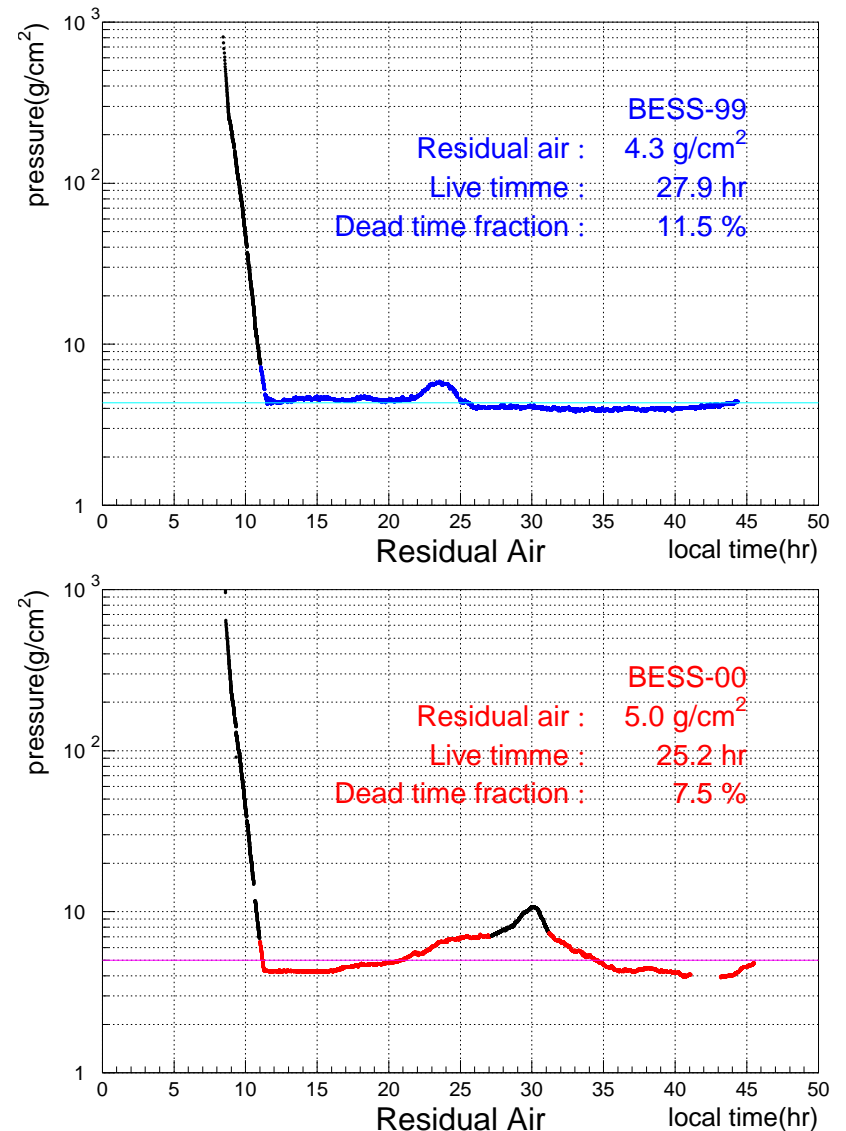
- **Aerogel Trigger**
 - High energy proton
Sanuki et al, ApJ, 2000.
 - e/μ
- **Low Energy Proton (ascent)**
 - atmospheric growth
- **High Charge (TOF)**
- **Filght 時間と Trigger Rate を予測し tune する.**
38/41/40 GB (98/99/00) exabytes.



Balloon Flights



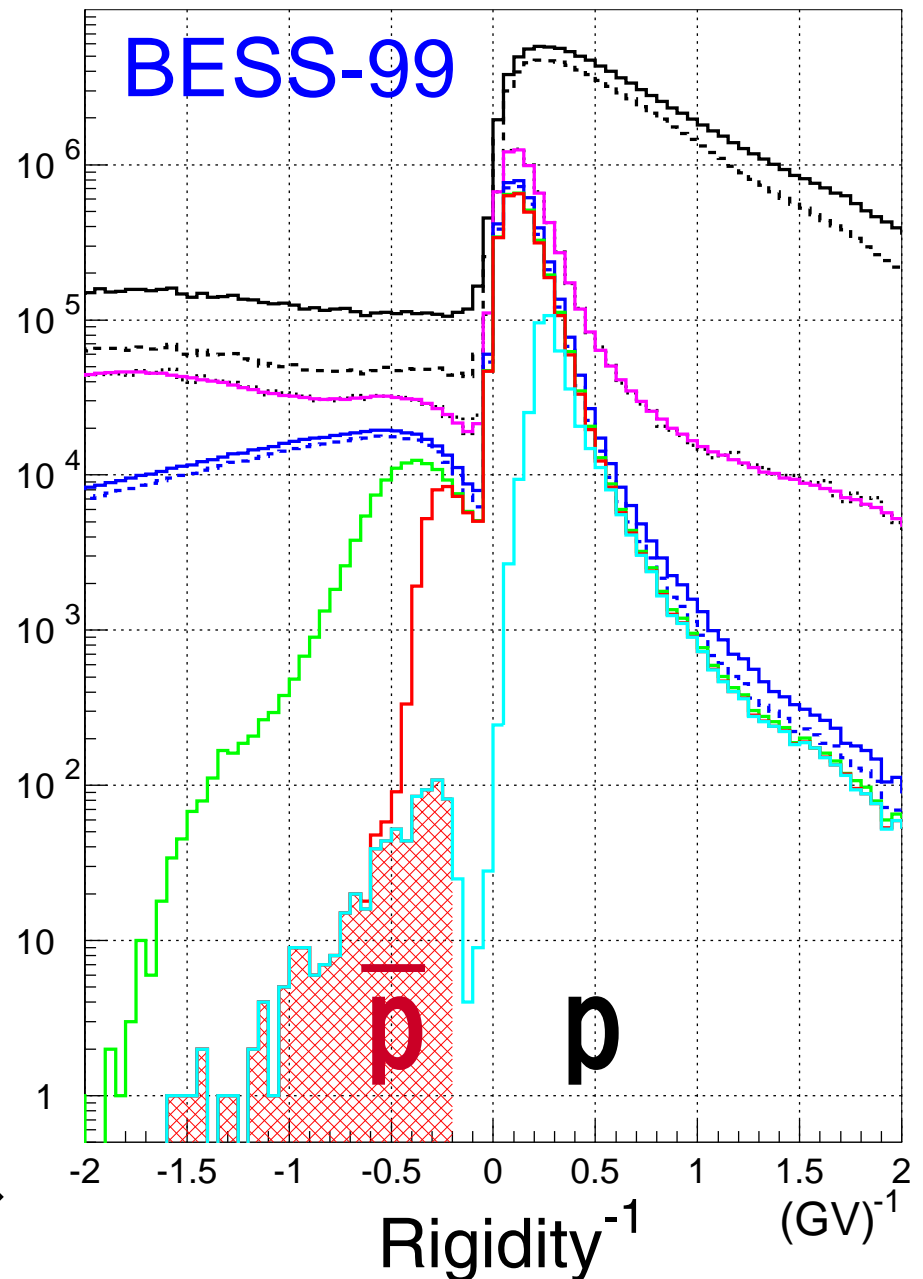
- LynnLake, Manitoba, Canada
low geomagnetic latitude
(cutoff rigidity $0.3\sim0.5$ GV)
- Floating altitude: $34\sim39$ km



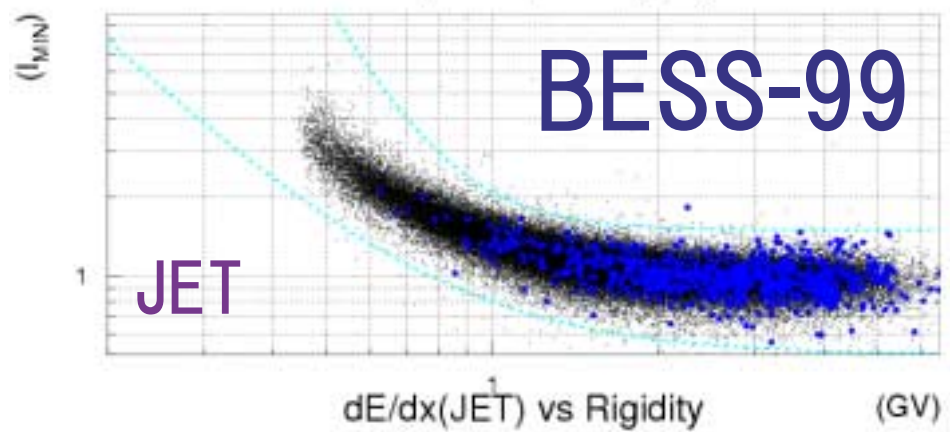
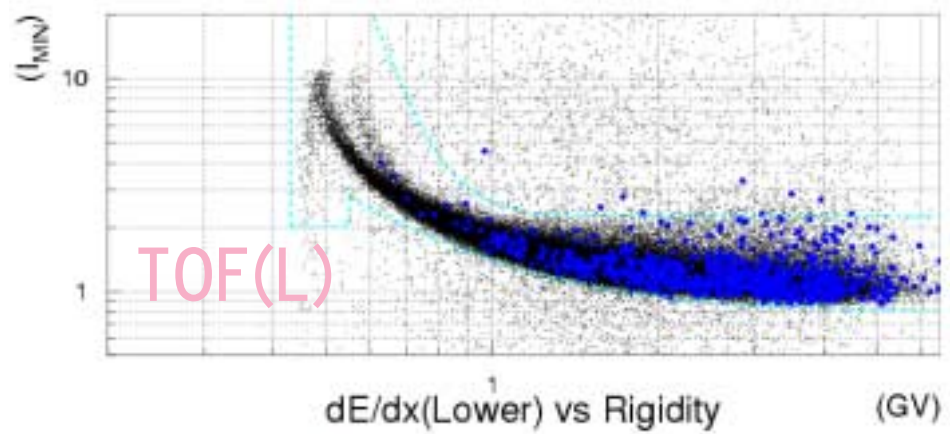
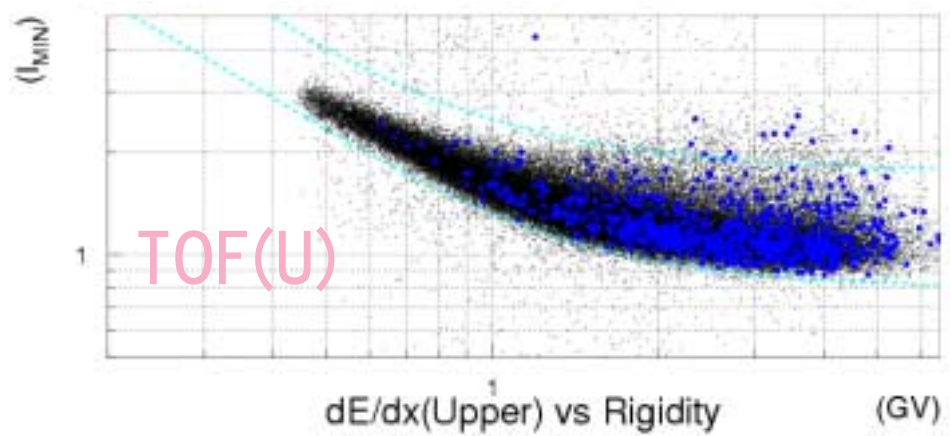
Event Reduction

1. first level trigger(TOF coincidence)
2. second level trigger
hit pattern & rigidity selection
3. fiducial volume cut
4. single particle selection
5. track quality cut
6. dE/dx cut
7. mass cut
8. aerogel Cherenkov veto

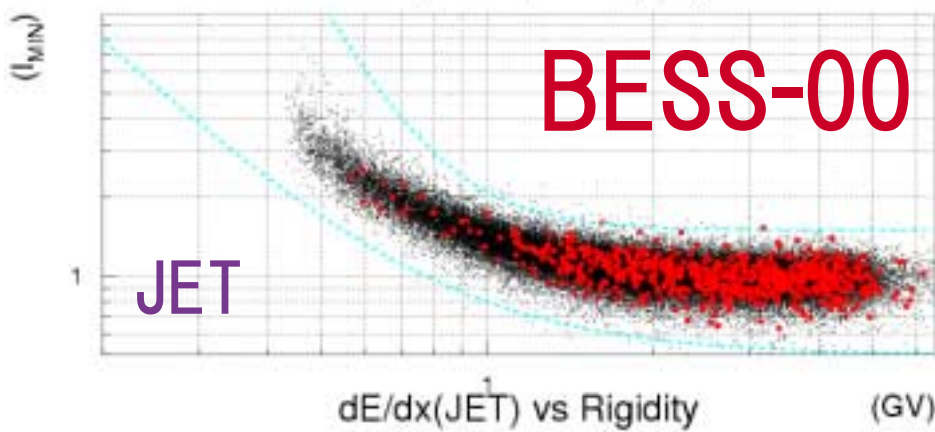
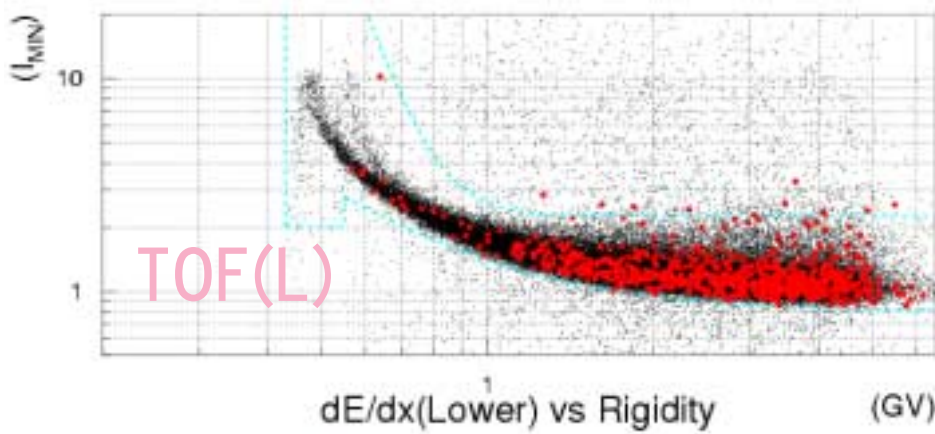
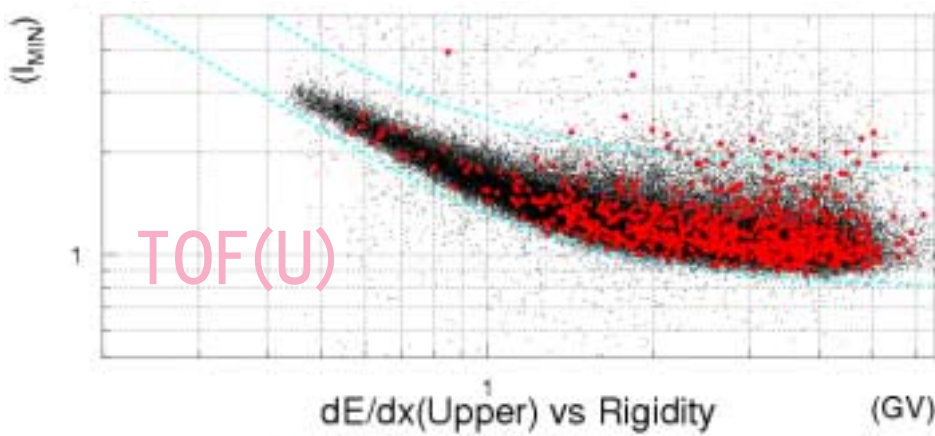
Rigidity = 運動量/電荷 \Rightarrow



dE/dx band cuts

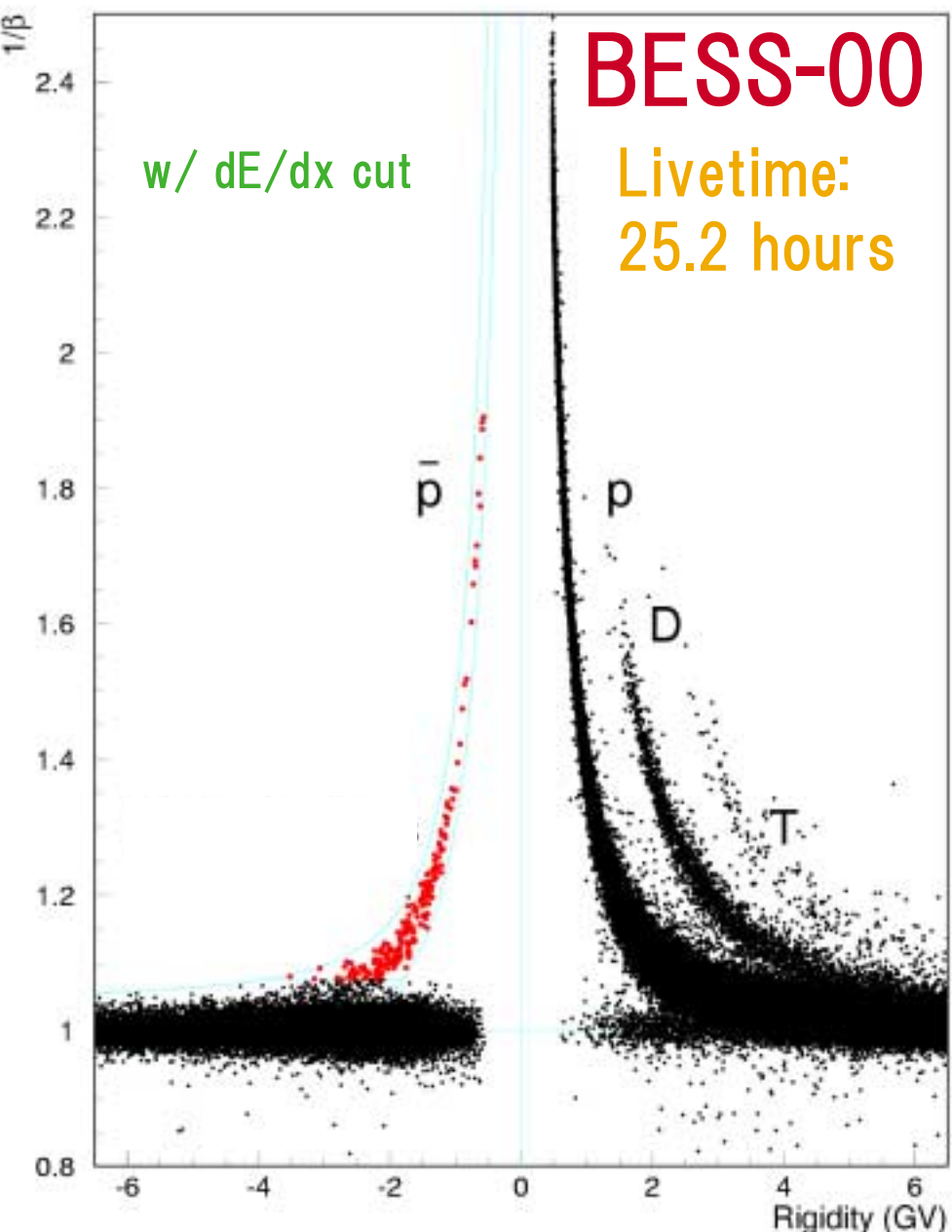
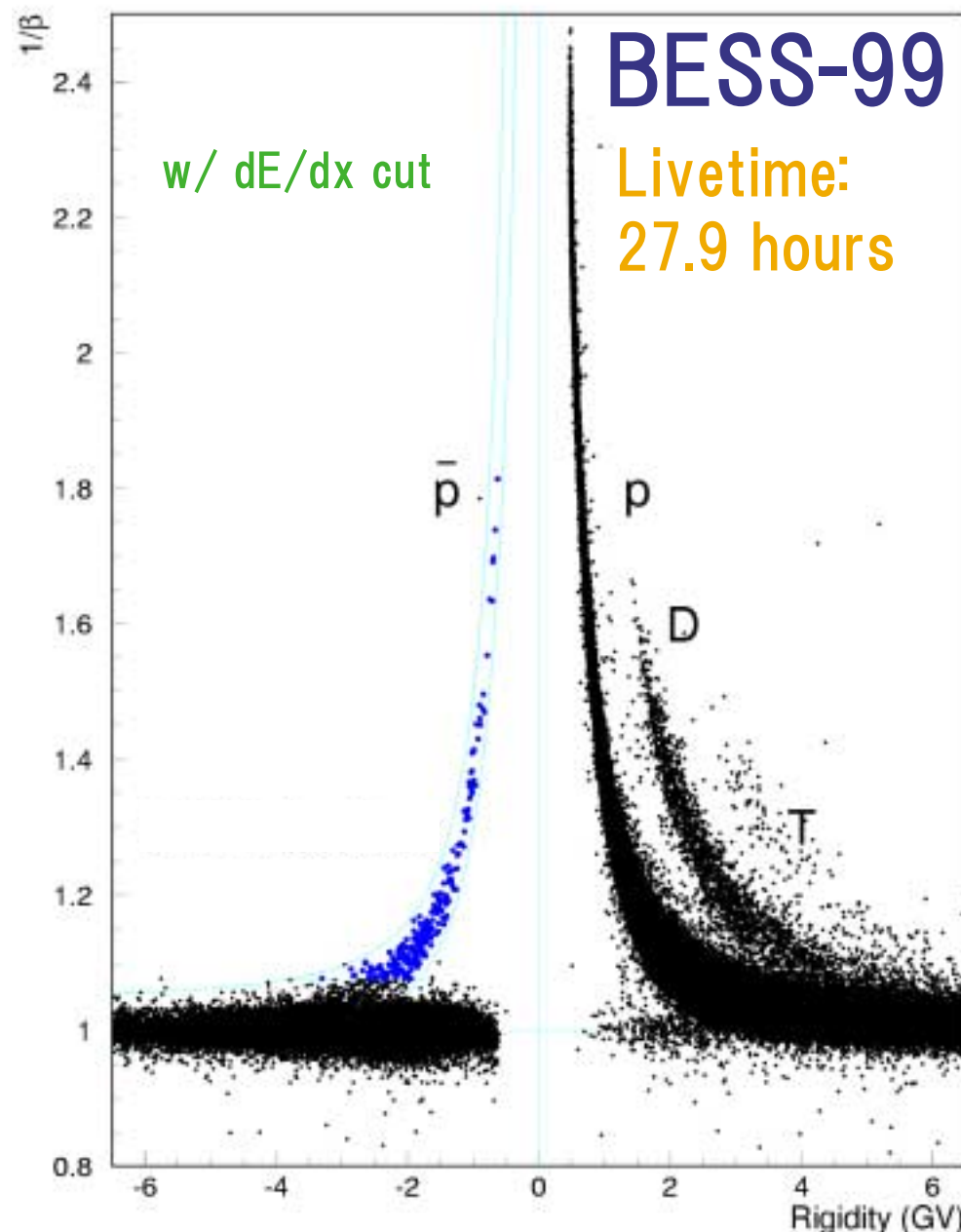


BESS-99

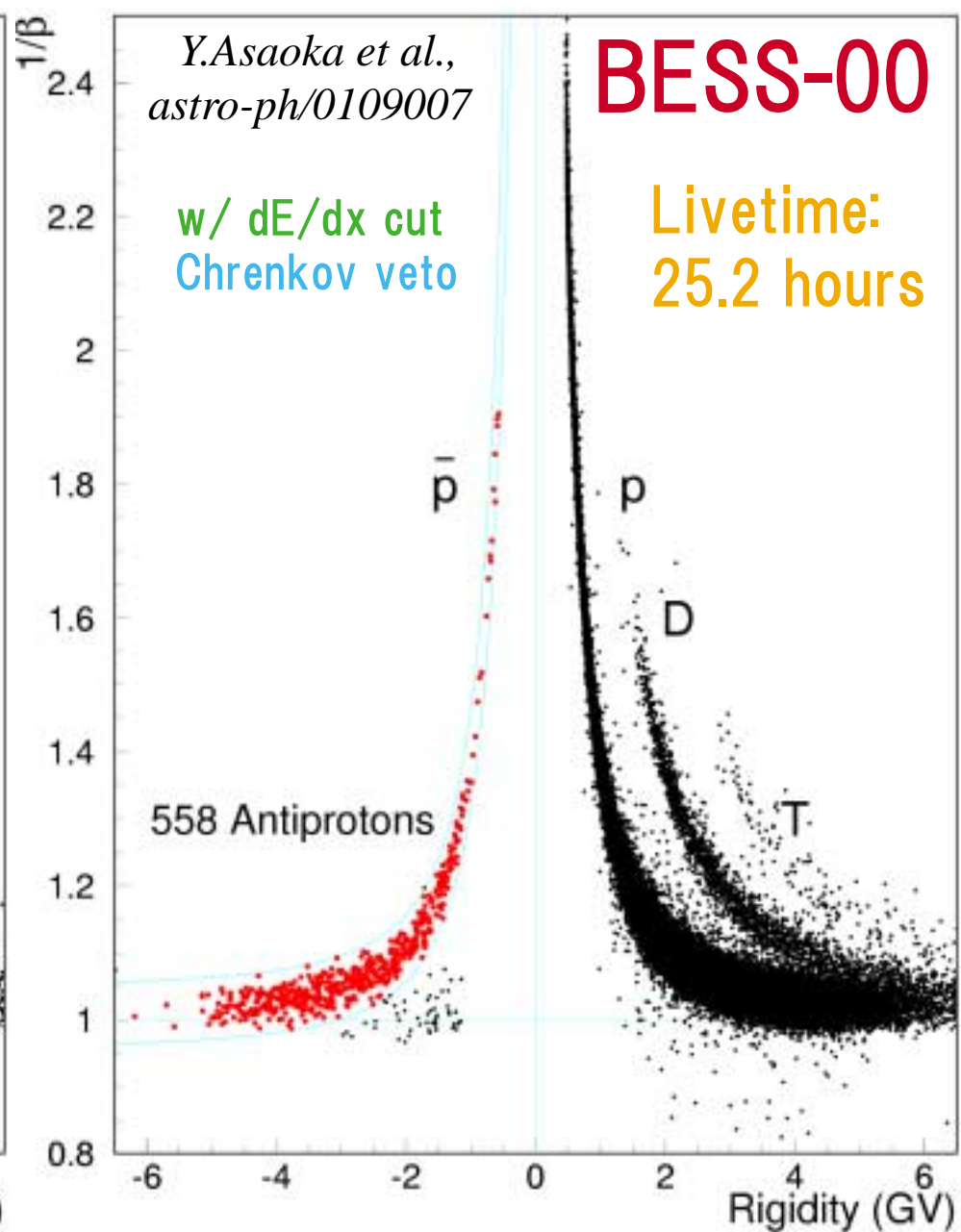
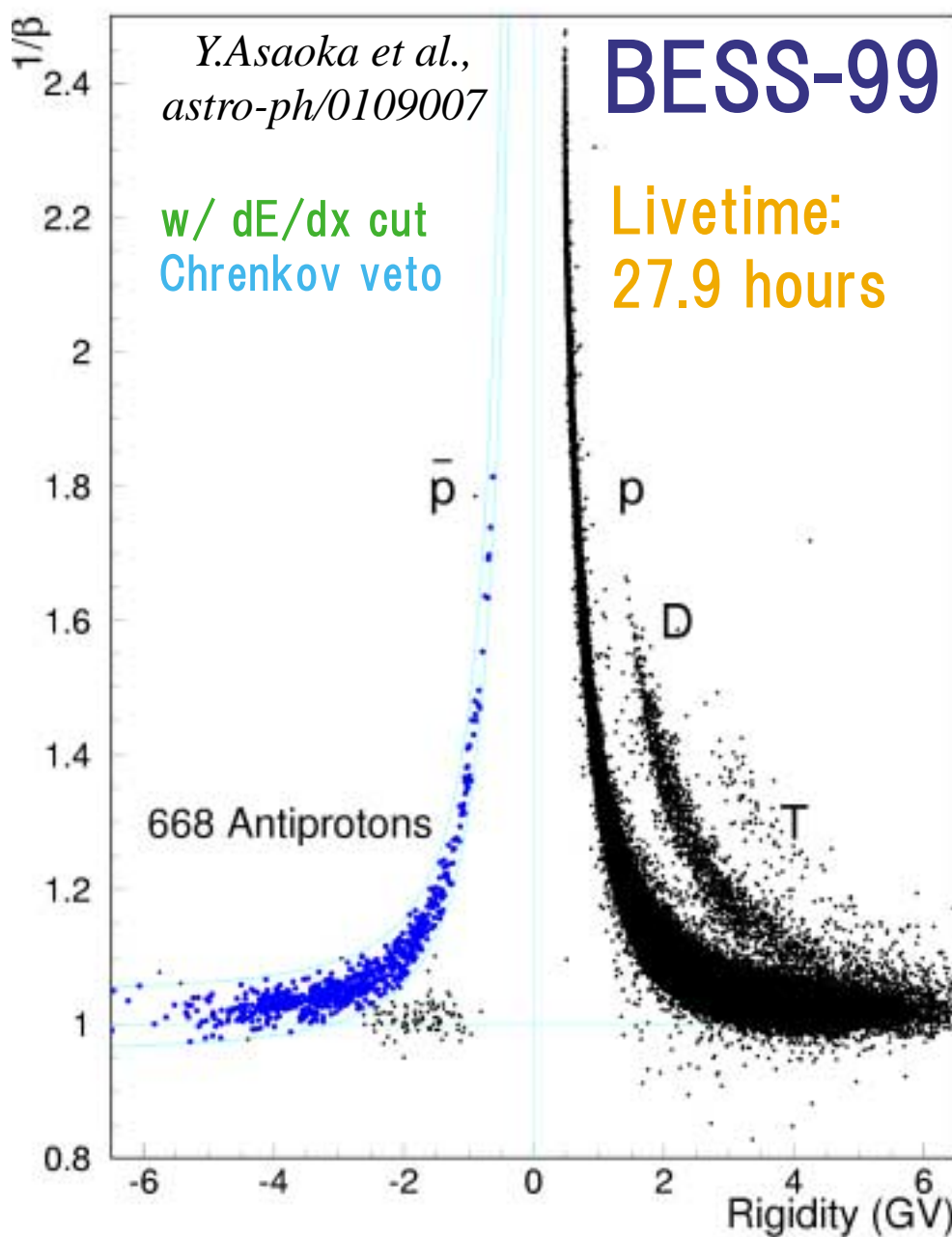


BESS-00

Antiproton Identification Plots



Antiproton Identification Plots

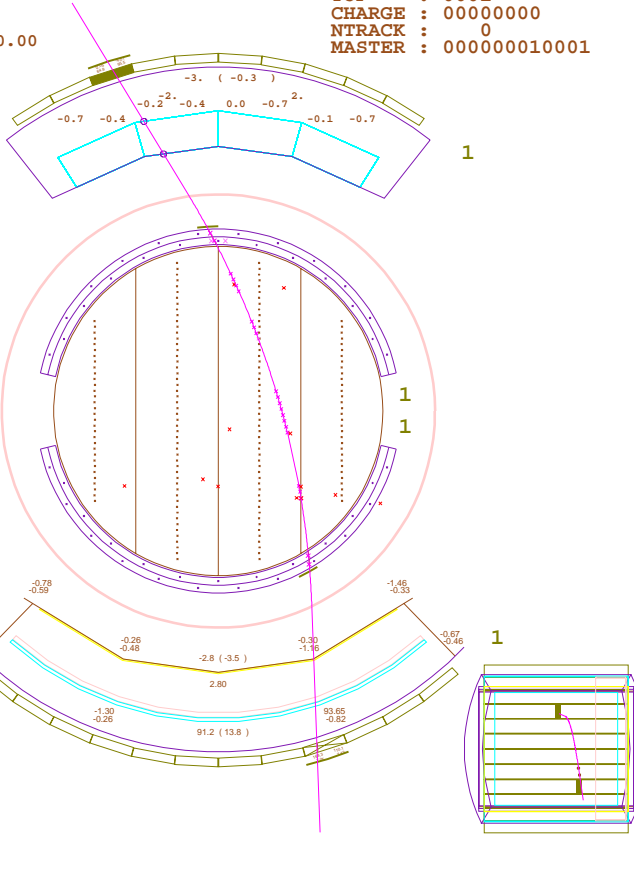


Event Display

/u/asaoka/exp30/evt/pb-5th.ntp
 Exp No: 30 Event No: 36111 Trigger : C5C50111 Event timing
 Run No: 8 CAMAC : 166 FADC : 760 003:36:56.8286

Ntk: 1 (Nex : 6)
 TID : 1
 Rigidity : -0.590
 1/Beta : 1.9008
 dE/dx(U/L/J) : 2.37/ 3.55/ 0.00
 Nht/Nsd : 19/20=0.95
 Nrf/Nzf/Ndr : 18/16/ 1
 Chi2-r(TK/JC) : 0.53/ 0.61
 Chi2-z(TK/JC) : 0.60/ 0.77
 DZ(U/L) : 10.6/ 20.4
 AZ(U/L) : -0.03/ 0.02

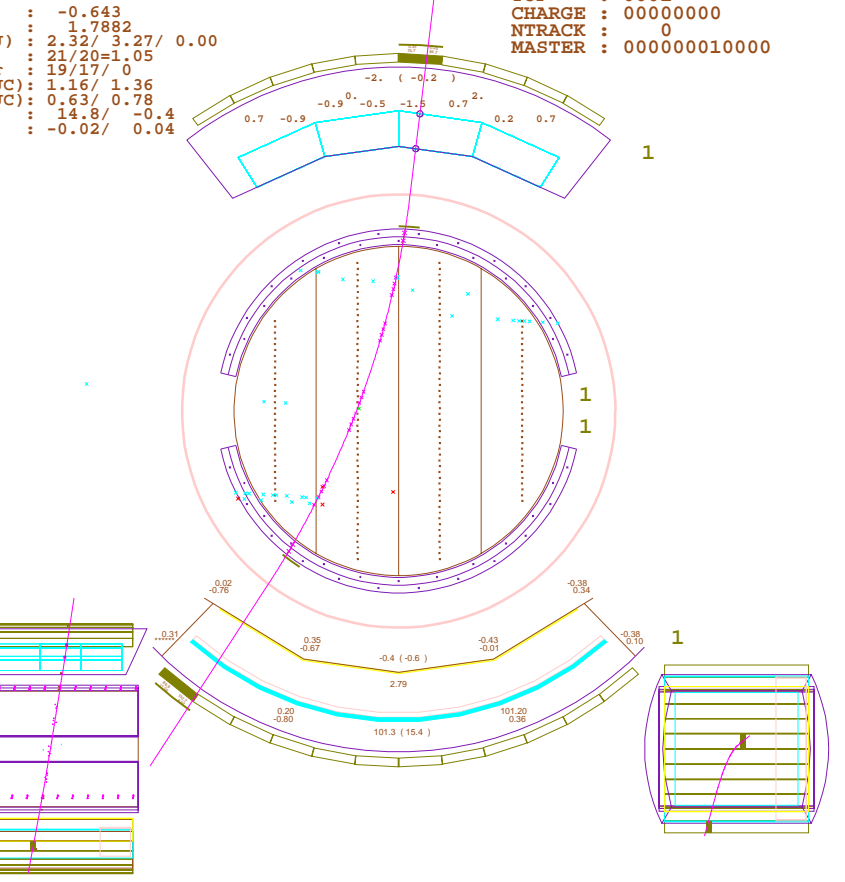
TOF : 0001
 CHARGE : 00000000
 NTRACK : 0
 MASTER : 000000010001



/u/asaoka/exp30/evt/pb-5th.ntp
 Exp No: 30 Event No: 500712 Trigger : 00000101 Event timing
 Run No: 14 CAMAC : 166 FADC : 1008 002:41:45.1479

Ntk: 1 (Nex : 2)
 TID : 1
 Rigidity : -0.643
 1/Beta : 1.7882
 dE/dx(U/L/J) : 2.32/ 3.27/ 0.00
 Nht/Nsd : 21/20=1.05
 Nrf/Nzf/Ndr : 19/17/ 0
 Chi2-r(TK/JC) : 1.16/ 1.36
 Chi2-z(TK/JC) : 0.63/ 0.78
 DZ(U/L) : 14.8/ -0.4
 AZ(U/L) : -0.02/ 0.04

TOF : 0001
 CHARGE : 00000000
 NTRACK : 0
 MASTER : 000000010000



Examples for BESS-00 Low Energy \bar{p} events

Absolute Flux Calculation

$$N(\bar{p}) = N_{\text{obs}} - N_{e/\mu} - N_{\text{atmos}}$$

$$J(\bar{p})dE = \frac{N(\bar{p})}{S \Omega \epsilon t}$$

Backgrounds

1. e/μ contamination

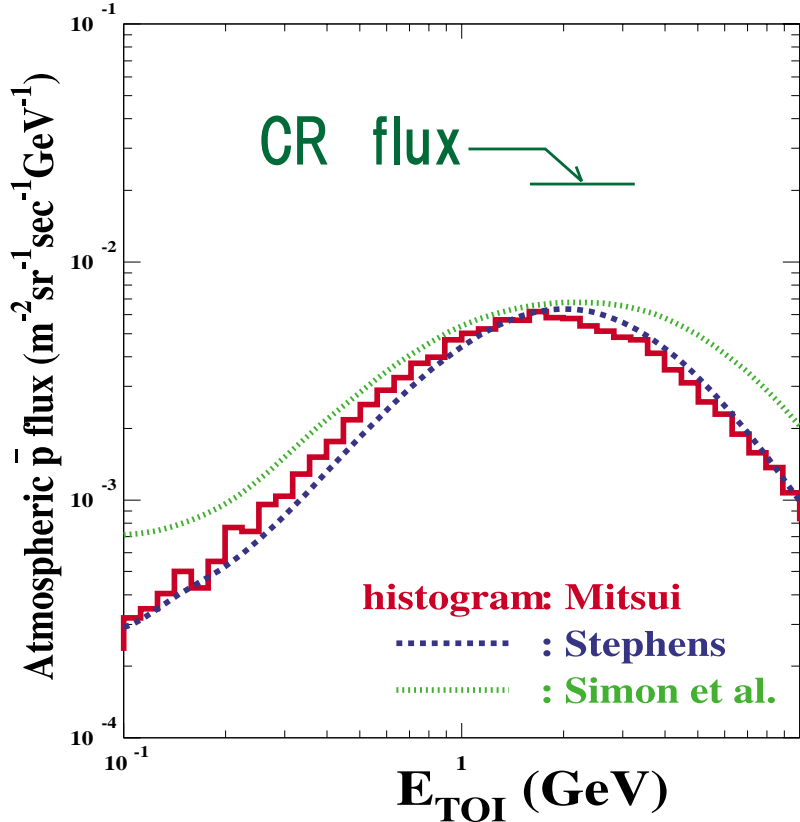
- Contamination < 5% (max. @ 4GeV)
- Aerogel rejection factor: ~4000

2. Atmospheric \bar{p} subtraction

- Subtraction < $25 \pm 7\%$ (syst.) (max. @ 2GeV)
- Calculations

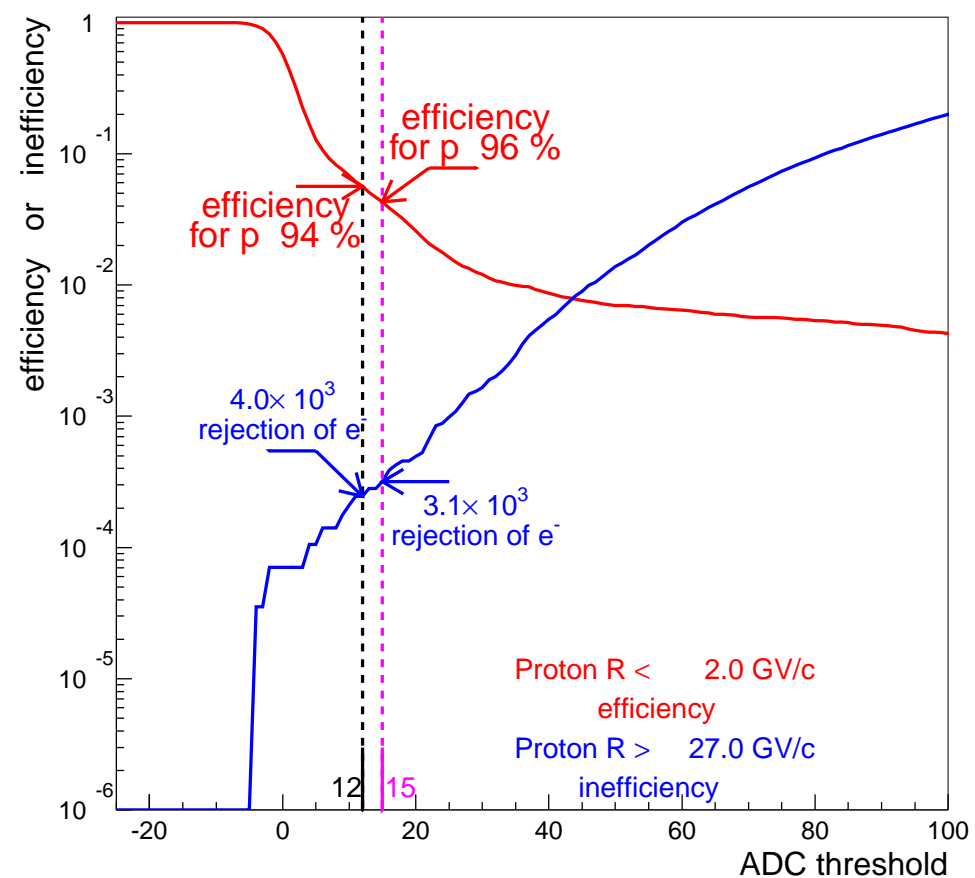
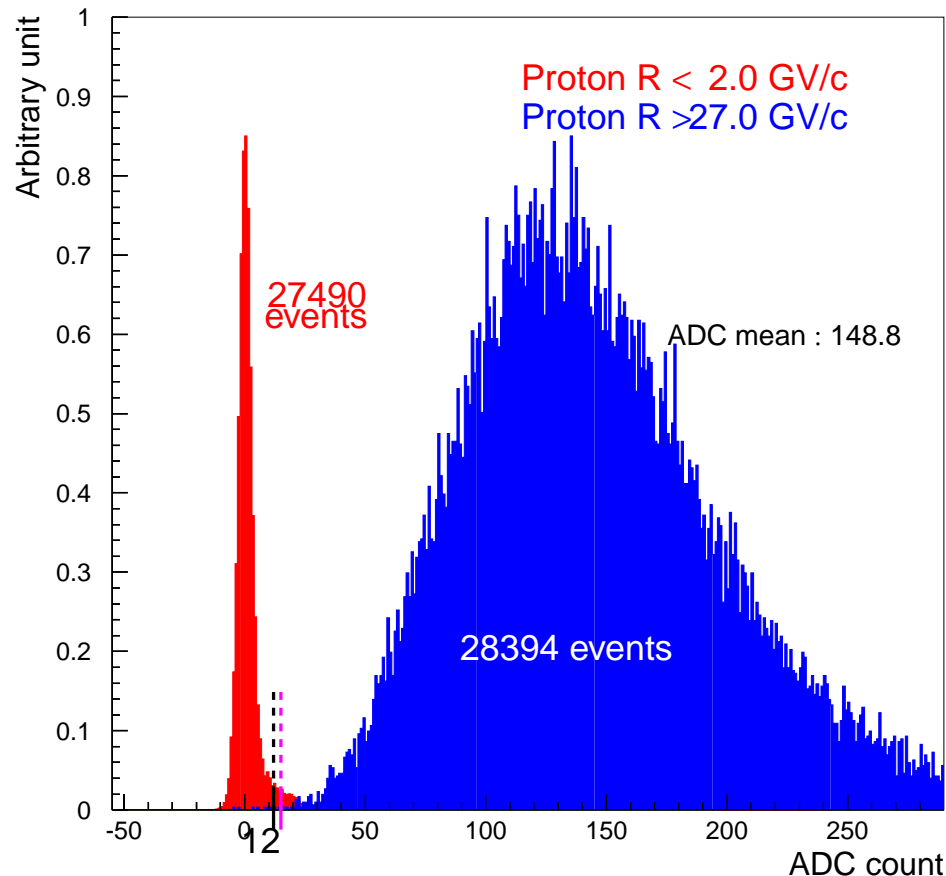
(Mitsui, Pfeifer et al,
S.A.Stephens)

山頂高度での
大気反陽子測定
⇒モデルの検証



Aerogel e/ μ Rejection Power

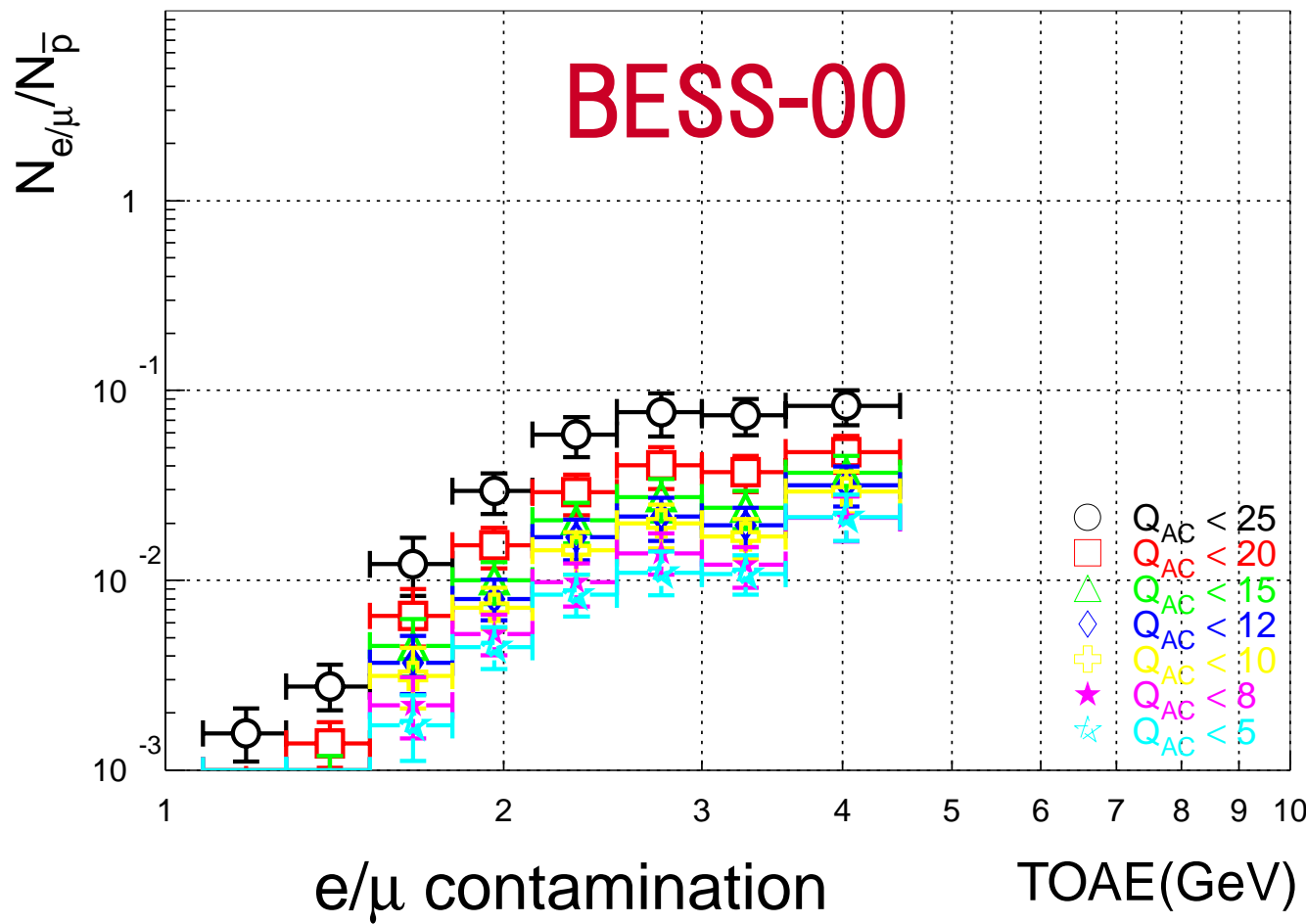
BESS-00



Rejection power estimated as a function of
ADC threshold using high energy proton samples.

Estimation of e/μ Contamination

- 1) No. of e/μ in the mass band were counted.
- 2) Rejection factor was obtained for a given ADC threshold.
- 3) No. of e/μ contamination in the \bar{p} candidates were calculated



⇒
 e/μ contamination
was kept below 5%
when applying $Q_{AC} < 12$.

Corrections

$$J(\bar{p})dE = \frac{N(\bar{p})}{S\Omega \epsilon t}$$

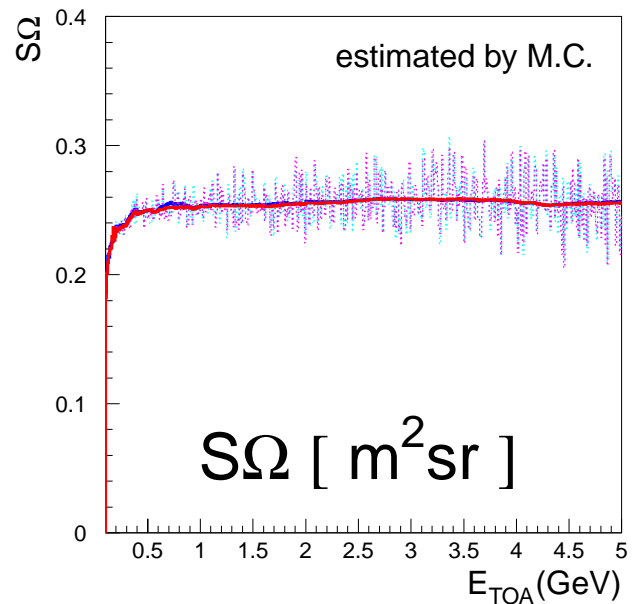
1. Exposure Factor ($S\Omega t$)

1). Live time (t):

- 1MHz clock,
directly measured
- dead time fraction
 $\sim 10\%$

2). $S\Omega$: M.C. simulation

- simple geometry



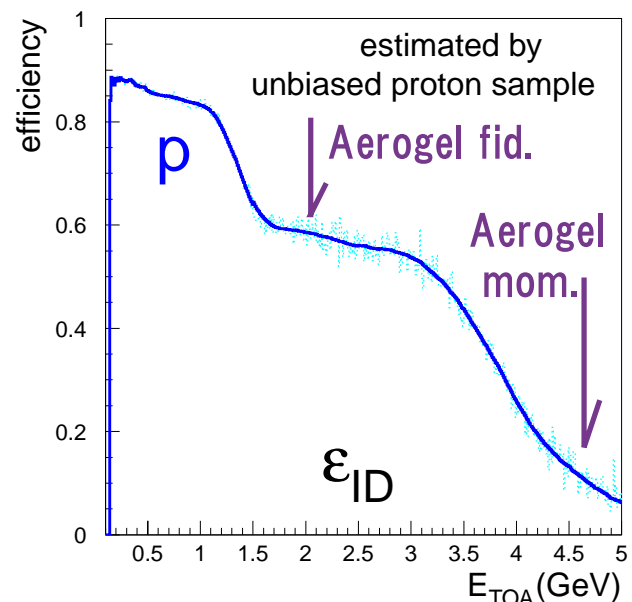
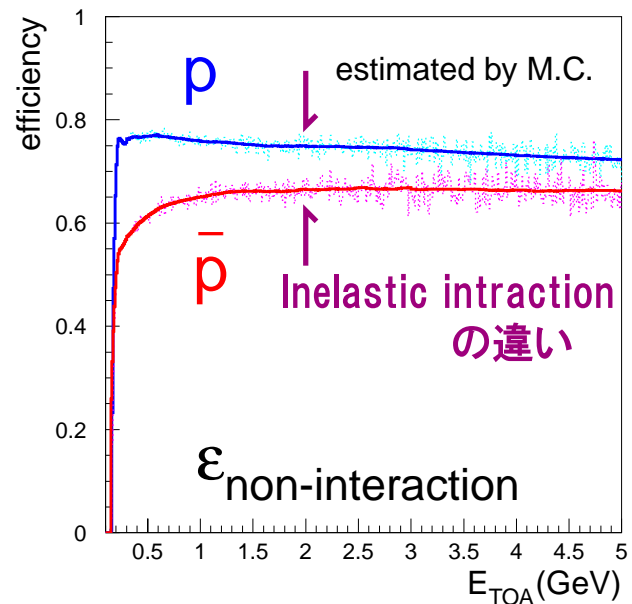
2. Detection Efficiencies (ϵ)

1). Interaction losses

M.C. simulation
calibrated by \bar{p} beam
@ KEK-PS K2 in 1999
 $\pm 15\% \Rightarrow \pm 5\% \text{ (syst.)}$

2). Event Selection

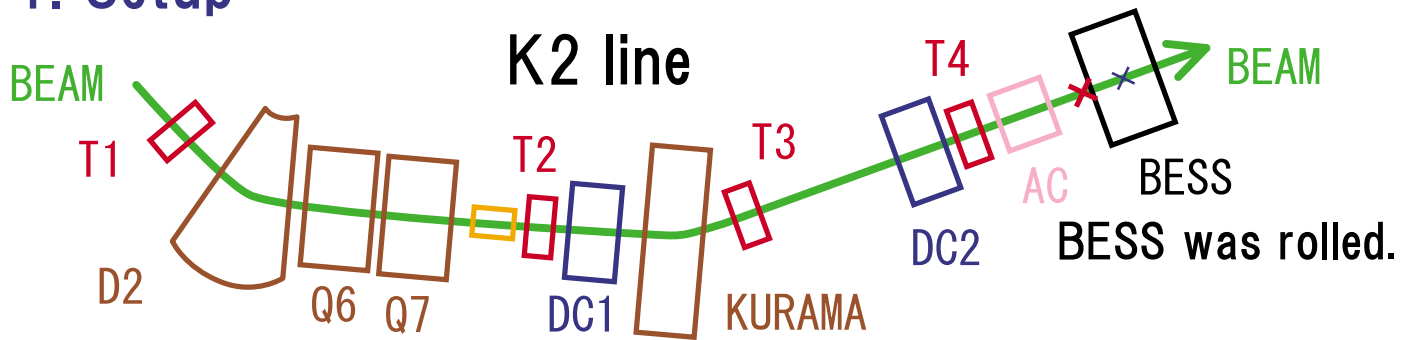
- unbiased proton sample
- high efficiencies



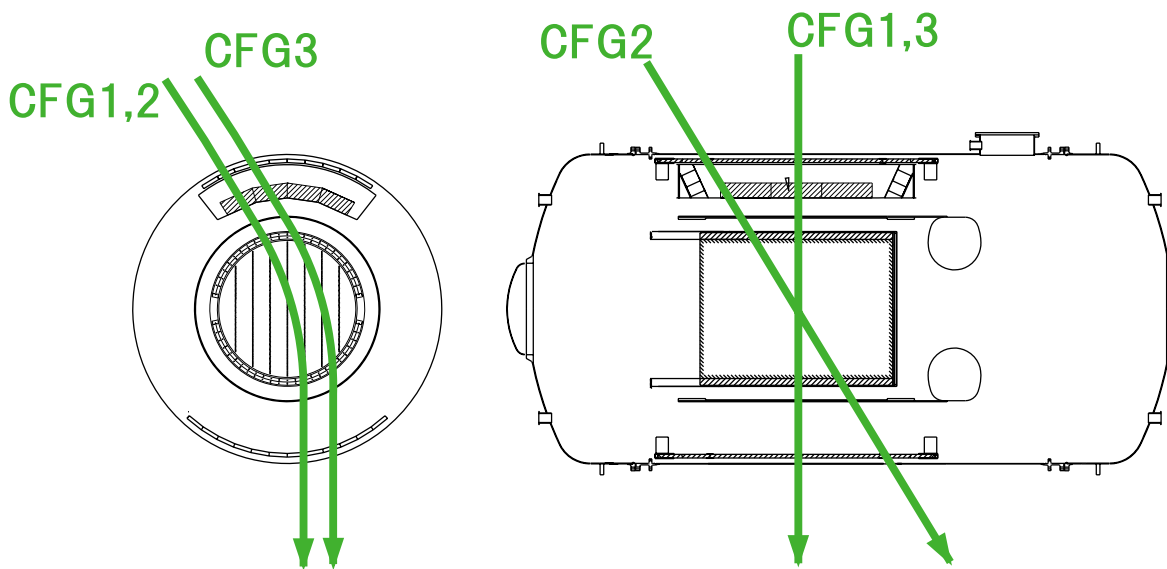
BESS detector beam test @ KEK

using low E antiproton and proton beam

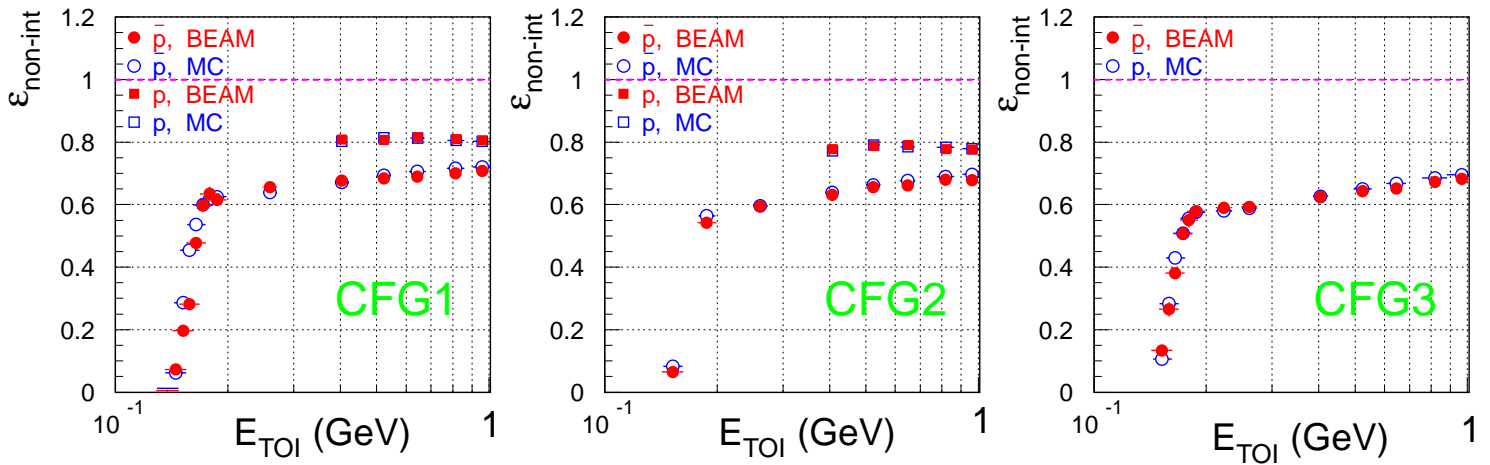
1. Setup



2. Beam incidence



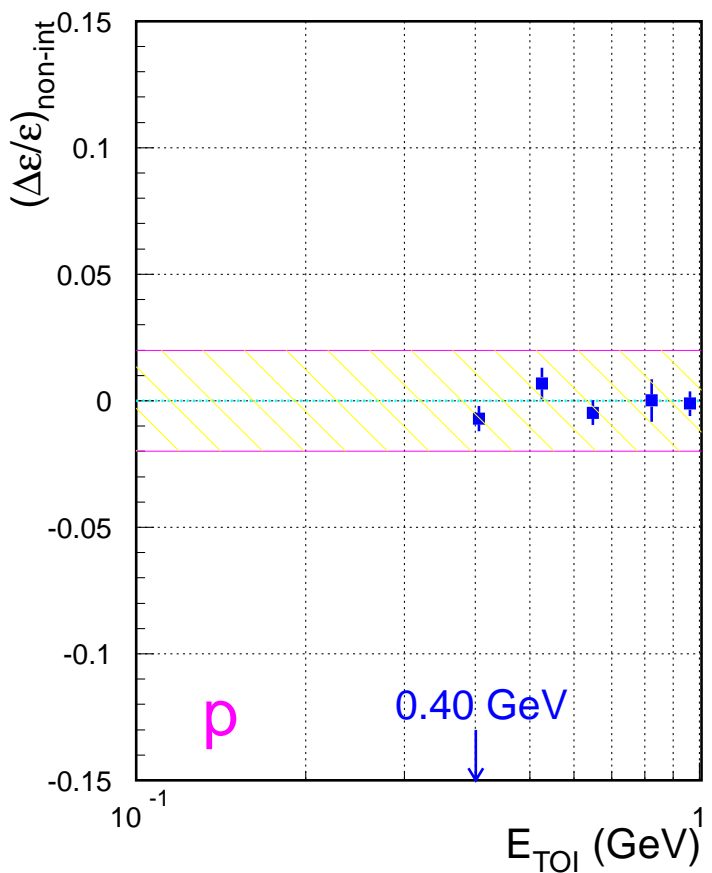
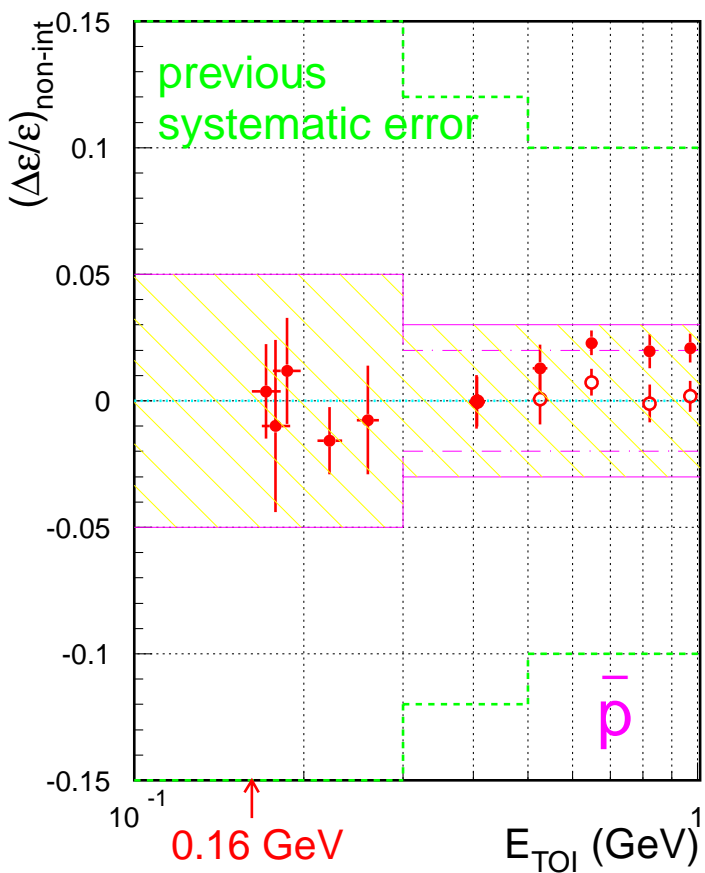
3. Direct measurement of the detection efficiencies



Systematic Uncertainty of the Detection Efficiencies

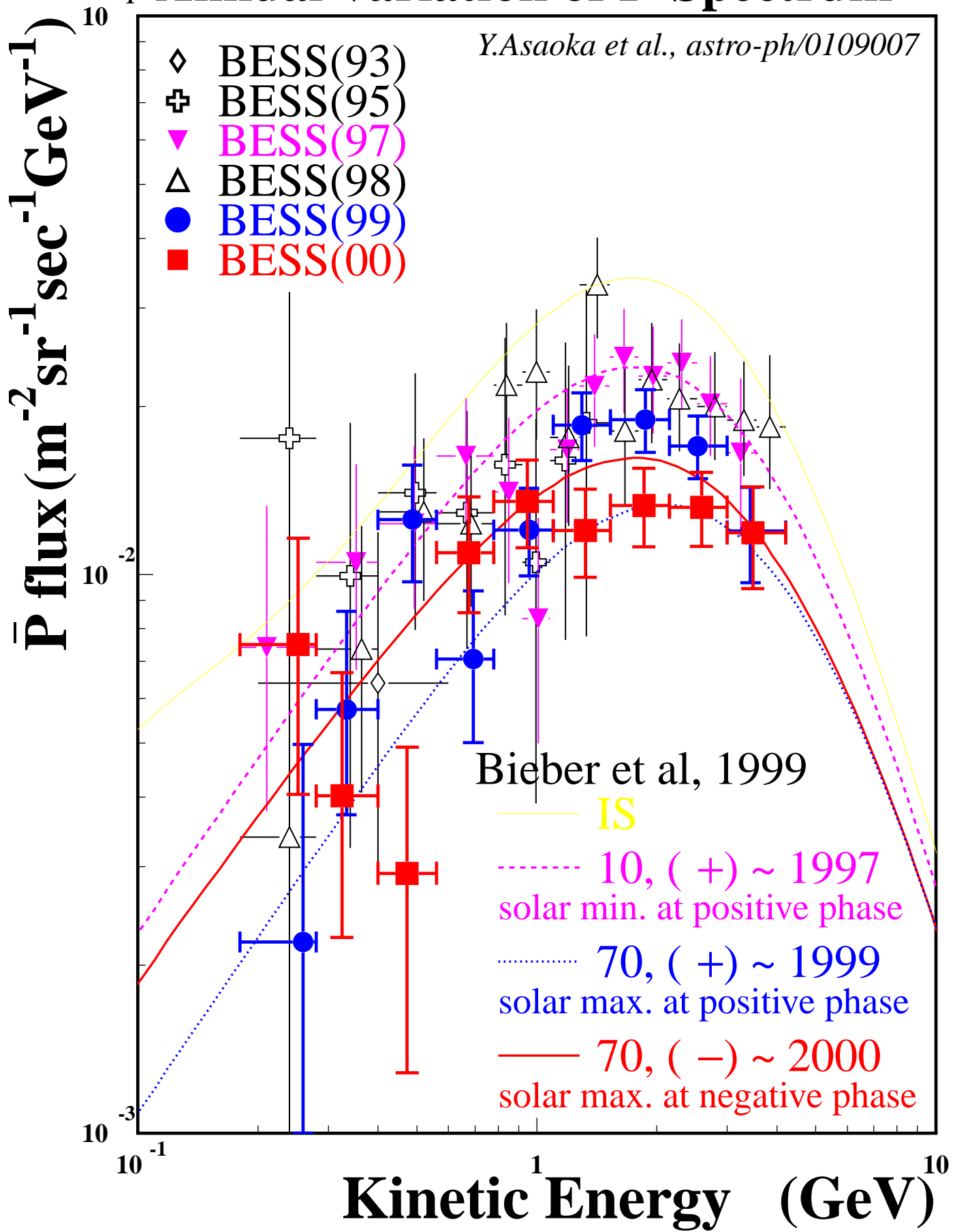
Y.Asaoka et al, physics/0105003, submitted to NIMA

- 1). The systematic errors of the beam test itself were estimated to be within $\pm 1\%$.
- 2). BESS M.C. simulation was verified by comparing with beam test data.
(hadronic interaction/material/detector response)
- 3). The relative systematic error of the detection efficiencies are kept within **5%**.

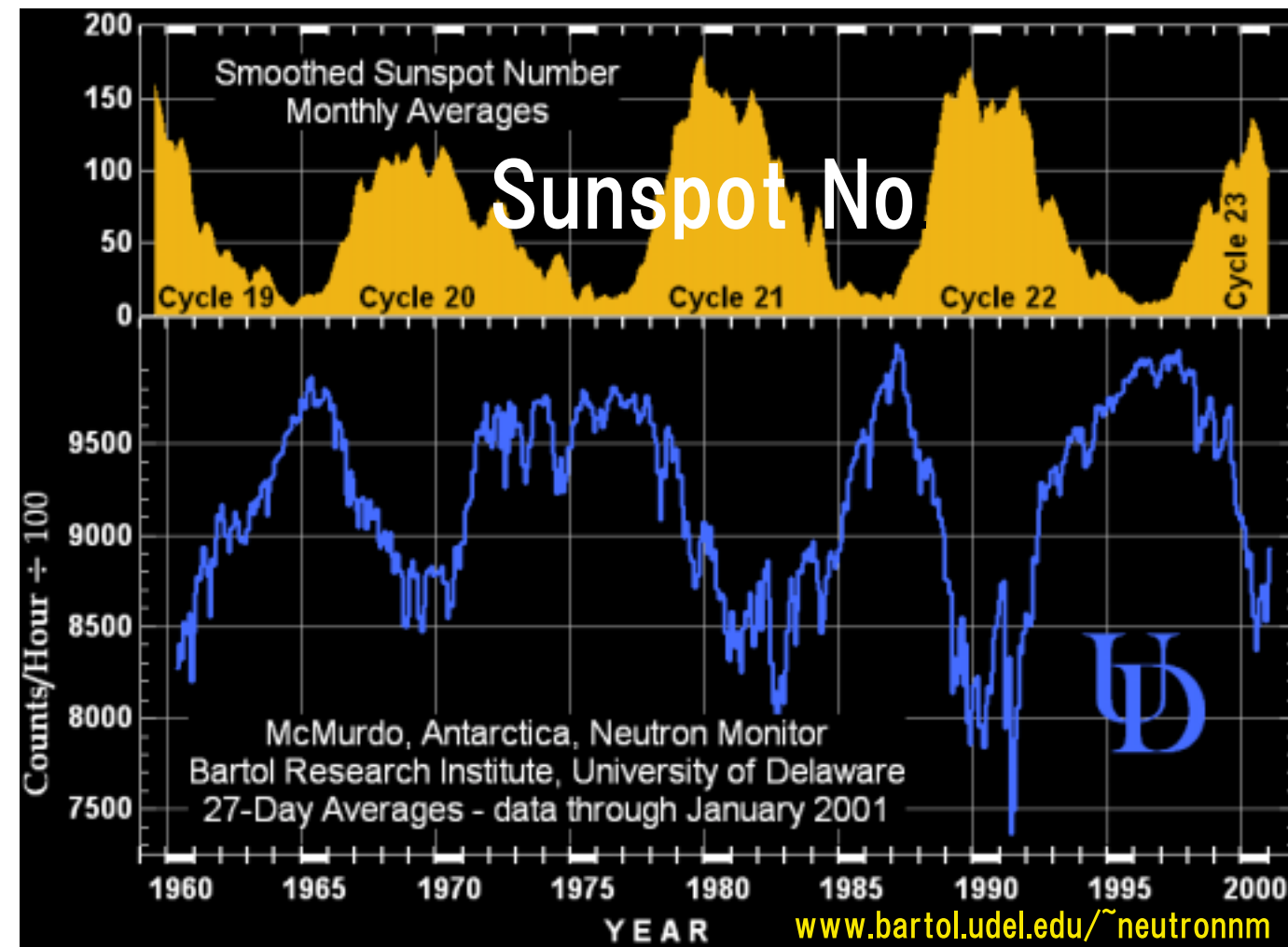


Annual Variation of \bar{P} Spectrum

Y.Asaoka et al., astro-ph/0109007



Solar Modulation



1960 1990
Neutron intensity

The process by which expanding solar wind modifies the energy spectrum of cosmic rays.

11-year cycle

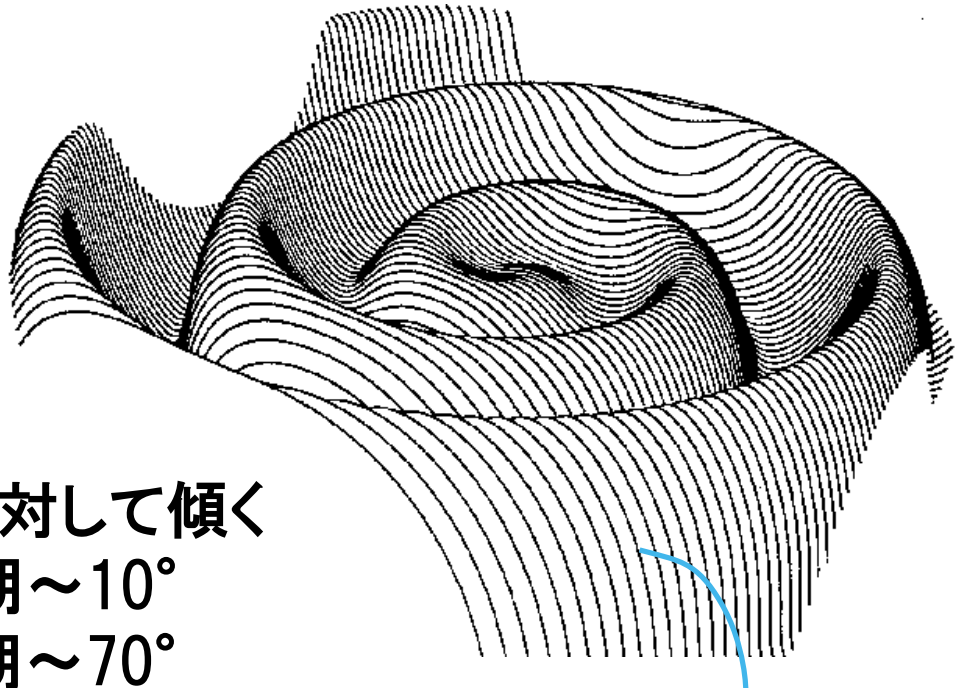
Sun's magnetic field polarity reverses at each solar maximum.



22-year cycle

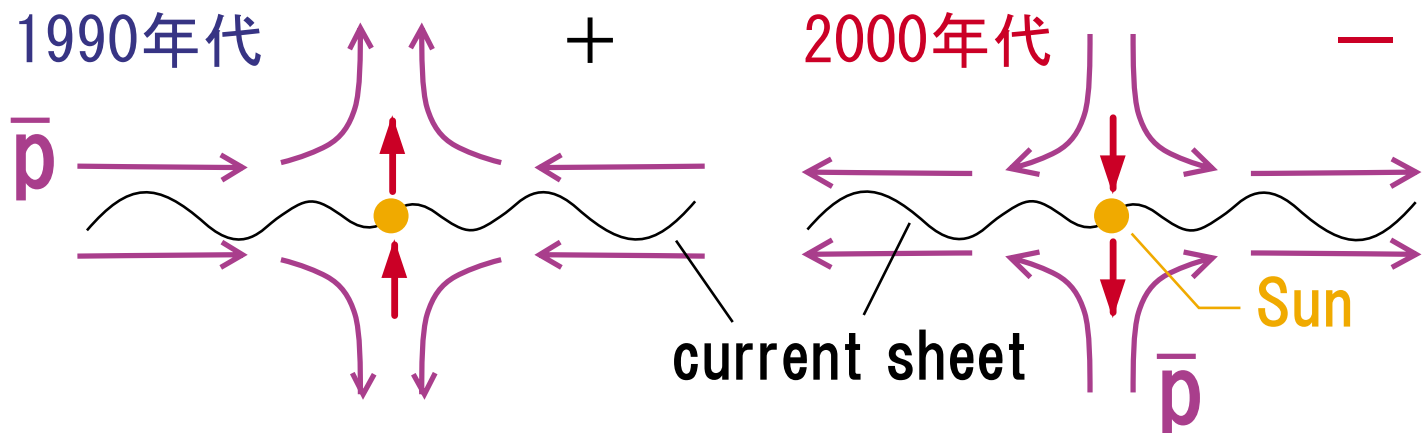
Charge Sign Dependence?

Sun's field



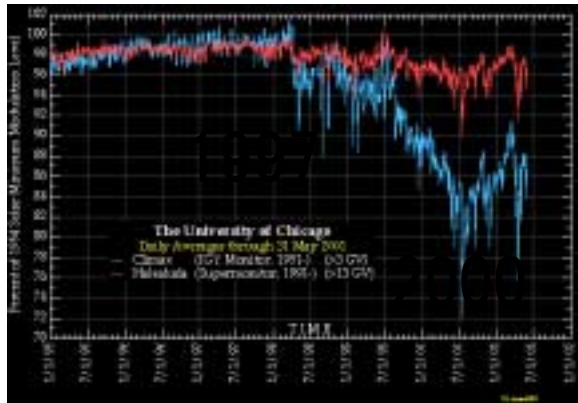
- ・太陽磁場: pole に対して傾く
太陽活動極小期～ 10°
極大期～ 70°
 - ・太陽磁場は太陽風の plasma 中に固定
 - ・太陽風の radial flow ($\sim 400\text{km/s}$)
 - ・25日周期の太陽の自転
- ⇒ wavy inclined current sheet

Drift in/out along current sheet
gradient and curvature drift



driftの向き \Leftrightarrow 粒子の電荷/太陽磁場のpolarity

Current Sheet Tilt Angle



Current sheet tilt angle governs the level of solar modulation.

1997 May
Quiet Sun
Tilt angle $\sim 10^\circ$

1998 May
Moderate Activity
Tilt angle $\sim 30^\circ$

1999 May-June
High Solar Activity

2000 May-June
High Solar Activity
Polarity has Reversed!

Current Evidence of Charge Sign Dependence

general consensus:

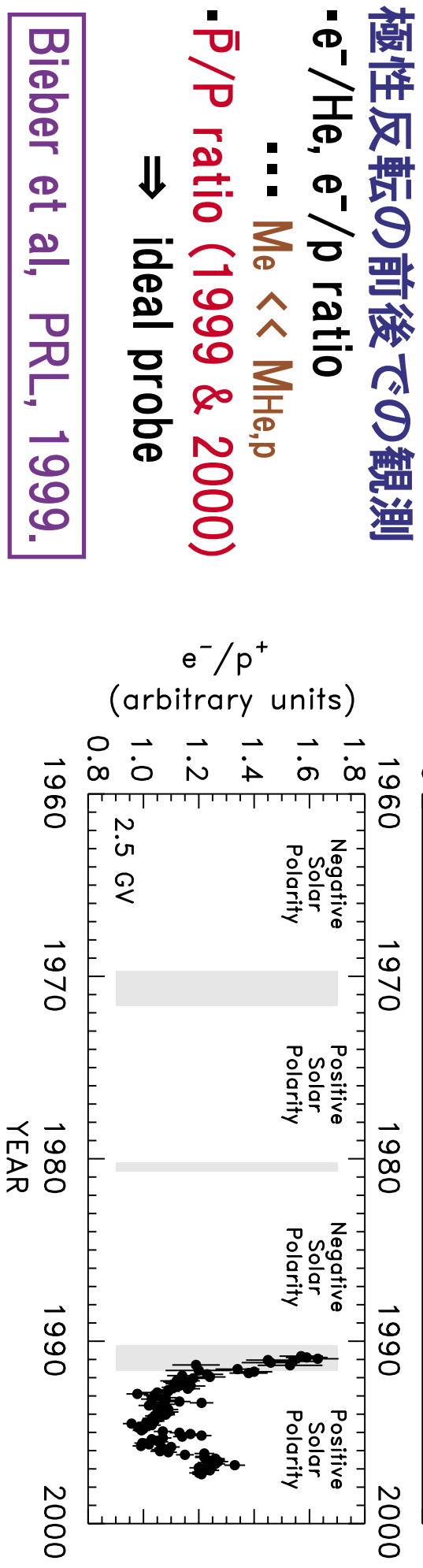
太陽活動極大期では
drift effect が無視できる

Bieber et al, 1999.

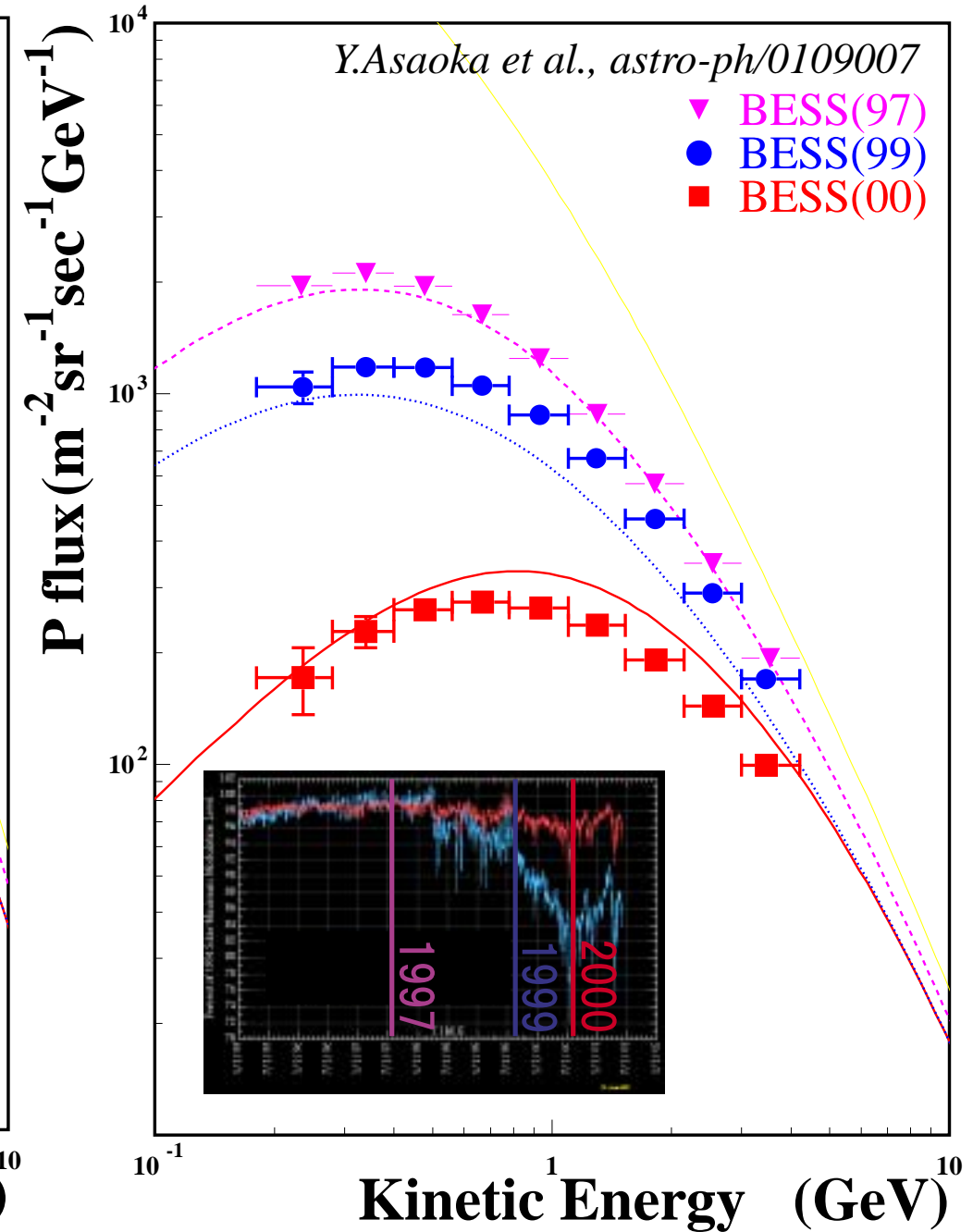
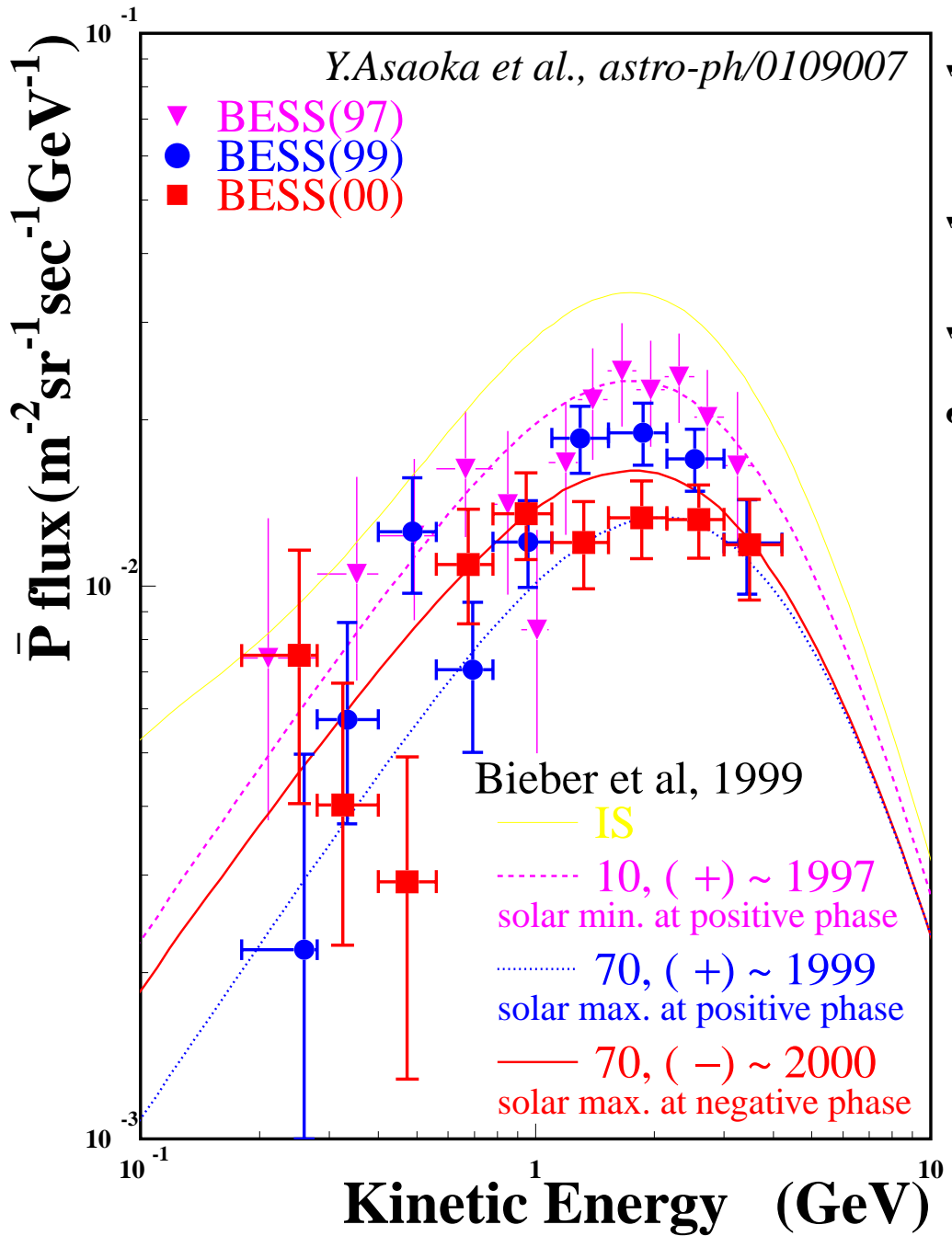
e^-/He : Balloon
 e^-/p : Ulysses

existing evidence:

極性反転の前後で
最も大きな変化

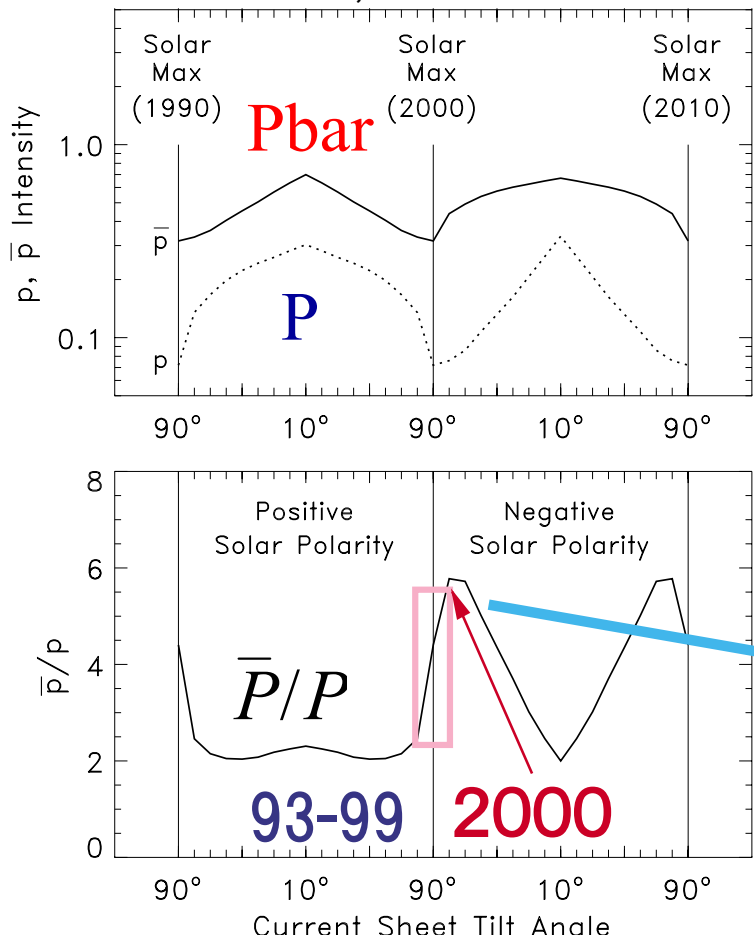


P and P spectrum following the solar field reversal

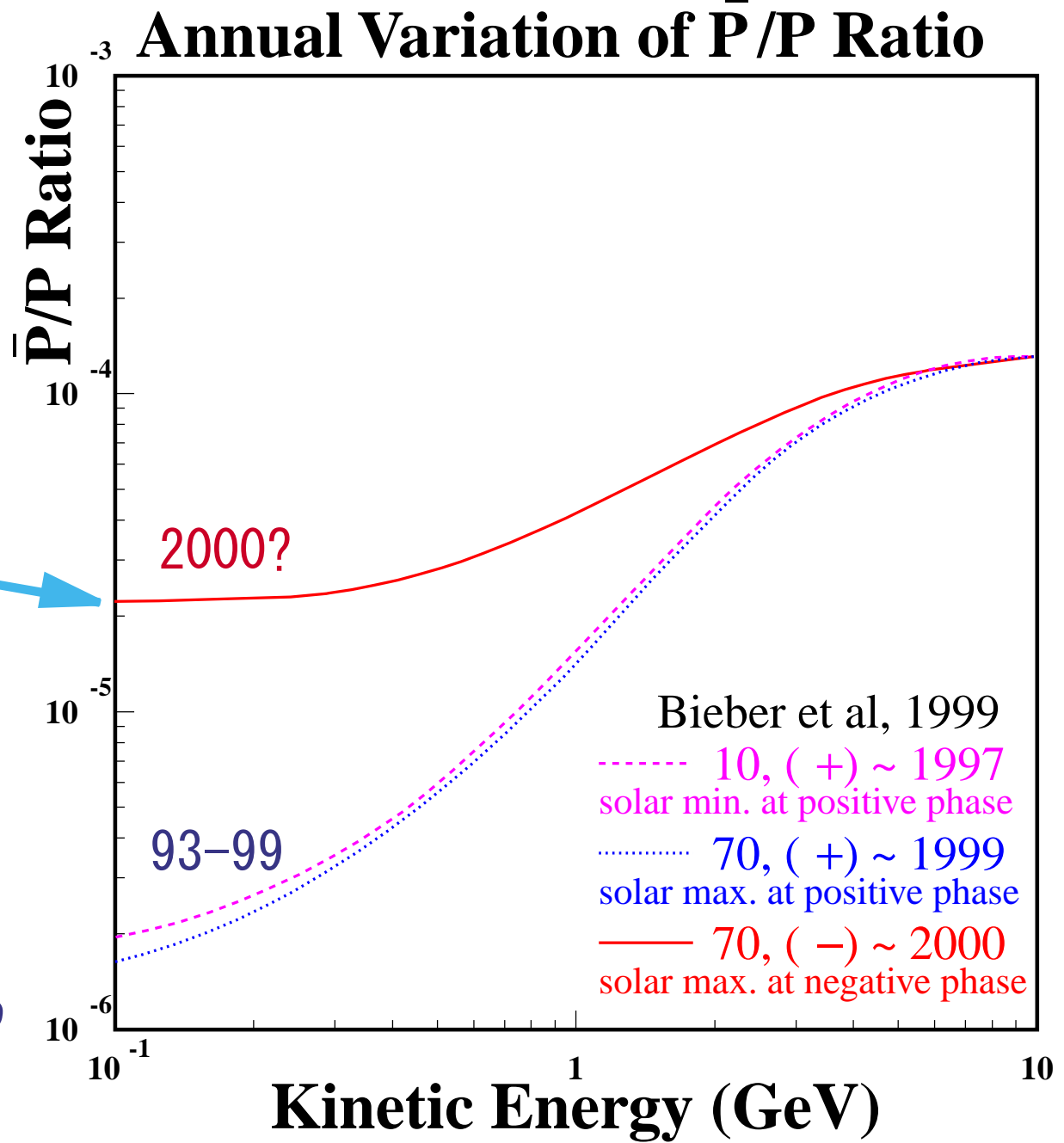


\bar{P}/P ratio following the solar field reversal

Bieber et al, 1999

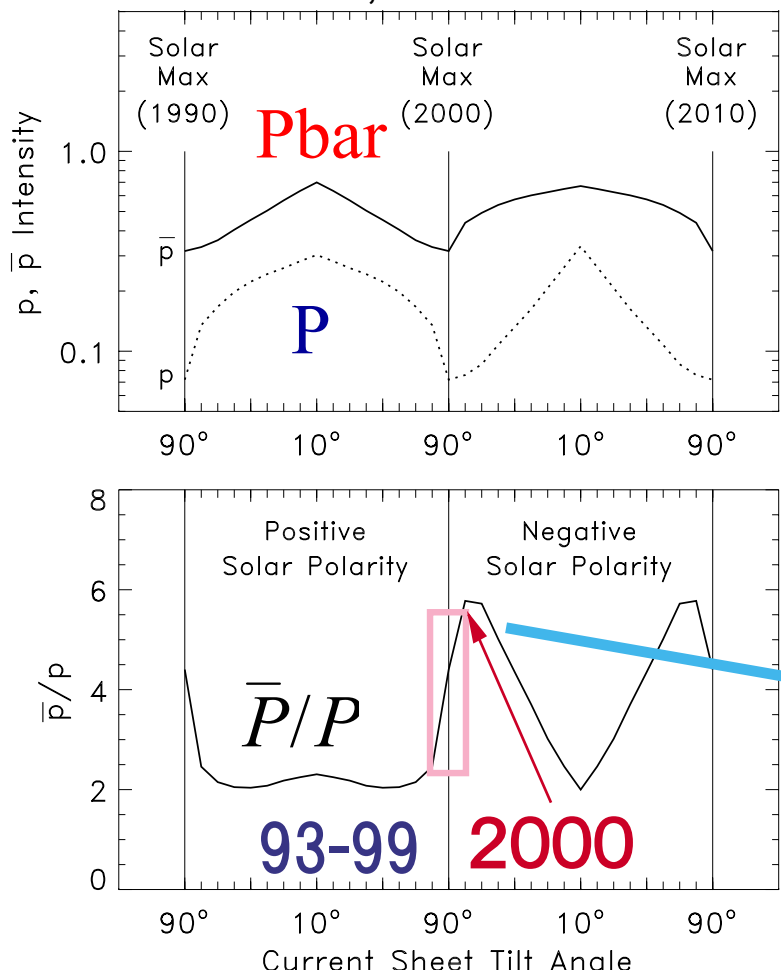


- IS spectrum の違い
- Charge sign の違い
- polarity (+) \Rightarrow 打ち消しあう
- (-) \Rightarrow 強めあう

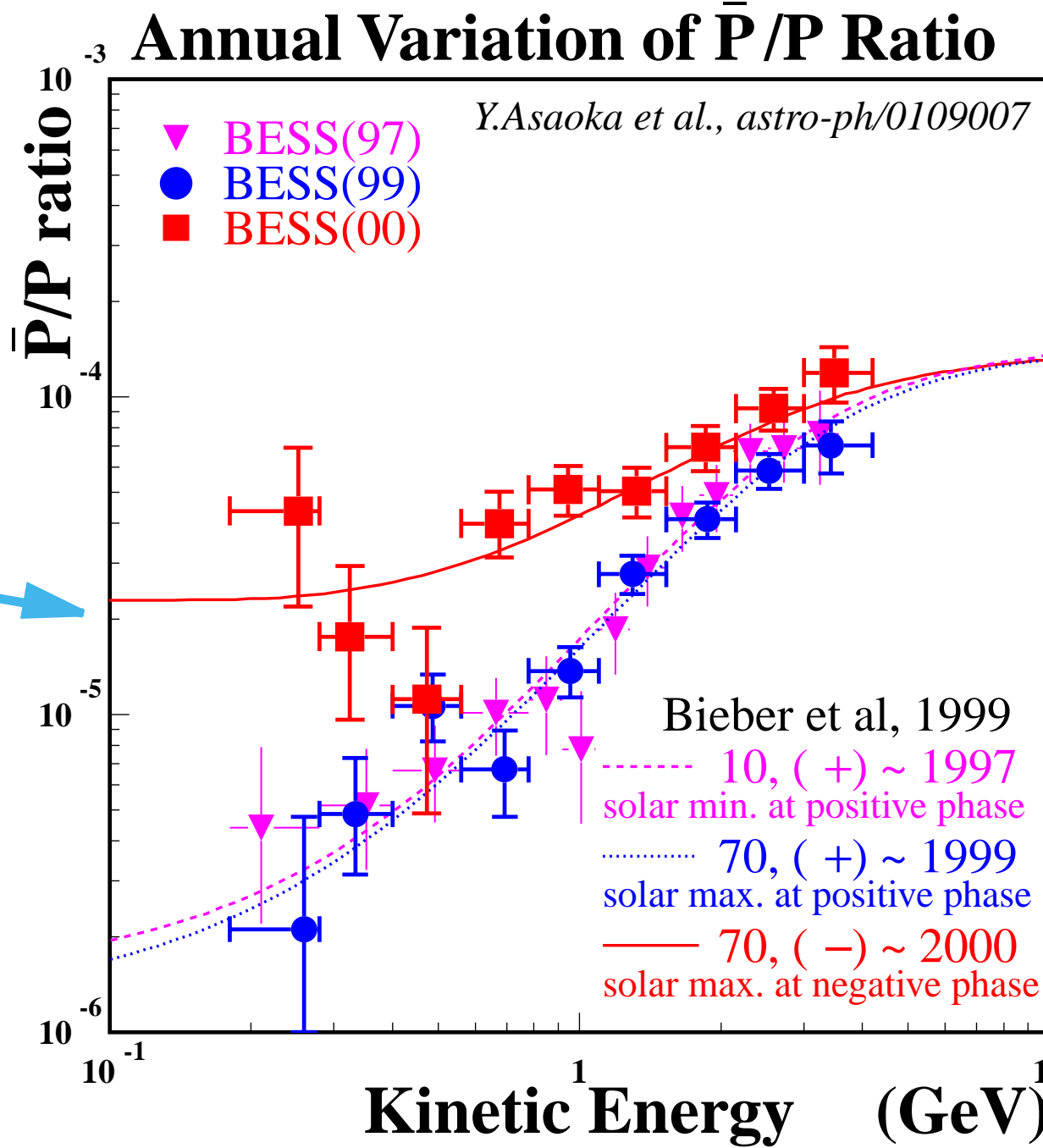


\bar{P}/P ratio following the solar field reversal

Bieber et al, 1999



- IS spectrum の違い
 - Charge sign の違い
- polarity (+) \Rightarrow 打ち消しあう
 (-) \Rightarrow 強めあう



Summary

BESSによる反陽子絶対流束の測定

1993 ~ 1994:

質量の同定による positive な検出

1995 ~ 1997:

太陽活動極小期における観測

- Energy Spectrum の測定
- 二次起源反陽子流束の peak を捉える.
⇒ 宇宙線伝播モデル
- 一次起源成分の流束に制限を与える.
↔ 低エネルギー領域での若干の過剰
一次起源成分の寄与の可能性残る.

1998 ~ 2000:

太陽活動極大期までの流束の経年変化

- Sun's polarity の反転の前後での測定
- 反陽子・陽子比の急激な上昇を捉える.
⇒ Charge sign dependence

Future:

BESS-Polar (南極周回飛翔)

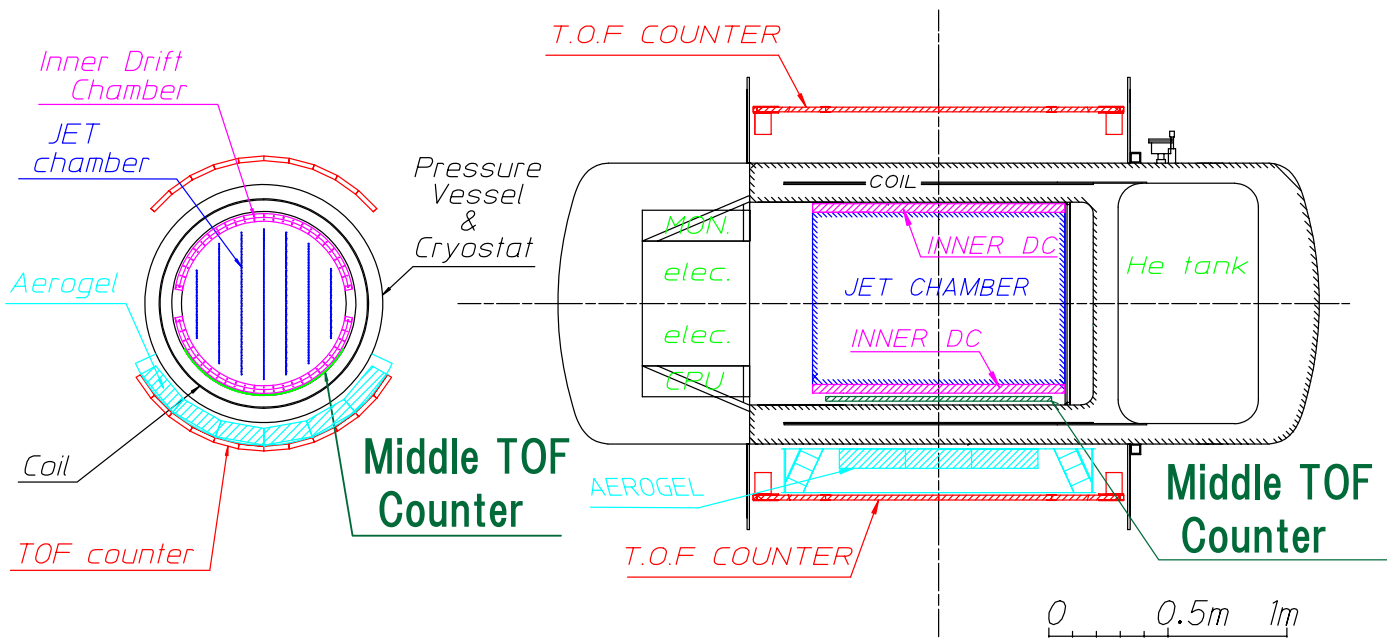
- 一次起源流束の有無に決着.

BESS Polar

AMSとも相補的な物理

No Vessel, New Mag (ultra thin)

\bar{p} 0.1-4.2 GeV by Middle TOF



2003-2004, 2006?

